PSFC/RR-11-2

Electric fields and transport in optimized stellarators

Landreman, M.

May 2011

Plasma Science and Fusion Center
Massachusetts Institute of Technology
Cambridge MA 02139 USA

This work was supported by the U.S. Department of Energy, Grant No. DE-FG02-91ER-54109. Reproduction, translation, publication, use and disposal, in whole or in part, by or for the United States government is permitted.

Electric fields and transport in optimized stellarators

by

Matthew Joseph Landreman

B.A., Swarthmore College (2003)
M.Sc., University of Oxford (2006)

Submitted to the Department of Physics
in partial fulfillment of the requirements for the degree of

Doctor of Philosophy

at the

MASSACHUSETTS INSTITUTE OF TECHNOLOGY

June 2011

Author . . . . . .
Department of Physics
May 10, 2011

Certified by . . . . . .
Peter J. Catto
Senior Research Scientist; Theory Head and Assistant Director, PSFC
Thesis Supervisor

Certified by . . . . . .
Miklos Porkolab
Professor; Director, PSFC
Thesis Co-Supervisor

Accepted by . . . . . .
Krishna Rajagopal
Professor, Associate Department Head for Education

Electric fields and transport in optimized stellarators

by

Matthew Joseph Landreman

Submitted to the Department of Physics on May 10, 2011,
in partial fulfillment of the requirements for the degree of Doctor of Philosophy

Abstract

Recent stellarator experiments have been designed with one of two types of neoclassical optimization: *quasisymmetry* or *quasi-isodynamism*. Both types of stellarator have perfectly confined collisionless particle orbits as well as one additional feature. Quasisymmetric plasmas have minimal flow damping, which may lead to reduced turbulent transport. Quasi-isodynamic plasmas can have vanishing bootstrap current, implying less variation in the magnetic configuration as the pressure changes and also implying greater stability.

Analytical expressions for neoclassical transport in a general stellarator are complicated, so it is desirable to find reduced expressions for ideal limiting cases to provide insight. Here, new neoclassical expressions are derived for a quasi-isodynamic plasma. The Pfirsch-Schlüter flow and current can be written concisely as an integral of B. The remaining components of the flow and bootstrap current are identical to those in a quasi-poloidally symmetric device. A compact expression is derived for the radial electric field E_r which is largely independent of the details of the magnetic field.

Another issue in the neoclassical theory of stellarators which has not been fully resolved is the validity of the so-called monoenergetic approximation, in which ad-hoc changes are made to E_r terms in the kinetic equation to expedite numerical computations. Here we show that at least in a quasisymmetric plasma, this approximate treatment of E_r leads to a significant and systematic underestimation of the trapped particle fraction. This distortion of the *collisionless* orbits is independent of any approximations made to the collision operator.

For ideal quasisymmetric and quasi-isodynamic plasmas, new neoclassical expressions are derived in which this problematic monoenergetic approximation is avoided. In the quasisymmetric case, results are presented in both the banana regime and plateau regime for the ion flow, ion radial heat flux, and bootstrap current. The bootstrap current is found to be enhanced. For the quasi-isodynamic case, new E_r-driven contributions to the distribution function are obtained. The flow and bootstrap current turn out to be modified by the same numerical coefficient as in the quasisymmetric case.

Thesis Supervisor: Peter J. Catto
Title: Senior Research Scientist; Theory Head and Assistant Director, PSFC

Thesis Co-Supervisor: Miklos Porkolab
Title: Professor; Director, PSFC

Acknowledgments

I am grateful to many people whose support and advice have made this work possible: to Peter Catto, for taking me on as a student, always making time to talk and work through the algebraic details, and making research fun; to Per Helander, for bringing this research topic to my attention, teaching me about stellarators and radial electric fields, and supporting my visit to Greifswald; to Tünde Fülöp for her generous hospitality at Chalmers Institute of Technology, where some of the work in this thesis was performed; to Jeff Freidberg, for many thought-provoking conversations; to Grisha Kagan, whose thesis work on tokamak pedestals laid the foundation for some of the stellarator calculations herein; to Antoine Cerfon, for being a sounding board and always indulging my naive plasma physics questions; to Chris Crabtree for being a friend and mentor; to my committee members Miklos Porkolab, Jan Egedal, and John Belcher for their advice; to Darin Ernst for his interest in this work and stimulating questions; and to Felix Parra and Istvan Pusztai for valuable conversations. Finally, I am grateful to Emily Kendall for her love and friendship.

Contents

CHAPTER 1

Introduction

The two most promising concepts for magnetic plasma confinement are tokamaks and stellarators. Tokamaks rely on a large current in the plasma, which has several negative consequences. The use of a transformer to induce this current makes tokamaks intrinsically pulsed rather than steady-state. If non-inductive current drive is used, a large fraction of any electricity produced in a reactor would need to be recirculated to run the current drive system. This large recirculating power fraction detracts from the overall economic viability of the concept. Finally, the large plasma current makes tokamaks susceptible to disruptions. The stellarator concept, in contrast, does not rely on any current in the plasma, so none of the the aforementioned problems apply [1, 2].

However, stellarators have a handicap compared to tokamaks when it comes to confinement. In axisymmetric plasmas, it can be proven that in the absence of collisions and turbulence, the guiding-center drift orbit of every particle is confined, a result known as Tamm's theorem [3]. However, in nonaxisymmetric plasmas, some trapped particles generally have drift trajectories that are not periodic, moving from the confined region outward to open field lines. This distinction between tokamaks and general stellarators is illustrated in figure 1-1. Alpha particles that are born on one of the unconfined trajectories in a stellarator are likely to collide with plasma-facing components before slowing down on the bulk plasma. In a reactor, the first wall would therefore suffer significant damage from this irradiation by high-energy alpha particles. Thermal ions and electrons may also follow these unconfined trajectories out of the core plasma. These unconfined particles carry heat away from the core, lowering the energy confinement of the system.

The particle and energy fluxes associated with these unconfined orbits can be calculated within the framework of neoclassical transport theory, in which the simplifying assumption is made that there is no turbulence in the plasma, but collisions are accounted for rigorously using kinetic theory. The collisional transport associated with guiding-center drifts is referred to as 'neoclassical' to distinguish it from the classical transport associated with Larmor motion. Neoclassical theory is important in both stellarators and tokamaks for un-

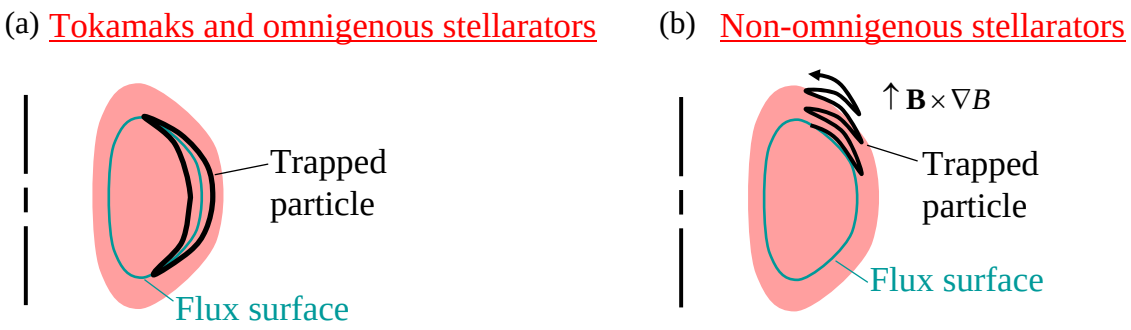

Figure 1-1: Trajectories of trapped particles. (a) In tokamaks and omnigenous stellarators, all collisionless trajectories are confined. (b) In contrast, trapped particles in other stellarators may have a radial drift that does not average to zero.

derstanding the flows and currents which arise in plasmas. However, neoclassical theory is particularly important in stellarators because *radial* neoclassical transport can be large in a stellarator due to the unconfined particle orbits, large enough to compete with or dominate turbulent transport in the plasma core. (Near the plasma edge, turbulent transport tends to be dominant due to the larger density and temperature gradients there, and also because neoclassical diffusion is a strong function of temperature.) As shown in figure 1-2, neoclassical theory has shown success at modeling radial transport in the core of stellarators. For the high temperatures typical of modern experiments, the electrons tend to be a "$1/\nu$" collisionality regime [4, 5], in which the radial diffusion coefficient is proportional to $1/\nu_e$, where ν_e is the total electron collision frequency.

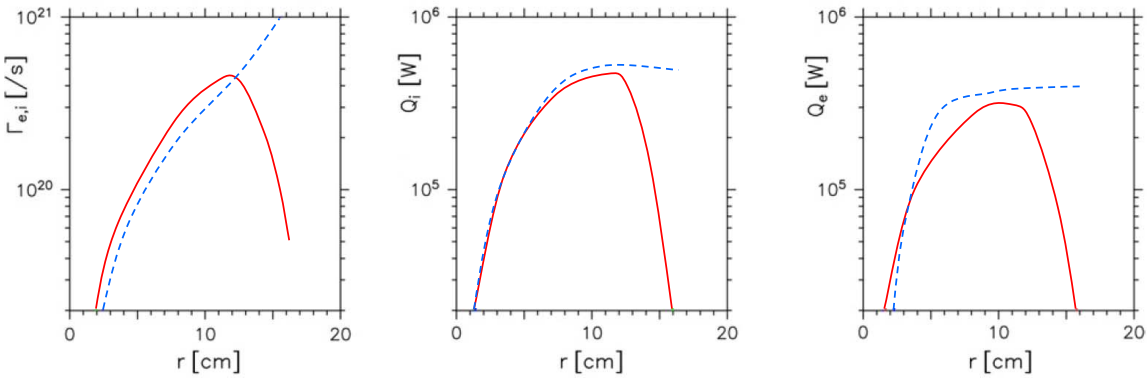

Figure 1-2: Comparison of neoclassical theory (solid red curves) to the transport inferred from experimental power balance (dashed blue curves) in W7-AS. Plots show the particle flux, ion heat flux, and electron heat flux respectively. Figure from [6].

In the last several decades it has become feasible to numerically search through the space of stellarator equilibria to minimize the fraction of particles that have unconfined orbits. A stellarator that was perfectly optimized in this sense would be "omnigenous,"

meaning that the time-averaged radial guiding center drift vanishes for all particles [7–10]. (This condition in fact only constrains the trapped particles, as this average radial drift automatically vanishes for passing particles). In an omnigenous stellarator, trapped particle orbits resemble the tokamak orbits in figure 1-1.a rather than the typical stellarator trapped particle trajectories of figure 1-1.b. An equivalent definition of omnigenity is that the longitudinal adiabatic invariant $J = \oint v_{\|} \, d\ell$ is constant on a flux surface. (Appendix A gives a proof that these two definitions are equivalent.) Axisymmetric plasmas are omnigenous due to Tamm's theorem. (Usage of the term "omnigenous" in the literature is inconsistent: some authors have used the term to mean a stricter condition, that the *instantaneous* (local) radial drift vanishes, which implies B is constant on a flux surface [11]. Herein we use the weaker definition given above.)

The condition of omnigenity places strong mathematical constraints on $\mathbf{B}(\mathbf{r})$. One remarkable feature which can be proven is that on any flux surface of an omnigenous field, the maximum and minimum of $B = |\mathbf{B}|$ form closed curves rather than isolated points. There are three topological possibilities: these maximum- and minimum-B curves can close toroidally, poloidally, or helically.

Many recent stellarator experiments and experiment designs fall into two sub-types of omnigenity: quasisymmetry and quasi-isodynamism. In this thesis we will focus attention on these two types of optimized stellarator. Both types of stellarator have perfectly confined collisionless particle orbits, and each type also has an additional feature relative to the more general class of omnigenous equilibria.

Quasisymmetric devices have minimal damping of plasma flows. As flows increase stability to MHD modes, and as sheared flows are expected to suppress turbulence, quasisymmetric plasmas are expected to have improved MHD stability and reduced turbulent transport [12]. In contrast to a general stellarator, in which flows turn out to be damped strongly in all directions, in a quasisymmetric plasma a direction exists in which strong flows are permitted. Associated with this direction, the *magnitude* of B has a symmetry in certain special coordinate systems, even if the full vector $\mathbf{B}$ has no obvious symmetry. More precisely, B varies on a flux surface only through a fixed linear combination of the toroidal and poloidal angles [13, 14]:

$$B(\psi, \theta, \zeta) = B(\psi, M\theta - N\zeta) \tag{1.1}$$

where M and N are fixed integers for a given device, ψ is any flux surface label, and θ and ζ are poloidal and toroidal angles that will be defined more precisely in the next chapter. It turns out that quasisymmetry can also be defined in several other equivalent ways which are independent of any coordinate system on a flux surface. For example, we shall prove in the next chapter that (1.1) is equivalent to

$$\mathbf{B} \cdot \nabla \left(\frac{\mathbf{B} \times \nabla \psi \cdot \nabla B}{\mathbf{B} \cdot \nabla B} \right) = 0. \tag{1.2}$$

It can be proven that any quasisymmetric magnetic field is omnigenous. As with all om-

nigenous fields, quasisymmetric fields fall into three classes based on the topology with which the constant-B curves close. These three varieties of quasisymmetry are known as quasi-axisymmetry ($N = 0$), quasi-poloidal symmetry ($M = 0$), and quasi-helical symmetry (both M and N nonzero). It also turns out quasisymmetric stellarators have many tokamak-like properties. The Helically Symmetric eXperiment (HSX) at the University of Wisconsin - Madison is nearly quasisymmetric [15], as is the design for the National Compact Stellarator eXperiment (NCSX), which was partially constructed at Princeton [16].

The second variety of optimized stellarator we will consider is one which is quasi-isodynamic. A quasi-isodynamic plasma is defined to be one in which the field is omnigenous and in which the B contours close poloidally, rather than toroidally or helically [17–21]. (While this definition is the one given by Helander and Nührenberg in [17], unfortunately the term "quasi-isodynamic" is defined inconsistently in the literature. For example, Mynick [22] defines the term to mean that the most deeply trapped particles are omnigenous, whereas barely trapped particles are not.) It turns out when the B contours close poloidally, the pressure-gradient-driven current known as the "bootstrap current" is minimized. As plasma currents can be a source of free energy to drive instability, quasi-isodynamic plasmas should have improved stability. Also, elimination of the bootstrap current minimizes the variation in the magnetic configuration as the pressure is varied. Therefore, the magnetic field can be optimized to be omnigenous over a wide range of pressures, rather than just for a specific pressure profile. The W7-X stellarator, currently under construction at the Max Planck Institute for Plasma Physics in Greifswald, Germany, is nearly quasi-isodynamic [17, 23–25]. Recent stellarator design studies have examined equilibria which are even closer to perfect quasi-isodynamism [20].

The various classes of stellarator are displayed in figure 1-3, in which contours of B are plotted for a given flux surface as a function of the toroidal and poloidal angles ζ and θ. Again, these angles will be defined precisely in the next chapter. Figures 1-3.a-c depict the three classes of quasisymmetric fields, showing the B contours are straight. The contour plot for a quasi-axisymmetric device (a) is identical to that for a tokamak. Omnigenous and quasi-isodynamic fields, depicted in (e) and (d), are more complicated, in that the B contours are not straight and there is no symmetry direction. Nonetheless, the B contours all encircle the plasma with the same topology: poloidally for the quasi-isodynamic case (d), and toroidally in (e). A general stellarator, shown in (f), is more complicated still. Here, different B contours close with different topology. For the particular case shown here, some contours (red and blue) do not encircle the plasma at all, whereas the orange, green, and cyan contours encircle the plasma toroidally.

The varying levels of complexity for these classes of stellarator can also be understood by considering how the magnitude of B varies along a field line. The corresponding plots for each class of stellarator are shown in figure 1-4. In quasisymmetric fields, as in tokamaks, B varies in a periodic manner along a field line. In omnigenous or quasi-isodynamic fields, the situation is more complicated because $B(\ell)$ is no longer periodic. However, each well in $B(\ell)$ has the same height and width. A general stellarator is much more complex, with many trapping wells of varying height and width.

The logical relationship among these classes of stellarators is displayed in figure 1-5.

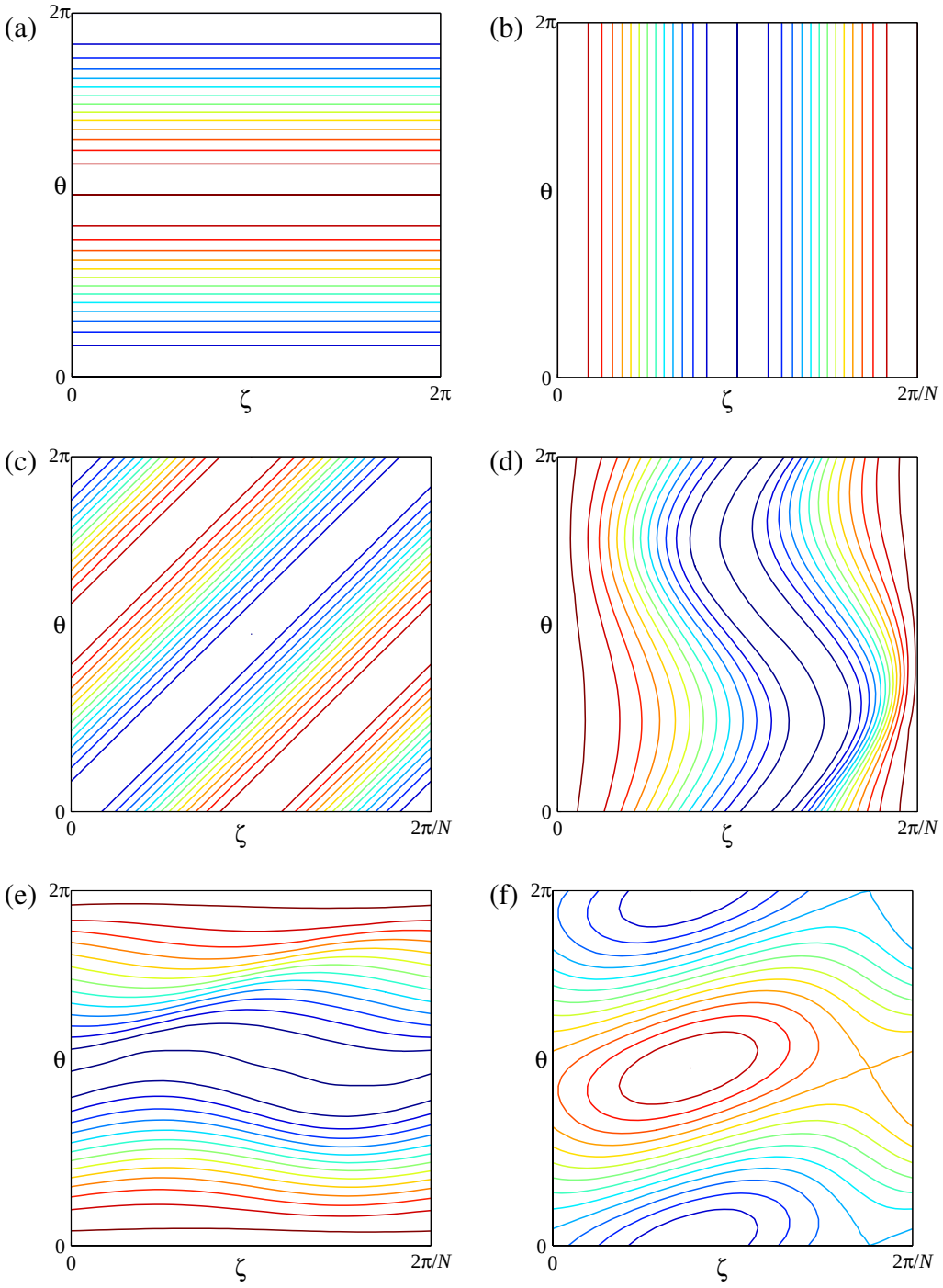

Figure 1-3: Contours of B on a flux surface for various types of stellarator. (a) A tokamak or quasi-axisymmetric stellarator. (b) Quasi-poloidal symmetry. (c) Quasi-helical symmetry. (d) A quasi-isodynamic device. (e) An omnigenous but non-quasi-isodynamic field. (f) A general (non-optimized) stellarator. In each case, red contours indicate the maximum B and blue contours indicate the minimum B, and the integer N indicates the number of identical toroidal segments.

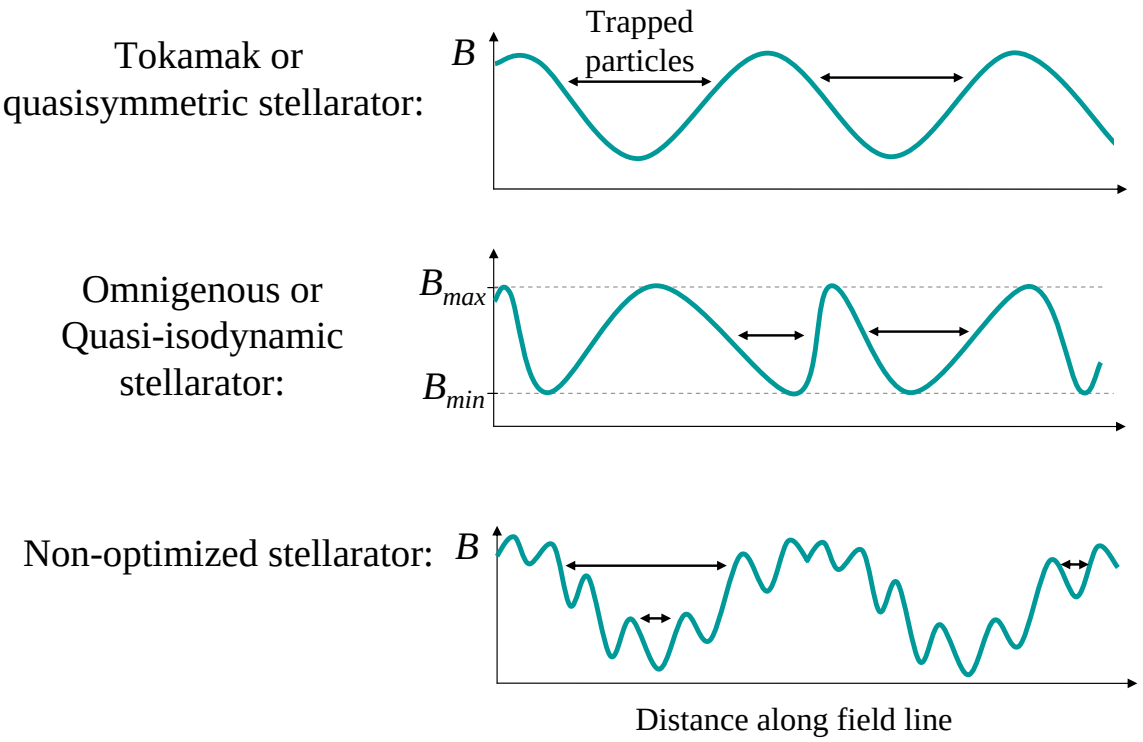

Figure 1-4: Variation of B along a field line for various types of toroidal magnetic field, in increasing order of complexity.

Axisymmetric plasmas are quasisymmetric (with $N = 0$ and $M = 1$), but nonaxisymmetric plasmas can be found which are quasisymmetric (to a close approximation.) Axisymmetric plasmas are not quasi-isodynamic, for the constant-B contours in an axisymmetric plasma close toroidally rather than poloidally. A quasi-poloidally symmetric plasma is quasi-isodynamic.

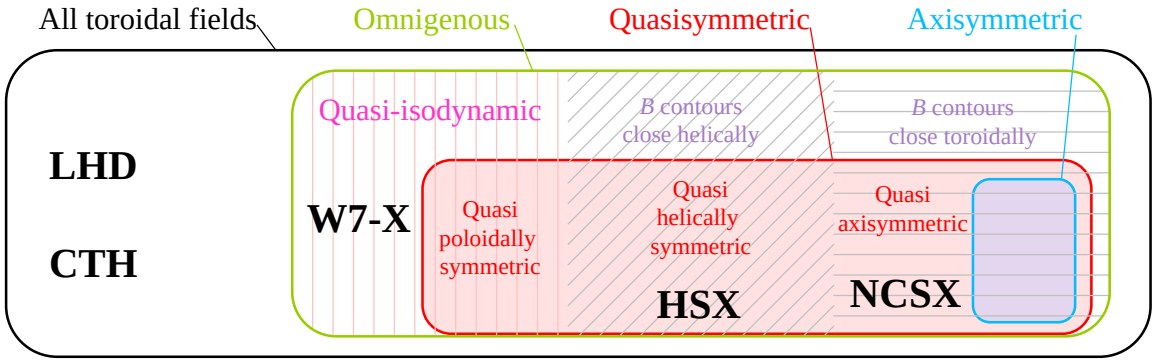

Figure 1-5: Relationship among the various classes of stellarators.

A wide literature exists on these and other concepts of stellarator optimization. Useful reviews include references [6, 18, 22, 26].

Analytical expressions for neoclassical transport in a general stellarator are quite complicated. For example, the bootstrap current in a general stellarator is given in appendix A of reference [27]. As shown there, to evaluate the bootstrap current it is necessary to solve two partial differential equations which depend on the magnetic field, and then compute several two- and three-dimensional integrals of the resulting solutions. While this evaluation can be done numerically for a specified magnetic equilibrium, it does not give the same insight as a compact and explicit analytic formula. It is therefore desirable to find limits in which the general formulae simplify. Quasisymmetry is one such limit. The equations of neoclassical transport for a quasisymmetric plasma were derived previously by Boozer in 1983 [28], who pointed out that the results turn out to be identical to the results for a tokamak if certain "isomorphism" substitutions are made. Helander and Nührenberg pointed out that quasi-isodynamic fields are another limit in which the problem of stellarator transport simplifies [17]. While these authors made important first steps, neoclassical theory in quasi-isodynamic fields has not been fully developed. In Chapt. 3, we further develop neoclassical theory in quasi-isodynamic plasmas, deriving several new results. The bootstrap current and parallel flow are found to resemble those in a quasi-poloidally symmetric plasma. The Pfirsch-Schlüter flow and current have a form which has no analogue in a quasisymmetric plasma, but which can be written concisely as an integral of B. In contrast to a quasisymmetric field, in a quasi-isodynamic field it is possible to calculate the radial electric field, and the result turns out to be largely independent of the details of the magnetic field.

The aforementioned calculations, as with the vast majority of neoclassical theory, em-

ploy an ordering in which the radial electric field is relatively small. More precisely, it is assumed that

$$|v_\parallel \mathbf{b} \cdot \nabla f| \gg |\mathbf{v}_\mathbf{E} \cdot \nabla f|, \tag{1.3}$$

where $\mathbf{v}_\mathbf{E} = cB^{-2}\mathbf{E}\times\mathbf{B}$ is the $\mathbf{E}\times\mathbf{B}$ drift, and we will refer to this ordering as the "small-E_r" regime. However, the approximation (1.3) is not always justified. The small-E_r ordering is particularly unrealistic in the HSX stellarator, for reasons which will be detailed in Chapt. 4. More generally, the radial electric field can have a significant effect on particle trajectories, thereby affecting the neoclassical properties of the plasma. To accurately determine the bootstrap current, which is particularly crucial for stellarators, "finite-E_r" effects need to be calculated by relaxing the ordering (1.3), allowing for larger E_r.

Such calculations are currently done in codes using a so-called monoenergetic approximation, in which ad-hoc changes are made to the E_r terms in order to enable rapid computation. Here we show that at least in a quasisymmetric plasma, this approximate treatment of E_r significantly distorts the particle orbits and leads to a systematic order-unity underestimation of the trapped particle fraction. These problems are related to the *collisionless* orbits and are therefore independent of other known problems arising from approximation of the collision operator.

For ideal quasisymmetric and quasi-isodynamic fields, new neoclassical expressions are derived in which this problematic monoenergetic approximation is avoided. In the quasisymmetric case, results are presented in both the banana regime and plateau regime for the ion flow, ion radial heat flux, and bootstrap current. The results resemble the conventional small-E_r expressions, but with a modified numerical coefficient for the ion temperature gradient terms. The bootstrap current is found to be enhanced. For the quasi-isodynamic case, new finite-E_r contributions to the distribution function are obtained. The flow and bootstrap current turn out to be modified by the same numerical function of E_r as in the quasisymmetric case.

The remaining chapters are organized as follows. In Chapt. 2 we give further background on quasisymmetry, and review the calculation of neoclassical transport in quasisymmetric plasmas when the radial electric field is small. Chapt. 3 presents the new neoclassical results for quasi-isodynamic stellarators with a small E_r. In Chapt. 4, we introduce the finite-E_r regime, and we explain the problem with previous calculations. Chapt. 5 and 6 present the new results for quasisymmetric and quasi-isodynamic stellarators with finite-E_r effects. We summarize and conclude in Chapt. 7. A number of noteworthy but technical issues are discussed in the appendices. Some of the work described herein has been published in references [29–31].

Throughout this thesis we will assume the magnetic field forms nested toroidal flux surfaces, ignoring the possibility of stochastic regions. Gaussian units are used throughout.

CHAPTER 2

Quasisymmetric stellarators

In this chapter we discuss quasisymmetric stellarators, the first of the two types of optimized stellarators analyzed in this thesis. We first motivate quasisymmetry using a novel coordinate-free approach. Discussions of quasisymmetry in the literature rely on magnetic coordinates and involve guiding-center drifts *parallel* to **B** or Lagrangian/Hamiltonian mechanics. These complexities are all avoided in the new approach given here in order to make the subject accessible to a wider audience. However, in this chapter we do also introduce Boozer coordinates, which allow us to give the more conventional definition of quasisymmetry. Boozer coordinates will also be used extensively in later chapters. Finally, we evaluate conventional (small-E_r) neoclassical transport in a quasisymmetric stellarator (demonstrating the isomorphism with axisymmetric systems) and we briefly discuss experiments.

2.1 Coordinate-free approach

2.1.1 Axisymmetry

To motivate quasisymmetry, it is instructive to first review some properties of axisymmetric plasmas, and in particular, the fact mentioned in the introduction that all particle orbits in an axisymmetric field are confined. For a charged particle moving in axisymmetric electromagnetic potentials, the canonical angular momentum $p_\phi = Rmv_\phi + ZeRA_\phi/c$ is conserved, where ϕ is the standard cylindrical angle, R is the major radius, Ze is the particle's charge, m is the mass, c is the speed of light, $v_\phi = R\mathbf{v}\cdot\nabla\phi$ is the toroidal component of the velocity, and A_ϕ is the toroidal component of the magnetic vector potential. Using $\psi_\mathrm{p} = -RA_\phi$, where $2\pi\psi_\mathrm{p}$ is the poloidal magnetic flux, it follows that

$$\hat{\Psi}_* = \psi_\mathrm{p} - \frac{mcRv_\phi}{Ze} \tag{2.1}$$

is conserved.

We now prove that all particle orbits in an axisymmetric field are confined to roughly a poloidal gyroradius $\rho_{\rm p} = \left(B/B_{\rm p}\right)\rho$ of a given flux surface, the result known as Tamm's theorem [3]. Here, $\rho = v/\Omega$ is the Larmor radius evaluated at the particle speed, $\Omega = ZeB/(mc)$ is the gyrofrequency, $B_{\rm p} = \sqrt{B_R^2 + B_z^2} = |\nabla\psi_{\rm p}|/R$ is the poloidal magnetic field, and we assume variation in the electrostatic potential is not too large so the speed v is nearly constant. First, consider that $|v_\phi|$ is bounded from above by v. The constancy of (2.1) then implies that the particle's radial coordinate $\psi_{\rm p}$ can only vary by $\sim mcRv/(Ze) = RB_{\rm p}\rho_{\rm p}$. As $\Delta\psi_{\rm p} \sim RB_{\rm p}\Delta r$ where Δr is the distance the particle departs from a given flux surface, then Δr is bounded from above by a distance $\sim \rho_{\rm p}$. Thus, as long as there is a poloidal field, all particle orbits are confined. This proof does not hold in a general stellarator because (2.1) only holds in axisymmetry.

Now suppose we want to find a quantity which is conserved by the *guiding-center* motion rather than by the exact particle motion. We first recall that any axisymmetric magnetic field can be written as $\mathbf{B} = \nabla\phi \times \nabla\psi_{\rm p} + I\nabla\phi$ where $I = RB_{\rm t}$ and $B_{\rm t} = R\mathbf{B}\cdot\nabla\phi$ is the toroidal field. It follows that

$$R^2B^2\nabla\phi = I\mathbf{B} - \mathbf{B}\times\nabla\psi_{\rm p} \tag{2.2}$$

and therefore

$$\hat{\Psi}_* = \psi_{\rm p} - \frac{Iv_\parallel}{\Omega} + \frac{\mathbf{v}_\perp\cdot\mathbf{b}\times\nabla\psi_{\rm p}}{\Omega}. \tag{2.3}$$

Here, $v_\parallel = \mathbf{v}\cdot\mathbf{b}$, $\mathbf{b} = \mathbf{B}/B$, and $\mathbf{v}_\perp = \mathbf{v} - v_\parallel\mathbf{b}$. The last term in (2.3) oscillates at the gyrofrequency about an average value of zero, whereas the other terms do not oscillate at the gyrofrequency to leading order. Since the guiding-center drifts are obtained by averaging over the gyromotion, it seems plausible that the quantity

$$\Psi_* = \psi_{\rm p} - \frac{Iv_\parallel}{\Omega} \tag{2.4}$$

will be conserved during motion of the guiding-center drifts.

To confirm rigorously that Ψ_* is indeed conserved, we will need to evaluate the total time derivative

$$\frac{d\Psi_*}{dt} = (v_\parallel\mathbf{b} + \mathbf{v}_{\rm d})\cdot\nabla\Psi_* \tag{2.5}$$

where the gradient holds the magnetic moment $\mu = v_\perp^2/(2B)$ and total energy $E = \left(v_\parallel^2/2\right) + \mu B + Ze\Phi/m$ fixed, and $\mathbf{v}_{\rm d}$ is the sum of the $\mathbf{E}\times\mathbf{B}$, ∇B, and curvature drifts:

$$\mathbf{v}_{\rm d} = \frac{c}{B^2}\mathbf{B}\times\nabla\Phi + \frac{v_\perp^2}{2\Omega B^2}\mathbf{B}\times\nabla B + \frac{v_\parallel^2}{\Omega B}\mathbf{B}\times\kappa \tag{2.6}$$

where $\kappa = \mathbf{b}\cdot\nabla\mathbf{b}$. It has been assumed for simplicity that $\mathbf{E} = -\nabla\Phi$, and we will also

assume the potential Φ is a flux function. As $\mathbf{b}\cdot\nabla\psi_{\rm p}=0$, then (2.5) can be written

$$\frac{d\Psi_*}{dt}=\mathbf{v}_{\rm d}\cdot\nabla\psi_{\rm p}+\upsilon_\parallel\mathbf{b}\cdot\nabla\left(\frac{I\upsilon_\parallel}{\Omega}\right)+\mathbf{v}_{\rm d}\cdot\nabla\left(\frac{I\upsilon_\parallel}{\Omega}\right). \tag{2.7}$$

Consider now that the two terms on the right-hand side of (2.4) are well separated in magnitude: estimating $\psi_{\rm p}\sim B_{\rm p}L^2$ for some scale-length L, and using $I\sim BL$, then

$$\frac{I\upsilon_\parallel/\Omega}{\psi_{\rm p}}\sim\frac{\rho_{\rm p}}{L}\ll 1 \tag{2.8}$$

where now $\rho_{\rm p}=(B/B_{\rm p})\upsilon_{\rm th}/\Omega$ is the *thermal* poloidal gyroradius. Similarly, the magnetic drifts in (2.5) are $\sim\rho/L$ smaller than the parallel motion term $\upsilon_\parallel\mathbf{b}$. The drifts (2.6) are derived assuming the $\mathbf{E}\times\mathbf{B}$ drift is comparable in magnitude to the magnetic drift speeds. Therefore, the last term in (2.7) is formally smaller than the others, so we will neglect it[1], leaving

$$\frac{d\Psi_*}{dt}\approx\mathbf{v}_{\rm d}\cdot\nabla\psi_{\rm p}-\upsilon_\parallel\mathbf{b}\cdot\nabla\left(\frac{I\upsilon_\parallel}{\Omega}\right). \tag{2.9}$$

Using the identity $\mathbf{B}\times\kappa\cdot\nabla\psi_{\rm p}=\mathbf{B}\times\nabla B\cdot\nabla\psi_{\rm p}$, we find the first right-hand-side term to be

$$\mathbf{v}_{\rm d}\cdot\nabla\psi_{\rm p}=\frac{2\upsilon_\parallel^2+\upsilon_\perp^2}{2\Omega B^2}\mathbf{B}\times\nabla B\cdot\nabla\psi_{\rm p}. \tag{2.10}$$

Next, we write $\upsilon_\parallel=\sqrt{2\left[E-\mu B-(Ze\Phi/m)\right]}$, so the last term in (2.9) can be evaluated using

$$-\upsilon_\parallel\mathbf{b}\cdot\nabla\left(\frac{\upsilon_\parallel}{\Omega}\right)=\frac{2\upsilon_\parallel^2+\upsilon_\perp^2}{2\Omega B^2}\mathbf{B}\cdot\nabla B. \tag{2.11}$$

In MHD equilibrium, I is a flux function so $\mathbf{b}\cdot\nabla I=0$. Finally, we take the ∇B component of (2.2) to find

$$I\mathbf{B}\cdot\nabla B=\mathbf{B}\times\nabla\psi_{\rm p}\cdot\nabla B. \tag{2.12}$$

Combining (2.9)-(2.12), a cancellation occurs, leaving $d\Psi_*/dt=0$ to leading order in ρ/L, as desired.

Notice that Tamm's theorem can be proven using the guiding-center conservation law (2.4) using the same reasoning we used earlier to prove the theorem from the true conservation law (2.1).

[1] It can actually be shown that $\mathbf{v}_{\rm d}\cdot\nabla(I\upsilon_\parallel/\Omega)$ is exactly zero, as shown in appendix B, but the proof requires that the guiding-center drift *parallel* to $\mathbf{b}$ be included in $\mathbf{v}_{\rm d}$. This subtlety concerning a formally negligible term is ignored here to make the present discussion accessible to a wider audience.

2.1.2 Quasisymmetry

Note that we did not need axisymmetry to derive (2.10) or (2.11). The proof of the conservation law for guiding-center motion above only used axisymmetry to derive (2.12), the fact that the ratio of $\mathbf{B} \times \nabla\psi_\mathrm{p} \cdot \nabla B$ to $\mathbf{B} \cdot \nabla B$ is the flux function I. Suppose we could find a *nonaxisymmetric* magnetic field in which a similar property held:

$$\frac{\mathbf{B} \times \nabla\psi_\mathrm{p} \cdot \nabla B}{\mathbf{B} \cdot \nabla B} = Y\left(\psi_\mathrm{p}\right) \tag{2.13}$$

for some flux function $Y\left(\psi_\mathrm{p}\right)$. Then we could use (2.10) and (2.11) to obtain

$$\frac{d\bar{\psi}_*}{dt} = 0 \tag{2.14}$$

to leading order in ρ/L where

$$\bar{\psi}_* = \psi_\mathrm{p} - \frac{Y v_\parallel}{\Omega} \tag{2.15}$$

and $d/dt = (v_\parallel \mathbf{b} + \mathbf{v}_\mathrm{d}) \cdot \nabla$ as in the axisymmetric case. Tamm's theorem then implies that all particle orbits in such a field are confined. (The proper component of B to use in place of B_p in Tamm's theorem is not immediately clear, but if all magnetic field components were estimated equally as $\sim B$, then particles could only drift $\sim \rho$ off a flux surface.) Such a field would therefore be omnigenous, and it should therefore exhibit reduced transport compared to a general stellarator.

We define quasisymmetry to be the property (2.13), which is equivalent to (1.2). It is shown in [32] that another equivalent definition of quasisymmetry is

$$\nabla B \times \nabla\psi_\mathrm{p} \cdot \nabla(\mathbf{B} \cdot \nabla B) = 0. \tag{2.16}$$

2.2 Properties of quasisymmetric plasmas

Axisymmetric fields are quasisymmetric due to (2.12). Garren and Boozer have shown that nonaxisymmetric fields can be exactly quasisymmetric only on isolated flux surfaces [33, 34]. However, in practice, nonaxisymmetric fields can be found which nearly satisfy (2.13) to a good approximation throughout the plasma [14, 15, 35, 36].

Although the quasisymmetry property (2.13) implies omnigenity, it turns out that omnigenous fields exist which are not quasisymmetric [9, 10]. Therefore quasisymmetry is a stricter condition than necessary for eliminating unconfined orbits. However, quasisymmetric fields are still desirable because they permit larger flow and flow shear than non-quasisymmetric omnigenous stellarators. This property can be understood in two ways. First, the flow in a nonaxisymmetric plasma can approach the ion thermal speed only in a quasisymmetric field [12]. Secondly, even when the flow speed is much lower than the ion thermal speed, in a general stellarator the flow is required to have a specific value, whereas

in a quasisymmetric field, the flow is not determined to leading order [37]. This flexibility permits both larger flows and larger flow shear. The possibility of larger flows and flow shear in a quasisymmetric device relative to non-quasisymmetric stellarators is important due to the effect of flows on instability and turbulent transport. Flows are understood to stabilize MHD modes [38]. Sheared flows are understood to break up turbulent eddies and thereby reduce cross-field transport [39]. Consequently, quasisymmetric stellarators should have not only reduced neoclassical transport compared to a non-optimized stellarator, but they may also have improved MHD stability and reduced turbulent transport.

The aforementioned property of quasisymmetric (and axisymmetric) plasmas that the flow is not automatically determined is known as "intrinsic ambipolarity." In a non-quasisymmetric stellarator, the ion and electron particle fluxes have differing dependencies on the radial electric field E_r. Therefore quasi-neutrality is established only for one or a small number of discrete values of E_r. Once E_r is thereby determined, the plasma flow is known. However, in quasisymmetric or axisymmetric plasmas, the ion and electron particle fluxes are always equal to each other to leading order, regardless of E_r. Consequently, it is not possible to solve for E_r by the requirement that the leading-order radial current be zero. In principle, an electric field could be calculated by finding higher-order corrections to the radial particle fluxes, but this procedure is too difficult to be practical.

2.3 Magnetic coordinates

2.3.1 General magnetic coordinates

In analyzing stellarators, both quasisymmetric and non-symmetric, it is useful to introduce "magnetic coordinates" θ and ζ. These quantities are defined to be poloidal and toroidal angle-like coordinates that satisfy the equation

$$\mathbf{B} = q\nabla\psi_{\mathrm{p}} \times \nabla\theta + \nabla\zeta \times \nabla\psi_{\mathrm{p}} \tag{2.17}$$

where $q\left(\psi_{\mathrm{p}}\right)$ is the safety factor, or equivalently,

$$\mathbf{B} = \nabla\psi_{\mathrm{t}} \times \nabla\theta + \iota\nabla\zeta \times \nabla\psi_{\mathrm{t}} \tag{2.18}$$

where $\iota(\psi_{\mathrm{t}}) = 1/q$ is the rotational transform. Here, "angle-like" means that θ increases by $2\pi k$ along any closed path which lies on a flux surface and which links the toroid k times in the poloidal direction, and ζ increases by $2\pi\ell$ along any closed path which lies on a flux surface and which links the toroid ℓ times in the toroidal direction. A proof that magnetic coordinates exist for any toroidal MHD equilibrium can be found in appendix C of [2]. From (2.17) it can be shown that field lines form straight lines in the (θ, ζ) plane.

The expressions (2.17) and (2.18) are known as the "contravariant" representations of $\mathbf{B}$. Another representation, known as the "covariant" form, can be obtained by decomposing the vector $\mathbf{B}$ in the $\nabla\psi_{\mathrm{p}}$, $\nabla\theta$, $\nabla\zeta$ basis: $\mathbf{B} = L\nabla\psi_{\mathrm{p}} + K\nabla\theta + I\nabla\zeta$. In general, the three coefficients L, K, and I will depend on all three coordinates $(\psi_{\mathrm{p}}, \theta, \zeta)$.

2.3.2 Boozer coordinates

Equation (2.17) does not uniquely determine the magnetic coordinates, and it turns out to be useful to introduce further constraints on the angles. The coordinates which will be used most in this and later chapters are "Boozer angles," which can be defined by the requirement that the K and I coefficients in the covariant representation be flux functions:

$$\mathbf{B} = L(\psi_{\rm p}, \theta, \zeta)\nabla\psi_{\rm p} + K(\psi_{\rm p})\nabla\theta + I(\psi_{\rm p})\nabla\zeta. \tag{2.19}$$

Appendix C of [2] gives a proof that Boozer coordinates can be constructed for any toroidal MHD equilibrium. In Boozer coordinates, the coefficients K and I acquire a physical meaning, which we now derive. From the rules of vector calculus in general coordinate systems (e.g. see pages 126-127 of [40] or the appendix of [41]) a differential step can be written

$$d\mathbf{r} = \frac{1}{\nabla\psi_{\rm p}\cdot\nabla\theta\times\nabla\zeta}\left[(\nabla\psi_{\rm p}\times\nabla\theta)d\zeta + (\nabla\theta\times\nabla\zeta)d\psi_{\rm p} + (\nabla\zeta\times\nabla\psi_{\rm p})d\theta\right]. \tag{2.20}$$

Now consider a loop at constant $\psi_{\rm p}$ and ζ, along which θ increases by 2π. Along this loop, then, $\mathbf{B}\cdot d\mathbf{r} = Kd\theta$, where we have used (2.19) and (2.20). It follows from Ampere's Law then that K equals $2/c$ times the toroidal current linked inside the flux surface. A similar argument using a constant-$\psi_{\rm p}$ constant-θ loop proves that I equals $2/c$ times the poloidal current linked outside the flux surface. (Some references on quasisymmetry instead use I to denote the $\nabla\theta$ coefficient. We choose the new convention because $RB_{\rm t}$ in an axisymmetric plasma is often denoted by I, as we have done in (2.2), and our I properly reduces to $RB_{\rm t}$ in axisymmetry.)

We can show that the terms in (2.19) are well separated in magnitude. First, observe that both currents in the plasma and in the external coils contribute to I, whereas only currents in the plasma contribute to K. Thus, typically $I \gg K$. Second, consider the limit of a vacuum field ($\mathbf{j} = 0$). In this case, the Ampere's Law argument above proves that $K \to 0$ and $I \to$ constant. It can also be shown that $L \to 0$ in this limit (if ζ is shifted by the proper flux function), so a vacuum field is described by $\mathbf{B} = I\nabla\zeta$ with I a constant.

In a substantial fraction of the stellarator literature, a different sub-class of magnetic coordinates called Hamada angles $(\theta_{\rm H}, \zeta_{\rm H})$ are used. These coordinates may be defined by the requirement that $\nabla\psi_{\rm p}\cdot\nabla\theta_{\rm H}\times\nabla\zeta_{\rm H}$ be a flux function. This definition turns out to be equivalent to the requirement $\nabla V\cdot\nabla\theta_{\rm H}\times\nabla\zeta_{\rm H} = 4\pi^2$, where V is the volume enclosed by a flux surface. Appendix C gives further discussion of Hamada coordinates and their relationship to quasisymmetry.

2.4 Quasisymmetry in Boozer coordinates

We now show that the definition of quasisymmetry (2.13) has a concise and equivalent definition in terms of the Boozer angles. The proof which follows is adapted from [37].

First, using (2.17) and (2.19), the quasisymmetry condition (2.13) can be written

$$I\frac{\partial B}{\partial \theta} - K\frac{\partial B}{\partial \zeta} = \left[q\frac{\partial B}{\partial \zeta} + \frac{\partial B}{\partial \theta}\right] Y. \tag{2.21}$$

Now consider a Fourier-decomposition of B,

$$B = \sum_{\tilde{M},\tilde{N}} \exp\left(i\left[\tilde{M}\theta - \tilde{N}\zeta\right]\right) B_{\tilde{M},\tilde{N}} \tag{2.22}$$

where the $B_{\tilde{M},\tilde{N}}$ are flux functions. Then (2.21) requires

$$\left(\tilde{N}K + \tilde{M}I + \left[\tilde{N}q - \tilde{M}\right] Y\right) B_{\tilde{M},\tilde{N}} = 0 \tag{2.23}$$

must be satisfied for every pair $\left(\tilde{M}, \tilde{N}\right)$. The quantity in parentheses in (2.23) can be zero only for a single value of the ratio $\tilde{M}/\tilde{N}$, so $B_{\tilde{M},\tilde{N}}$ can be nonzero only for a single value of $\tilde{M}/\tilde{N}$. It follows that

$$B = B\left(\psi_{\rm p},\ M\theta - N\zeta\right) \tag{2.24}$$

for some integers M and N. Thus, (2.13) implies (2.24).

We can also prove the converse. Suppose (2.24) is satisfied. Then

$$M\frac{\partial B}{\partial \zeta} = -N\frac{\partial B}{\partial \chi}. \tag{2.25}$$

It follows from (2.21) that (2.13) is then satisfied, with

$$Y = \frac{NK + MI}{M - Nq}. \tag{2.26}$$

Thus, (2.24) and (2.13) are two equivalent statements of quasisymmetry.

In the proof of section 2.1, we dropped a small term in going from (2.5) to (2.9). However, using Boozer coordinates it can be shown that this small term actually vanishes if we slightly redefine the conserved quantity and if we use a slightly different definition of the guiding-center drift:

$$\mathbf{v}_{\rm d} = (v_\parallel/\Omega)\nabla \times (v_\parallel \mathbf{b}), \tag{2.27}$$

where the curl is taken at fixed μ and total energy E. This form of the guiding center drifts is equivalent to (2.6) to leading order, but the two forms differ in a higher-order correction to the parallel velocity. In appendix B it is shown that with this new form of the drift, an exact constant of the motion is

$$\psi_* = \psi_{\rm h} - \frac{I_{\rm h} v_\parallel}{\Omega} \tag{2.28}$$

where

$$\psi_{\rm h} = M\psi_{\rm p} - N\psi_{\rm t} \tag{2.29}$$

and

$$I_{\rm h} = NK + MI. \tag{2.30}$$

This proof in the appendix also shows that the conservation law still holds if electrostatic potential varies in time and space, as long as the spatial variation has the same single helicity as B.

2.5 Quasisymmetry-axisymmetry isomorphism

In an axisymmetric field $B = B(\psi_{\rm p}, \Theta)$, where Θ is a poloidal angle (not necessarily the Boozer angle), we have seen that $\mathbf{B} \times \nabla\psi_{\rm p} \cdot \nabla B / \mathbf{B} \cdot \nabla B = I$. In a quasisymmetric field $B = B(\psi_{\rm p}, \chi)$, where

$$\chi = M\theta - N\zeta \tag{2.31}$$

is a helical angle, we have seen that $\mathbf{B} \times \nabla\psi_{\rm p} \cdot \nabla B / \mathbf{B} \cdot \nabla B = Y$, where Y is defined in (2.26). Due to the parallelism in these fundamental geometric relations, we might expect that other tokamak formulae may be applicable to a quasisymmetric stellarator if we make the replacements

$$\Theta \to \chi, \qquad I \to Y. \tag{2.32}$$

In fact, it turns out that all the important formulae for neoclassical transport in a quasisymmetric plasma can indeed be obtained by naive application of the substitutions (2.32) to the corresponding tokamak formulae. However, it turns out to be somewhat advantageous to take the fundamental isomorphism to be

$$\Theta \to \chi, \qquad I \to I_{\rm h}, \qquad \psi_{\rm p} \to \psi_{\rm h} \tag{2.33}$$

with $I_{\rm h}$ and $\psi_{\rm h}$ given in (2.29)-(2.30). The isomorphism (2.33) correctly implies $\mathbf{B} \times \nabla\psi_{\rm h} \cdot \nabla B / \mathbf{B} \cdot \nabla B = I_{\rm h}$, so it is at least equally valid to (2.32). However, (2.33) has the advantage that it gives the exact conserved quantity ψ_* for a quasisymmetric field, whereas (2.32) instead suggests the conserved quantity would be $\bar{\psi}_*$, and this latter quantity is conserved only to leading order rather than exactly. Both versions of the isomorphism give correct results for all neoclassical transport formulae.

As mentioned earlier, $I \gg K$, so if the symmetry is not quasi-poloidal (i.e. if $M \neq 0$), then it can be useful to approximate $I_{\rm h} \approx MI$.

The existence of the isomorphism was pointed out by Boozer in [28]. The isomorphism does not hold for all quantities, however. For example, classical transport does not obey the isomorphism rules [42]. To ascertain whether the isomorphism holds for a given quantity, therefore, care is required, and it must be rigorously shown that the equation(s) which determine the quantity in a quasisymmetric plasma are isomorphic to the equations which determine the quantity in an axisymmetric plasma. In the next section we sketch the proof that the isomorphism indeed holds for the conventional (low-flow) banana-regime neoclassical fluxes and flows.

2.6 Neoclassical transport in quasisymmetric plasmas

We begin with the drift kinetic equation $(\upsilon_\parallel \mathbf{b} + \mathbf{v}_\mathrm{d}) \cdot \nabla f = C$ (derived in e.g. [43]) for any particle species in a quasisymmetric plasma, using $(\psi_\mathrm{h}, \chi, \zeta)$ as the spatial coordinates. (For $M = 0$ quasi-poloidal symmetry, χ and ζ are degenerate, in which case θ could be substituted for ζ as the third coordinate throughout.) We make an ansatz that $(\partial f/\partial\zeta)_\chi = 0$, and the f we find will be consistent with this assumption. The leading order equation is taken to be $\upsilon_\parallel (\mathbf{b}\cdot\nabla\chi)\,\partial f_0/\partial\chi = C\{f_0\}$. The conventional entropy production argument then shows that f_0 is a Maxwellian and a flux function. The next order equation is then

$$\upsilon_\parallel (\mathbf{b}\cdot\nabla\chi)\frac{\partial f_1}{\partial\chi} + (\mathbf{v}_\mathrm{d}\cdot\nabla\psi_\mathrm{h})\frac{\partial f_0}{\partial\psi_\mathrm{h}} = C\{f_1\}. \tag{2.34}$$

Next, we apply the following identity (proven in appendix B):

$$\mathbf{v}_\mathrm{d}\cdot\nabla\psi_\mathrm{h} = \upsilon_\parallel\mathbf{b}\cdot\nabla\left(I_\mathrm{h}\upsilon_\parallel/\Omega\right) = \upsilon_\parallel(\mathbf{b}\cdot\nabla\chi)\frac{\partial}{\partial\chi}\left(I_\mathrm{h}\upsilon_\parallel/\Omega\right). \tag{2.35}$$

This result is what one would expect by naively applying the substitutions (2.32) to the corresponding identity for axisymmetry. We can then combine (2.34)-(2.35) as

$$\upsilon_\parallel(\mathbf{b}\cdot\nabla\chi)\frac{\partial g}{\partial\chi} = C\left\{g - \frac{I_\mathrm{h}\upsilon_\parallel}{\Omega}\frac{\partial f_0}{\partial\psi_\mathrm{h}}\right\} \tag{2.36}$$

where

$$g = f_1 + I_\mathrm{h}\upsilon_\parallel\Omega^{-1}\partial f_0/\partial\psi_\mathrm{h}. \tag{2.37}$$

A subsidiary expansion $g = g^{(0)} + g^{(1)} + ...$ is then made in the smallness of the right side of (2.36) compared to the left. The leading order equation is $\partial g^{(0)}/\partial\chi = 0$. The $g^{(1)}$ term in the next order equation is then annihilated by a transit average to give the constraint

$$0 = \overline{C\left\{g^{(0)} - I_\mathrm{h}\upsilon_\parallel\Omega^{-1}\partial f_0/\partial\psi_\mathrm{h}\right\}} \tag{2.38}$$

which determines $g^{(0)}$, thereby determining f_1. Here, the transit average of any quantity X is defined by

$$\overline{X} = \frac{\oint d\chi\, X/\left(\upsilon_\parallel\mathbf{b}\cdot\nabla\chi\right)}{\oint d\chi/\left(\upsilon_\parallel\mathbf{b}\cdot\nabla\chi\right)}. \tag{2.39}$$

For passing regions of (E,μ,ψ_h)-space (in which any χ is allowed), $\oint(\cdot)\,d\chi$ indicates $\int_0^{2\pi M}(\cdot)\,d\chi$. For trapped regions (in which not all χ are allowed), the integral $\oint(\cdot)\,d\chi$ denotes $\sum_\varsigma \varsigma\int_{\chi\mathrm{min}}^{\chi\mathrm{max}}(\cdot)\,d\chi$ where $\varsigma = \mathrm{sgn}(\upsilon_\parallel)$.

To justify our assumption that $\partial f/\partial\zeta = 0$, we need to show that neither $\mathbf{b}\cdot\nabla\chi$ nor C introduce ζ-dependence in $g^{(0)}$ through (2.38)-(2.39). First, by forming the product of (2.17) with (2.19) we find $\mathbf{B}\cdot\nabla\theta = B^2/(qI+K)$, so $\mathbf{b}\cdot\nabla\chi = B^{-1}(M-Nq)\,\mathbf{B}\cdot\nabla\theta$ is independent of ζ. Second, as argued in the footnote of [17], the linearized and gyro-averaged collision

operator only introduces spatial dependence through B, so no ζ-dependence is introduced. The pitch-angle scattering model operators have this same property. Thus, $g^{(0)}$ is independent of ζ, so f_1 is as well. The problem of finding f_1 in a 3D field has thereby become 2D if the field is quasisymmetric and the χ variable is used.

Equations (2.37)-(2.38) can be obtained by applying the substitutions (2.32) to the corresponding tokamak expressions, so f_1 can be obtained by these same substitutions. Forming $\int d^3v\, v_\parallel f_1$, then the parallel flows and currents obey the isomorphism as well. Finally, as shown in appendix D, the moment equations used to obtain the particle and heat fluxes from f_1 also obey the isomorphism. Thus, all the banana-regime neoclassical fluxes and flows follow the isomorphism. A similar argument shows that plateau-regime fluxes and flows do so as well.

Table 2.1 summarizes the isomorphism rules. Care must be taken in two regards. First, whereas in axisymmetric plasmas it is common to apply $\mathbf{b}\cdot\nabla\Theta \approx (qR_0)^{-1}$, it is not generally true that $\mathbf{b}\cdot\nabla\chi \approx (qR_0)^{-1}$ in a quasisymmetric stellarator. Second, tokamak calculations often use the model field magnitude $B = B_0\left[1 + 2\varepsilon\sin^2(\Theta/2)\right]$ with $\varepsilon = a/R_0$. In a stellarator, however, it will not generally be true that the relative field variation equals twice the inverse aspect ratio. We can use the expression $B = B_0\left[1 + 2\varepsilon\sin^2(\chi/2)\right]$ in stellarator calculations only if we understand the ε therein to be *defined* as $\left(\hat{B} - \check{B}\right)/\left(2\check{B}\right)$, where $\hat{B}$ and $\check{B}$ are the maximum and minimum of B on the flux surface respectively. Thus, the isomorphism substitutions must be made in tokamak expressions *before* either $\mathbf{b}\cdot\nabla\Theta \approx (qR_0)^{-1}$ or $\varepsilon = a/R_0$ are invoked.

Table 2.1: Axisymmetry- quasisymmetry isomorphism

	Axisymmetry	**Quasisymmetry**
Symmetry of B	$B = B\left(\psi_\mathrm{p}, \Theta\right)$	$B = B\left(\psi_\mathrm{h}, \chi\right)$
Angle on which B depends	Poloidal angle Θ	Helical angle $\chi = M\theta - N\zeta$
Radial coordinate	Poloidal flux ψ_p	Helical flux $\psi_\mathrm{h} = M\psi_\mathrm{p} - N\psi_\mathrm{t}$
B component flux function	$I = RB_\mathrm{t}$	$I_\mathrm{h} = NK + MI$
Conserved quantity	$\Psi_* = \psi_\mathrm{p} - Iv_\parallel/\Omega$	$\psi_* = \psi_\mathrm{h} - I_\mathrm{h}v_\parallel/\Omega$
Inverse connection length	$\mathbf{b}\cdot\nabla\Theta \approx 1/(qR)$	$\mathbf{b}\cdot\nabla\chi = (M - Nq)B/(qI + K)$
Relative B variation	$\varepsilon = a/R$	$\varepsilon = \left(\hat{B} - \check{B}\right)/\left(2\check{B}\right)$

2.7 Existence of quasisymmetric equilibria

Strictly speaking, toroidal equilibria with $M \neq 1$ symmetry are not possible for the following reason. On the magnetic axis, the pressure gradient vanishes, and so

$$0 = \mathbf{j} \times \mathbf{B} \propto (\nabla \times \mathbf{B}) \times \mathbf{B} = \kappa B^2 - \nabla_\perp (B^2/2). \tag{2.40}$$

In a toroidal device, the curvature of the axis κ cannot be zero everywhere, since the axis must close. Assuming B is nonzero, then (2.40) implies $\nabla_\perp B \neq 0$ on axis. Therefore, expanding $B(\psi_\mathrm{p}, \theta, \zeta)$ in distance from the axis $\sqrt{\psi_\mathrm{p}}$, the term that is linear in $\sqrt{\psi_\mathrm{p}}$ must have a $\sin(\theta - \theta_0(\zeta))$ component. Consequently, $M = 1$ harmonics must be present, and so symmetries with $M \neq 1$ cannot be realized exactly. However, in analyzing quasisymmetric systems it can still be useful to allow for the possibilities of $M \neq 1$ symmetries, since $M \neq 1$ symmetry can be approximately obtained away from the magnetic axis. For instance, the Quasi Poloidal Stellarator (QPS) which has been partially designed at Oak Ridge has an equilibrium with approximate $M = 0$ symmetry in almost all of the plasma volume [44].

In extrapolations to a power reactor, quasi-axisymmetric plasmas have an advantage over quasi-helically symmetric plasmas for the following reason. In an axisymmetric plasma, the B spectrum has a "toroidal" ($N = 0$, $M = 1$) harmonic associated with the approximate proportionality of B to $1/R$. To obtain a quasi-helically symmetric ($N \neq 0$) equilibrium, this toroidal harmonic must be canceled out. As the amplitude of the toroidal harmonic in an axisymmetric field increases with decreasing aspect ratio, quasi-helically symmetric equilibria tend to have large aspect ratio. Quasi-axisymmetric designs do not have the same minimum limit on the aspect ratio. In a power reactor, it is desirable to minimize the aspect ratio in order to minimize the reactor size, which in turn reduces the total reactor cost. Consequently, quasi-axisymmetry appears more promising than quasi-helical symmetry in a reactor-scale stellarator.

2.8 Experiments

The first identification of a non-axisymmetric equilibrium which was nearly quasisymmetric was in a numerical study by Nührenberg and Zille [14], published in 1988. This symmetry of this first equilibrium was $N = 6$, $M = 1$.

Inspired by this success, a similar optimization procedure was used to design the Helically Symmetric eXperiment (HSX) at the University of Wisconsin – Madison [15, 45]. HSX is currently the only operating quasisymmetric stellarator. The field of the device possesses ($N = 4, M = 1$) helical symmetry. HSX is equipped with a set of additional planar coils which can be energized to spoil the quasisymmetry, thereby allowing comparisons between quasisymmetric and non-symmetric plasmas which are otherwise similar. By inducing flows with biased probes and measuring the rate of flow decay when the probe potential is allowed to float, it has been demonstrated that damping of plasma flows is indeed reduced in the symmetric configuration compared to the asymmetric configuration

[46]. Also, the energy confinement has been measured to be significantly higher in the symmetric configuration compared to the asymmetric configuration [47].

In parallel with this development of quasi-helically symmetric stellarators, in 1996 Garabedian identified equilibria with quasi-axisymmetry [35, 36]. Quasi-axisymmetric equilibria were refined, leading to the design of the National Compact Stellarator eXperiment (NCSX) [16], which was to be built at the Princeton Plasma Physics Laboratory. The US Department of Energy terminated the construction of NCSX in 2008, citing construction delays and cost overruns, although fabrication of the nonplanar coils had already been completed. It remains to be seen whether a quasi-axisymmetric stellarator will be constructed.

CHAPTER 3

Quasi-isodynamic stellarators

In this chapter we discuss quasi-isodynamic stellarators, the second of the two types of optimized stellarators which will be analyzed in this thesis. Quasi-isodynamism is the design principle behind the W7-X stellarator, presently under construction at the Max Planck Institute for Plasma Physics in Greifswald, Germany. A quasi-isodynamic magnetic field can be defined as one which is both omnigenous and in which the constant-B contours close poloidally. After giving further background on the concept of quasi-isodynamism, we will next derive several geometric relations among the magnetic field components and the field strength in a quasi-isodynamic field. Using these relations, the forms of the flow and current will be obtained for arbitrary collisionality. The flow, radial electric field, and bootstrap current are then determined explicitly for the long-mean-free-path regime.

3.1 Introduction

The quasisymmetric fields discussed in the previous chapter have two desirable properties: all collisionless orbits are confined (omnigenity), and flows are not strongly damped. However, quasisymmetry places a strong constraint on the magnetic field geometry. It is therefore desirable to examine the larger design space of non-quasisymmetric fields which are still nearly omnigenous. Such fields would still have minimal neoclassical transport, but they would likely have somewhat larger turbulent transport compared to a quasisymmetric plasma.

We should first ask whether or not there *are* in fact any omnigenous fields which are non-quasisymmetric. This issue has been investigated by Cary and Shasharina [9, 10], and the answer is somewhat complicated. These authors showed that any analytic and perfectly omnigenous field *must* be quasisymmetric, but analytic fields can be constructed which are *nearly* omnigenous and yet are far from being quasisymmetric. Therefore, in practice a magnetic field can be omnigenous without being quasisymmetric.

Omnigenous fields have many remarkable mathematical and physical properties. For example, it is proven in [9] that the maximum and minimum of B are the same for each field line on a flux surface. In contrast to a general stellarator, the vanishing of the time-averaged radial drift implies that no $D \propto 1/\nu$ regime exists in a perfectly omnigenous device, where D is any radial transport coefficient and ν is the relevant collision frequency.

As the maximum and minimum of B on a flux surface form curves, rather than isolated points, these curves will close in one of three ways: toroidally, poloidally, or helically. A quasi-isodynamic field is an omnigenous field in which these constant-B curves close poloidally [17, 19–21]. Note that axisymmetric fields are not quasi-isodynamic since constant-B contours close toroidally.

In the analysis which follows, we will restrict our attention to quasi-isodynamic fields, rather than considering the more general case of omnigenous fields, for several reasons. Quasi-isodynamic fields are experimentally relevant, as the W7-X stellarator is designed to be approximately quasi-isodynamic [24**?**], and recent stellarator design studies have examined equilibria which are even closer to perfect quasi-isodynamism [20]. The reason these designs have emphasized quasi-isodynamic fields over other varieties of omnigenous fields is that quasi-isodynamism results in minimal bootstrap current. More precisely, it is proven in [17, 20] that in a quasi-isodynamic field, it is consistent to have zero toroidal current ($K = 0$ in the notation of (2.19)) and zero bootstrap current density $\langle j_\parallel B \rangle$. The minimization of the bootstrap current is desirable for two reasons. First, as the bootstrap current is proportional to the pressure gradient, then the magnetic field of a plasma with zero bootstrap current will remain optimized over a wide range of plasma pressures. Secondly, plasma currents can be a source of free energy to drive instability, so a plasma with zero bootstrap current should be generally more stable than a comparable plasma with large $\langle j_\parallel B \rangle$.

In contrast to quasisymmetric fields, in which neoclassical transport had been calculated previously [28, 48], neoclassical transport in quasi-isodynamic fields has not been fully explored. Some initial work was done by Helander and Nührenberg in [17]. These authors showed that the part of the long-mean-free-path- (banana) regime distribution function determined by the collisional constraint is found from an equation which is identical in form to the analogous equation for an axisymmetric plasma. However, several new results for quasi-isodynamic fields are obtained in the following sections.

In section 3.2, we give new derivations for some of the properties of quasi-isodynamic fields discussed in [17], and new expressions are also derived which relate the components of $\mathbf{B}$ to derivatives of B and of the Boozer angles. In section 3.3, we use these relations to derive novel expressions for the flow and current in a quasi-isodynamic field. It is shown that the distribution function obtained in [17] for the long-mean-free-path regime is consistent with these forms, but our forms of the flow and current are valid for all regimes of collisionality. In section 3.4, we use ambipolarity to determine the radial electric field in the long-mean-free-path regime. The bootstrap current is given in section 3.5, and we conclude in section 3.6. Emphasis is given throughout on practical calculations for a specified $B(\theta, \zeta)$, and the figures show an example calculation of the key quantities for a model field.

Although the field of any real stellarator will not be perfectly quasi-isodynamic, the re-

sults which follow are useful in several regards. A perfectly quasi-isodynamic model field can be provided as input to transport codes, so the results herein can be used to validate such codes. In addition, the flow, current, and radial electric field in a plasma which is approximately quasi-isodynamic can be expected to resemble the analytic forms derived here. Therefore, the results herein may give insight into the physics of W7-X-like stellarators.

3.2 Geometric properties of quasi-isodynamic fields

We begin by recalling the contravariant and covariant representations of the magnetic field in Boozer coordinates:

$$\mathbf{B} = \nabla\psi_\mathrm{t} \times \nabla\theta + q^{-1}\nabla\zeta \times \nabla\psi_\mathrm{t} \tag{3.1}$$

and

$$\mathbf{B} = I\nabla\zeta + K\nabla\theta + L\nabla\psi_\mathrm{p}, \tag{3.2}$$

where $2\pi\psi_\mathrm{t}$ is the toroidal flux, $cI(\psi_\mathrm{t})/2$ is the poloidal current linked outside the flux surface, $cK(\psi_\mathrm{t})/2$ is the toroidal current inside the flux surface, and $q(\psi_\mathrm{t})$ is the safety factor. We introduce the field line label $\alpha = \theta - q^{-1}\zeta$, so $\mathbf{B} = \nabla\psi_\mathrm{t} \times \nabla\alpha$. Let $\check{B}$ and $\hat{B}$ denote the minimum and maximum of B along a field line, respectively. Omnigenity requires that the most deeply trapped particles (those with $v_\parallel = 0$) have no radial drift, so if the electrostatic potential is a flux function, the radial ∇B drift $\propto \mathbf{B} \times \nabla B \cdot \nabla\psi_\mathrm{t}$ must vanish. As these particles also lie at $B = \check{B}$ where $\mathbf{B} \cdot \nabla B = 0$, then $\check{B}$ must be independent of field line ($\partial\check{B}/\partial\alpha = 0$). By considering the action of marginally trapped particles, it is proven in [9] that $\hat{B}$ must be independent of field line as well. As the range of allowed B is thus independent of α, and as a 2π increase in α at fixed B is a closed poloidal loop, it becomes convenient to use $(\psi_\mathrm{t},\ \alpha,\ B)$ as the spatial coordinates. However, specifying $(\psi_\mathrm{t},\ \alpha,\ B)$ does not uniquely determine a location on the flux surface – there are two possible locations in each magnetic well, one on either side of $\check{B}$ along the field line. We denote this discrete degree of freedom by $\gamma = \pm 1$, which Helander and Nührenberg term the *branch* [17].

In an omnigenous field, the longitudinal adiabatic invariant $J = \oint v_\parallel\, d\ell$ must be constant on a flux surface. This requirement implies [9]

$$\left(\frac{\partial}{\partial\alpha}\right)_B \sum_\gamma \frac{\gamma}{\mathbf{b} \cdot \nabla B} = 0, \tag{3.3}$$

a result which is termed the "Cary-Shasharina Theorem" in [17]. Here and throughout, subscripts on partial derivatives indicate quantities which are held fixed. A proof of (3.3) is given in appendix A. It is shown in [9] that (3.3) implies the contours of $B = \hat{B}$ are straight in Boozer coordinates. In a quasi-isodynamic field, the B contours close poloidally, and so $B = \hat{B}$ contours must be curves of constant ζ.

It is useful to express $\mathbf{B}$ in terms of its covariant components in the $(\psi_\mathrm{t},\ \alpha,\ B)$ coordinates:

$$\mathbf{B} = B_\psi \nabla\psi_\mathrm{t} + B_\alpha \nabla\alpha + B_B \nabla B. \tag{3.4}$$

From the dot product of this expression with $\mathbf{B} = \nabla\psi_\mathrm{t} \times \nabla\alpha$ we find

$$B_B = \frac{B^2}{\mathbf{B} \cdot \nabla B}. \tag{3.5}$$

The dot product of (3.4) with $\nabla\psi_\mathrm{t} \times \nabla B$ gives $B_\alpha = -\mathbf{B} \times \nabla\psi_\mathrm{t} \cdot \nabla B / \mathbf{B} \cdot \nabla B$, and the dot product of (3.4) with $\nabla\alpha \times \nabla B$ gives $B_\psi = \mathbf{B} \times \nabla\alpha \cdot \nabla B / \mathbf{B} \cdot \nabla B$.

We note that an incremental step can be written in the $(\psi_\mathrm{t},\, \alpha,\, B)$ coordinates as

$$d\mathbf{r} = \frac{1}{\mathbf{B} \cdot \nabla B} \left[(\nabla\alpha \times \nabla B)\, d\psi_\mathrm{t} + (\nabla B \times \nabla\psi_\mathrm{t})\, d\alpha + \mathbf{B} dB \right] \tag{3.6}$$

and in the $(\psi_\mathrm{t},\, \theta,\, \zeta)$ coordinates by

$$d\mathbf{r} = \frac{1}{\mathbf{B} \cdot \nabla\zeta} \left[(\nabla\theta \times \nabla\zeta)\, d\psi_\mathrm{t} + (\nabla\zeta \times \nabla\psi_\mathrm{t})\, d\theta + (\nabla\psi_\mathrm{t} \times \nabla\theta)\, d\zeta \right]. \tag{3.7}$$

By applying Ampere's law to a constant-B poloidal loop on a flux surface, and using (3.6) to write $\mathbf{B} \cdot d\mathbf{r} = B_\alpha d\alpha$ for this path, we find $\int_0^{2\pi} B_\alpha d\alpha = 2\pi K$, where $K(\psi_\mathrm{t})$ is the same quantity as in (3.2). It follows that [17]

$$B_\alpha = -\frac{\mathbf{B} \times \nabla\psi_\mathrm{t} \cdot \nabla B}{\mathbf{B} \cdot \nabla B} = K + \left(\frac{\partial h}{\partial \alpha} \right)_B \tag{3.8}$$

for some single-valued function h. As shown in section 2.1.2, $\mathbf{B} \times \nabla\psi_\mathrm{t} \cdot \nabla B / \mathbf{B} \cdot \nabla B$ is a flux function if and only if the field is quasisymmetric, so the $(\partial h/\partial\alpha)_B \to 0$ limit corresponds to quasisymmetry. More precisely, $(\partial h/\partial\alpha)_B \to 0$ corresponds to quasi-*poloidal* symmetry ($B = B(\psi_\mathrm{t},\, \zeta)$) since, by definition, B contours in a quasi-isodynamic field close poloidally.

Next, we use the fact that $(\nabla \times \mathbf{B}) \times \mathbf{B}$ is parallel to $\nabla\psi_\mathrm{t}$ in a scalar-pressure MHD equilibrium, so

$$0 = (\nabla \times \mathbf{B}) \cdot \nabla\psi_\mathrm{t} = \nabla \cdot (\mathbf{B} \times \nabla\psi_\mathrm{t}) = (\mathbf{B} \cdot \nabla B) \left[\left(\frac{\partial B_B}{\partial \alpha} \right)_B - \left(\frac{\partial B_\alpha}{\partial B} \right)_\alpha \right]. \tag{3.9}$$

Plugging in (3.5) and (3.8), we obtain the useful identity

$$\left(\frac{\partial}{\partial \alpha} \right)_B \frac{B^2}{\mathbf{B} \cdot \nabla B} = \frac{\partial^2 h}{\partial\alpha \partial B}. \tag{3.10}$$

Applying (3.3), then $\sum_\gamma \gamma\, \partial^2 h / \partial\alpha\partial B = 0$. The integral of this result from $\check{B}$ to B gives $\sum_\gamma \gamma\, (\partial h/\partial\alpha)_B = 0$, i.e. $(\partial h/\partial\alpha)_B$ must be branch-independent everywhere. In this integration, the contribution from the $\check{B}$ boundary has vanished because $\gamma = +1$ and $\gamma = -1$ refer to the same location there, so B_α is branch-independent there, and so $(\partial h/\partial\alpha)_B$ is branch-independent there as well. Although $(\partial h/\partial\alpha)_B$ must therefore be γ-independent everywhere, h itself may depend on the branch. However, consider the quantity $h_\Sigma =$

$[h(\gamma = 1) + h(\gamma = -1)]/2$. By applying $(\partial/\partial\alpha)_B$ to $h(\gamma) = h_\Sigma + \frac{1}{2}[h(\gamma) - h(-\gamma)]$, we then find $(\partial h/\partial\alpha)_B = (\partial h_\Sigma/\partial\alpha)_B$, so h could be replaced by h_Σ in (3.8), the equation which defined h. Thus, it is no loss in generality to assume h is branch-independent. This proof differs somewhat from the one given in [17], though the underlying principles are the same. In the sections which follow, we will only ever need $(\partial h/\partial\alpha)_B$ rather than h itself, so the calculation of h_Σ will not be necessary.

For completeness, we now present one additional relation which can be found for B_ψ. We use (3.4) to form

$$(\nabla \times \mathbf{B}) \times \mathbf{B} = (\mathbf{B} \cdot \nabla B)\left[\left(\frac{\partial B_\psi}{\partial B}\right)_\alpha - \left(\frac{\partial}{\partial \psi_\mathrm{t}}\right)_{\alpha,B}\left(\frac{B^2}{\mathbf{B}\cdot\nabla B}\right)\right]\nabla\psi_\mathrm{t}. \tag{3.11}$$

Then, from MHD equilibrium $4\pi\nabla p = (\nabla \times \mathbf{B}) \times \mathbf{B}$ it follows that

$$\left(\frac{\partial B_\psi}{\partial B}\right)_\alpha = \left(\frac{\partial}{\partial \psi_\mathrm{t}}\right)_{\alpha,B}\left(\frac{B^2}{\mathbf{B}\cdot\nabla B}\right) + \frac{4\pi}{\mathbf{B}\cdot\nabla B}\frac{dp}{d\psi_\mathrm{t}}. \tag{3.12}$$

We now relate the components of $\mathbf{B}$ in the $(\psi_\mathrm{t},\ \alpha,\ B)$ basis to the more familiar quantities θ and ζ. The results will be important in later sections for calculating the parallel flow and current. First, the dot product of (3.1) with (3.2) gives $\mathbf{B}\cdot\nabla\theta = B^2/(qI + K) = q^{-1}\mathbf{B}\cdot\nabla\zeta$, and it follows that

$$\frac{B^2}{\mathbf{B}\cdot\nabla B} = (qI + K)\left[\left(\frac{\partial B}{\partial\theta}\right)_\zeta + q\left(\frac{\partial B}{\partial\zeta}\right)_\theta\right]^{-1}. \tag{3.13}$$

Using $(\partial B/\partial\theta)_\alpha = (\partial B/\partial\theta)_\zeta + q\,(\partial B/\partial\zeta)_\theta$, then

$$\frac{B^2}{\mathbf{B}\cdot\nabla B} = (qI + K)\left(\frac{\partial\theta}{\partial B}\right)_\alpha = \frac{qI + K}{q}\left(\frac{\partial\zeta}{\partial B}\right)_\alpha. \tag{3.14}$$

Also, from (3.2) we can form

$$\mathbf{B}\times\nabla\psi_\mathrm{t}\cdot\nabla B = (\mathbf{B}\cdot\nabla\theta)\,q\left[I\left(\frac{\partial B}{\partial\theta}\right)_\zeta - K\left(\frac{\partial B}{\partial\zeta}\right)_\theta\right]. \tag{3.15}$$

Plugging this result into (3.8) we obtain

$$\left(\frac{\partial h}{\partial\alpha}\right)_B = -(qI + K)\left(\frac{\partial B}{\partial\theta}\right)_\zeta\left[\left(\frac{\partial B}{\partial\theta}\right)_\zeta + q\left(\frac{\partial B}{\partial\zeta}\right)_\theta\right]^{-1}. \tag{3.16}$$

Using $(\partial B/\partial\theta)_\zeta = (\partial B/\partial\theta)_\alpha + (\partial B/\partial\alpha)_\theta$, then (3.16) implies

$$\left(\frac{\partial h}{\partial\alpha}\right)_B = (qI + K)\left[\left(\frac{\partial\theta}{\partial\alpha}\right)_B - 1\right] = \frac{qI + K}{q}\left(\frac{\partial\zeta}{\partial\alpha}\right)_B \tag{3.17}$$

where we have used

$$0 = \left(\frac{\partial B}{\partial \theta}\right)_B = \left(\frac{\partial B}{\partial \theta}\right)_\alpha + \left(\frac{\partial \alpha}{\partial \theta}\right)_B \left(\frac{\partial B}{\partial \alpha}\right)_\theta . \tag{3.18}$$

Comparing (3.14) and (3.17), it is evident that (3.10) is satisfied. Equations (3.16) and (3.17) will be needed for computations in section 3.

As the $B = \hat{B}$ contours are constant-ζ curves, then $(\partial\zeta/\partial\alpha)_B = 0$ along these contours. Equation (3.17) then implies $(\partial h/\partial\alpha)_B \to 0$ along these contours as well.

Let $\Delta\zeta(B) = \sum_\gamma \gamma \int_{\check{B}}^{B} (\partial\zeta'/\partial B')_\alpha \, dB'$ be the difference in ζ between the two points of field magnitude B on either side of $\check{B}$, where $\zeta' = \zeta(B')$. By (3.14) and (3.3),

$$(\partial(\Delta\zeta)/\partial\alpha)_B = 0 \tag{3.19}$$

for a quasi-isodynamic field. In section IV of [9], Cary and Shasharina give a procedure to construct a function $B(\theta, \zeta)$ with the property (3.19) and with $\hat{B}$ straight in Boozer coordinates. This construction is reviewed briefly in appendix E since we will use it to obtain the figures. Differentiating (3.19), then

$$\sum_\gamma \gamma \frac{\partial^2 \zeta}{\partial\alpha \partial B} = 0 \tag{3.20}$$

which, due to (3.14), implies (3.3). Thus, any field generated by the Cary-Shasharina construction will be quasi-isodynamic, in the sense that all the properties described in this section will apply. For example, $(\partial h/\partial\alpha)_B$ can be calculated from (3.16), and the result will automatically be branch-independent. (This last fact can also be seen by integrating (3.20) from $\check{B}$ and using (3.17).)

Figure 3-1 shows a quasi-isodynamic field generated using the Cary-Shasharina construction, with parameters specified in appendix E. The property (3.19) is illustrated in figure 3-1 by the fact that the two thick line segments, both of which are parallel to the field lines, have the same $\Delta\zeta$. Figure 3-2 shows $(\partial h/\partial\alpha)_B$ which is calculated for this field using (3.16).

3.3 Parallel flows and current

3.3.1 General collisionality case

We now derive the form of the equilibrium flow for any particle species in a quasi-isodynamic field. We assume the species density n, pressure p, and electrostatic potential Φ are all flux functions to leading order. The perpendicular flow is given to leading order by the sum of the $\mathbf{E} \times \mathbf{B}$ and diamagnetic flows: $\mathbf{V}_\perp = \omega B^{-2} \mathbf{B} \times \nabla\psi_t$, where $\omega(\psi_t) = c(d\Phi/d\psi_t) + c(dp/d\psi_t)/(Zen)$ and Ze is the species charge. Writing the total flow as

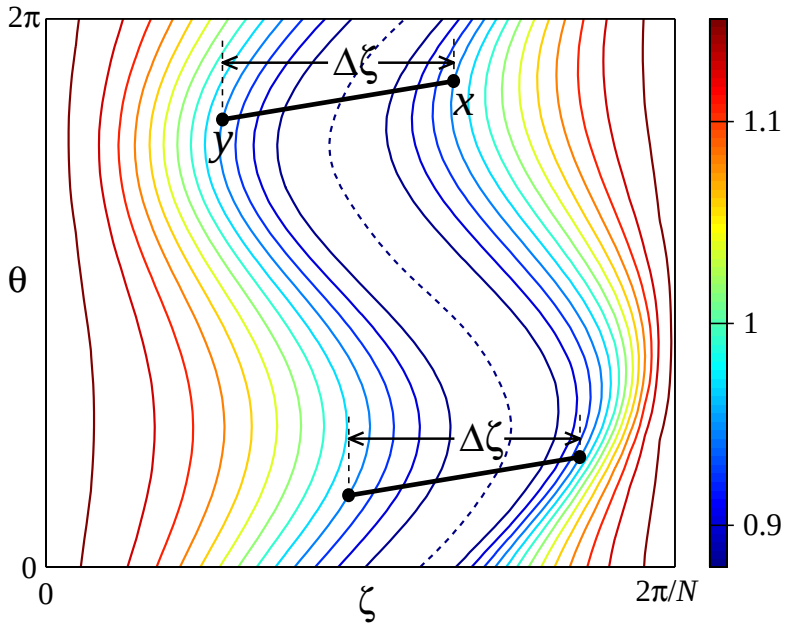

Figure 3-1: Contours of the normalized magnetic field magnitude $b = B/\left\langle B^2\right\rangle^{1/2}$ for the model quasi-isodynamic field specified in appendix E. The dashed contour indicates $\check{B}/\left\langle B^2\right\rangle^{-1} = 0.88$, and $\hat{B}/\left\langle B^2\right\rangle^{-1} = 1.15$ occurs at the left and right edges. The two thick line segments, which are parallel to field lines, illustrate the property (3.19). Points x and y refer to the analysis preceding (E.3).

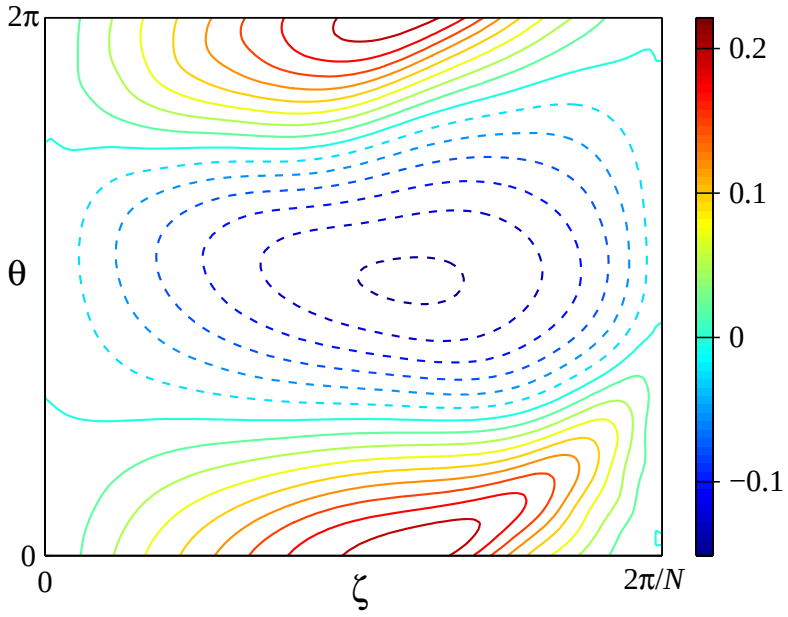

Figure 3-2: The normalized departure from quasisymmetry $q\,(qI + K)^{-1}\,(\partial h/\partial\alpha)_B$, calculated for the model field of figure 3-1 using (3.16). Dashed contours are negative.

$\mathbf{V} = \mathbf{V}_\perp + V_\parallel B^{-1}\mathbf{B}$, then from the mass conservation relation $\nabla\cdot(n\mathbf{V}) = 0$ we can write

$$\mathbf{B}\cdot\nabla\left(\frac{V_\parallel + \omega U}{B}\right) = 0 \tag{3.21}$$

where U is defined to be a single-valued and continuous solution of

$$\mathbf{B}\cdot\nabla\,(U/B) = \mathbf{B}\times\nabla\psi_\mathrm{t}\cdot\nabla\left(1/B^2\right). \tag{3.22}$$

The solvability condition of (3.22) is satisfied for any scalar-pressure MHD equilibrium. Applying (3.8), we find

$$\left(\frac{\partial\,(U/B)}{\partial B}\right)_\alpha = \frac{2}{B^3}\left[K + \left(\frac{\partial h}{\partial\alpha}\right)_B\right]. \tag{3.23}$$

Integrating in B,

$$Y = \frac{U}{B} + \frac{K + \Upsilon}{B^2} \tag{3.24}$$

where Y is the integration constant, and

$$\Upsilon\,(\psi_\mathrm{t},\,\alpha,\,B) = 2B^2\int_B^{\hat{B}}\frac{dB'}{B'^3}\left(\frac{\partial h'}{\partial\alpha}\right)_B. \tag{3.25}$$

Again, primes indicate a quantity indicate it is evaluated using the dummy integration variable B' rather than using the local value of B. We will see the quantity Υ appears repeatedly in the analysis of quasi-isodynamic fields.

While Y is by definition independent of B, additional work is required to show that Y is also independent of α and γ, which we do as follows. At $B = \check{B}$, both signs of γ refer to the same location, so U is γ-independent there. Consequently the entire right-hand side of (3.24) is γ-independent at $B = \check{B}$, so Y must be γ-independent. Next, the right-hand side of (3.24) is continuous across the curve $B = \hat{B}$ when θ is held fixed. Therefore Y must have this same property, implying $Y(\alpha) = Y(\alpha + 2\pi/(qN))$ for all α, where again N is the number of identical stellarator cells. It follows that Y must be independent of α, and therefore Y is a flux function. Had $\check{B}$ been chosen as the limit of integration in (3.25) instead of $\hat{B}$, then the right-hand side of (3.24) would not be continuous across the curve $B = \hat{B}$ when θ is held fixed, and so Y would need to depend on α.

We choose to specify Y by requiring $\langle UB \rangle = 0$, where the brackets denote a flux surface average. For any quantity Q, this average is

$$\langle Q \rangle = \frac{\displaystyle\sum_\gamma \gamma \int_{\check{B}}^{\hat{B}} dB \int_0^{2\pi} d\alpha \frac{Q}{\mathbf{B}\cdot\nabla B}}{\displaystyle\sum_\gamma \gamma \int_{\check{B}}^{\hat{B}} dB \int_0^{2\pi} d\alpha \frac{1}{\mathbf{B}\cdot\nabla B}}. \tag{3.26}$$

Note that $\langle \Upsilon \rangle = 0$, since the α integral can be performed by parts, and (3.3) applied. We thereby obtain

$$U = -\frac{1}{B}\left[\left(1 - \frac{B^2}{\langle B^2 \rangle}\right) K + \Upsilon\right]. \tag{3.27}$$

Next, it follows from (3.21) that $V_\parallel B + \omega U B = B^2 A$ for some flux function $A(\psi_t)$. Flux-surface-averaging this equation to find A, we obtain our final form for the parallel flow of each species in a quasi-isodynamic field:

$$V_\parallel = \frac{B\langle V_\parallel B\rangle}{\langle B^2\rangle} + V_\parallel^{\mathrm{PS}}, \tag{3.28}$$

where the "Pfirsch-Schlüter flow" is

$$V_\parallel^{\mathrm{PS}} = \frac{c}{B}\left(\frac{d\Phi}{d\psi_t} + \frac{1}{Zen}\frac{dp}{d\psi_t}\right)\left[\left(1 - \frac{B^2}{\langle B^2\rangle}\right)K + \Upsilon\right] \tag{3.29}$$

and satisfies $\left\langle V_\parallel^{\mathrm{PS}} B \right\rangle = 0$. For $(\partial h/\partial\alpha)_B \to 0$, then $\Upsilon \to 0$, and (3.29) reduces properly to the result for a quasi-poloidally symmetric field.

The parallel current has a similar form to (3.28)-(3.29), which can be obtained by mul-

tiplying these equations by Zen and summing over species. The result is

$$j_\parallel = \frac{B\left\langle j_\parallel B\right\rangle}{\left\langle B^2\right\rangle} + j_\parallel^{\mathrm{PS}}, \tag{3.30}$$

where the "Pfirsch-Schlüter current" is

$$j_\parallel^{\mathrm{PS}} = \frac{c}{B}\left(\frac{dp_{\mathrm{tot}}}{d\psi_{\mathrm{t}}}\right)\left[\left(1-\frac{B^2}{\left\langle B^2\right\rangle}\right)K + \Upsilon\right] \tag{3.31}$$

and satisfies $\left\langle j_\parallel^{\mathrm{PS}} B\right\rangle = 0$, and p_{tot} is the sum of the pressures of each species.

We emphasize that (3.28)-(3.31) are valid in a quasi-isodynamic stellarator at arbitrary collisionality.

3.3.2 Long-mean-free-path regime

We now show that the distribution function obtained in [17] for the long-mean-free-path regime indeed gives a flow of the form (3.28)-(3.29). The distribution function obtained in that reference was

$$f = f_0 - f_0\frac{e\Phi_1}{T} + g + K\frac{\upsilon_\parallel}{\Omega}\frac{\partial f_0}{\partial\psi_{\mathrm{t}}} - \frac{cm}{Ze}\int_B^{B_x} dB'\left(\frac{\partial h'}{\partial\alpha}\right)_{B'}\frac{\partial}{\partial B'}\frac{\upsilon_\parallel'}{B'}\frac{\partial f_0}{\partial\psi_{\mathrm{t}}} \tag{3.32}$$

where f_0 is a stationary Maxwellian flux function, $\Phi_1\left(\psi_{\mathrm{t}},\,\theta,\,\zeta\right)$ is the next-order correction to the potential, and $\Omega = ZeB/\left(mc\right)$ is the gyrofrequency. The $\partial/\partial\psi_{\mathrm{t}}$ derivatives and the B' integral are performed holding the leading-order energy $\upsilon^2/2 + Ze\Phi/m$ and the magnetic moment $\upsilon_\perp^2/2B$ fixed. Also,

$$B_x = \begin{cases} \hat{B} & \text{if } \lambda < \check{B}/\hat{B} \\ \check{B}/\lambda & \text{if } \lambda > \check{B}/\hat{B}, \end{cases} \tag{3.33}$$

where $\lambda = \upsilon_\perp^2\check{B}/\left(\upsilon^2 B\right)$, and g is a flux function which vanishes for trapped particles. Applying $\int d^3\upsilon\,\upsilon_\parallel$ to (3.32) gives

$$\begin{aligned} nV_\parallel \;=\; & X + \frac{cnK}{B}\left(\frac{d\Phi}{d\psi_{\mathrm{t}}} + \frac{1}{Zen}\frac{dp}{d\psi_{\mathrm{t}}}\right) \\ & -\frac{cm}{Ze}\int d^3\upsilon\,\upsilon_\parallel f_0\left[\frac{1}{p}\frac{dp}{d\psi_{\mathrm{t}}} + \frac{Ze}{T}\frac{d\Phi}{d\psi_{\mathrm{t}}} + \left(\frac{m\upsilon^2}{2T}-\frac{5}{2}\right)\frac{1}{T}\frac{dT}{d\psi_{\mathrm{t}}}\right]\int_B^{B_x} dB'\left(\frac{\partial h'}{\partial\alpha}\right)_{B'}\frac{\partial}{\partial B'}\frac{\upsilon_\parallel'}{B'} \end{aligned} \tag{3.34}$$

where $X = \int d^3\upsilon\,\upsilon_\parallel g$. We can write $X = (B/\check{B})\pi\sum_\varsigma \varsigma\int_0^\infty d\upsilon\,\upsilon^3\int_0^{\check{B}/\hat{B}} d\lambda\, g$, where $\varsigma = \mathrm{sgn}\left(\upsilon_\parallel\right)$, and the upper limit of the λ integral is changed from $\check{B}/B$ to $\check{B}/\hat{B}$ since g is zero for trapped particles. As g is a flux function at fixed υ and λ, then $X \propto B$, so X has the form of the $B\left\langle V_\parallel B\right\rangle / \left\langle B^2\right\rangle$ term in (3.28). Finally, we evaluate the last line of (3.34), obtaining

as a first step

$$\int d^3v\, v_\parallel f_0 \int_B^{B_x} dB' \left(\frac{\partial h'}{\partial \alpha}\right)_{B'} \frac{\partial}{\partial B'} \frac{v'_\parallel}{B'} = -\frac{3nTB}{4m\check{B}} \int_0^{\check{B}/B} d\lambda \int_B^{B_x} dB' \left(\frac{\partial h'}{\partial \alpha}\right)_{B'} \frac{\left(2-\lambda B'/\check{B}\right)}{B'^2\sqrt{1-\lambda B'/\check{B}}}. \tag{3.35}$$

The contribution from the $dT/d\psi_t$ term in (3.34) vanishes in the v integration. We now switch the order of the λ and B' integrations, so B' ranges over $\left(B,\, \hat{B}\right)$ and λ ranges over $\left(0,\, \check{B}/B'\right)$. The λ integral can then be evaluated, giving precisely the Υ term in (3.29). Thus, the flow associated with the distribution (3.32) indeed has the form (3.28)-(3.29).

As described in [17], the g component of the distribution function for passing particles is computed from the constraint $\langle (B/v_\parallel)\, C\rangle = 0$, where C is the collision operator. If we consider the ions in a pure plasma, we can explicitly calculate g_i and X using the standard momentum-conserving model operator

$$C_i = \nu\mathcal{L}\left\{f_{i1} - f_{i0}\frac{m_i u v_\parallel}{T_i}\right\} \tag{3.36}$$

where

$$\mathcal{L} = \frac{2v_\parallel \check{B}}{v^2 B}\frac{\partial}{\partial\lambda}\lambda v_\parallel \frac{\partial}{\partial\lambda} \tag{3.37}$$

is the pitch-angle scattering operator,

$$u = \left[\int d^3v\, f_{i0}\frac{m_i v^2}{3T_i}\nu\right]^{-1} \int d^3v\, f_{i1}\nu v_\parallel, \tag{3.38}$$

$$\nu = \frac{2\pi Z^4 e^4 n_i \ln\Lambda}{\sqrt{2m_i}T_i^{3/2}} \frac{[\mathrm{erf}\,(x) - \Psi(x)]}{x^3}, \tag{3.39}$$

$\Psi(x) = [\mathrm{erf}\,(x) - x\,(d\,\mathrm{erf}\,(x)/dx)]/\left(2x^2\right)$, $\mathrm{erf}\,(x) = \left(2/\sqrt{\pi}\right)\int_0^x \exp\left(-t^2\right)dt$ is the error function, and $x = v/\sqrt{2T_i/m_i}$. The analysis then closely resembles the standard tokamak calculation [8], giving

$$g_i = -f_{i0}\frac{Km_i c}{ZeT_i}\frac{dT_i}{d\psi_t}\left[\frac{m_i v^2}{2T_i} - 1.33\right]\frac{\varsigma v}{2\check{B}} H \int_\lambda^{\check{B}/\hat{B}} \frac{d\lambda'}{\left\langle\sqrt{1-\lambda' B/\check{B}}\right\rangle} \tag{3.40}$$

where $H = H\left(\check{B}/\hat{B} - \lambda\right)$ is a Heavyside function which is 1 for passing particles and 0 for trapped particles. The final expression for the parallel ion flow in the long-mean-free-path regime becomes

$$V_{i\parallel} = -1.17 f_c \frac{KcB}{Ze\langle B^2\rangle}\frac{dT_i}{d\psi_t} + \frac{c}{B}\left(\frac{d\Phi}{d\psi_t} + \frac{1}{Zen_i}\frac{dp_i}{d\psi_t}\right)(K+\Upsilon) \tag{3.41}$$

where the effective fraction of circulating particles

$$f_c = \frac{3}{4}\frac{\left\langle B^2\right\rangle}{\check{B}^2}\int_0^{\check{B}/\hat{B}}\frac{\lambda\, d\lambda}{\left\langle\sqrt{1-\lambda B/\check{B}}\right\rangle} \tag{3.42}$$

is approximately one if the variation in B is small. As expected, (3.41) has the form (3.28)-(3.29).

Notice that the distribution function (3.32) was derived in [17] only for the long-mean-free-path regime, whereas the general form of the flow (3.28)-(3.29) was derived here without any assumption about the collisionality.

3.3.3 Computation of geometric integral

For any particular quasi-isodynamic field, the Υ quantity (3.25) which appears in the Pfirsch-Schlüter flow (3.29) and Pfirsch-Schlüter current (3.31) can be evaluated numerically in a number of ways. One approach is to use (3.17) to write

$$\Upsilon = 2B^2\frac{qI+K}{q}\int_B^{\hat{B}}\frac{dB'}{B'^3}\left(\frac{\partial\zeta'}{\partial\alpha}\right)_{B'}. \tag{3.43}$$

The function $\zeta(\alpha, B)$ can be computed from a given field $B(\theta, \zeta)$ or specified directly. The integrand in (3.43) can then be computed, the integral evaluated, and if desired, the result mapped to (θ, ζ) coordinates. Figure 3-3 shows Υ computed using this method for the model field of figure 3-1.

In an alternative approach, we begin by transforming (3.25) as follows:

$$\Upsilon = -2B^2\int_{\zeta_x}^{\zeta}\frac{d\zeta'}{B'^3}\left(\frac{\partial B'}{\partial\zeta'}\right)_\alpha\left(\frac{\partial h'}{\partial\alpha}\right)_{B'} = -\frac{2B^2}{q}\int_{\zeta_x}^{\zeta}\frac{d\zeta'}{B'^3}\left[\left(\frac{\partial B'}{\partial\theta'}\right)_{\zeta'}+q\left(\frac{\partial B'}{\partial\zeta'}\right)_{\theta'}\right]\left(\frac{\partial h'}{\partial\alpha}\right)_{B'}. \tag{3.44}$$

For points between $\check{B}$ and $\zeta = 0$, the integration bound ζ_x is 0, and for points on the other side of $\check{B}$, $\zeta_x = 2\pi/N$, where again N is the number of toroidal periods of the stellarator (i.e. the number of $\hat{B}$ or $\check{B}$ curves). Applying (3.16), then

$$\Upsilon = 2B^2\frac{qI+K}{q}\int_{\zeta_x}^{\zeta}\frac{d\zeta'}{B'^3}\left(\frac{\partial B'}{\partial\theta'}\right)_{\zeta'}. \tag{3.45}$$

This expression can also be obtained from (3.43) using (3.18), with θ replaced by ζ in the latter. Depending on the particular application, either the form (3.43) or (3.45) for Υ may be more convenient to evaluate.

Notice that the integrals throughout this section are performed along constant-α paths.

As the right-hand side of (3.25) is branch-independent, then the integrals in (3.43) and (3.45) must be so as well. These integrals can still be computed for a $B(\theta, \zeta)$ which is not quasi-isodynamic, but the result will be discontinuous at $B = \check{B}$. For a *nearly* quasi-

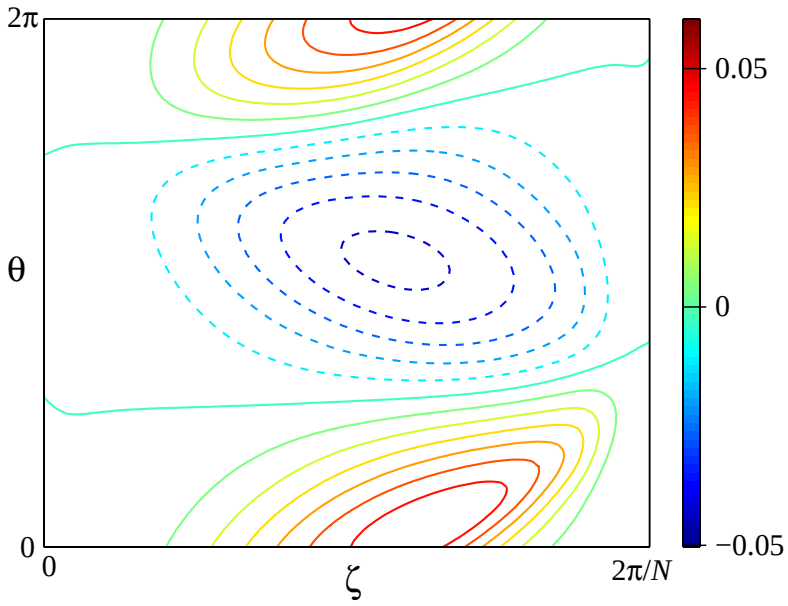

Figure 3-3: Contours of the dimensionless quantity $\Upsilon q/(qI + K)$, where Υ appears in the parallel flow and current and is defined in (3.25). The calculation is performed for the model field of figure 3-1 using (3.43). Dashed contours are negative.

isodynamic $B(\theta, \zeta)$, such as the one obtained in [9, 10] by Fourier-filtering a perfectly quasi-isodynamic field, the discontinuity in Υ is small.

3.4 Particle flux and radial electric field

We now derive an expression for the radial flux of each particle species at any collisionality. The neoclassical part of the flux is

$$\langle \mathbf{\Gamma} \cdot \nabla \psi_t \rangle = \left\langle \int d^3 v \, f \mathbf{v}_d \cdot \nabla \psi_t \right\rangle \tag{3.46}$$

where $\mathbf{v}_d = (v_\parallel/\Omega)\nabla \times (v_\parallel \mathbf{b})$ is the drift velocity. As in section 3.3.2, derivatives throughout this section will hold the leading-order energy $v^2/2 + Ze\Phi/m$ and the magnetic moment $v_\perp^2/2B$ fixed. It can be shown using (3.8) that $\mathbf{v}_d \cdot \nabla \psi_t = v_\parallel \mathbf{b} \cdot \nabla \Delta$ where

$$\Delta = -K \frac{v_\parallel}{\Omega} + S \tag{3.47}$$

and

$$S = \int_B^{B_x} dB' \left(\frac{\partial h'}{\partial \alpha} \right)_{B'} \frac{\partial}{\partial B'} \frac{v_\parallel'}{\Omega'}. \tag{3.48}$$

Using

$$\int d^3\upsilon\,(\ \cdot\ ) = \pi\frac{B}{\check{B}}\sum_{\varsigma}\varsigma\int_0^\infty \upsilon^2 d\upsilon\int_0^{\check{B}/B}\frac{d\lambda}{\sqrt{1-\lambda B/\check{B}}}\,(\ \cdot\ ) \tag{3.49}$$

and the fact that $\langle \mathbf{B}\cdot\nabla Q\rangle = 0$ for any single-valued Q, we find

$$\langle \boldsymbol{\Gamma}\cdot\nabla\psi_{\rm t}\rangle = \left\langle \int d^3\upsilon\, f\upsilon_\parallel \mathbf{b}\cdot\nabla\Delta\right\rangle = -\left\langle\int d^3\upsilon\,\upsilon_\parallel\Delta\mathbf{b}\cdot\nabla f\right\rangle. \tag{3.50}$$

In the last equation we have also used the fact that $\Delta = 0$ at $\lambda = \check{B}/B$. Substituting in the drift kinetic equation

$$\upsilon_\parallel\mathbf{b}\cdot\nabla f + \mathbf{v}_{\rm d}\cdot\nabla\psi_{\rm t}\frac{\partial f_0}{\partial\psi_{\rm t}} = C \tag{3.51}$$

where C is the collision operator, we then obtain

$$\langle \boldsymbol{\Gamma}\cdot\nabla\psi_{\rm t}\rangle = -\left\langle\int d^3\upsilon\,\Delta C\right\rangle. \tag{3.52}$$

We now specialize to the case of the ion flux in a pure plasma, so ion collisions with electrons and the radial electron particle flux can be ignored to leading order in $\sqrt{m_{\rm e}/m_{\rm i}}$. We also specialize to the long-mean-free-path collisionality regime. The model collision operator (3.36) is again employed. This operator is constructed to have the momentum conservation property $\int d^3\upsilon\,\upsilon_\parallel C = 0$, so (3.52) can be written

$$\langle \boldsymbol{\Gamma}_{\rm i}\cdot\nabla\psi_{\rm t}\rangle = -\left\langle\int d^3\upsilon\, S\nu\mathcal{L}\left\{-\Delta\frac{\partial f_{\rm i0}}{\partial\psi_{\rm t}} + g_{\rm i} - f_{\rm i0}\frac{m_{\rm i}u\upsilon_\parallel}{T_{\rm i}}\right\}\right\rangle \tag{3.53}$$

where we have applied the distribution function (3.32).

We next make use of the property $\langle(\partial Q/\partial\alpha)_B\rangle = 0$ for any branch-independent Q. This property follows from (3.26) and (3.10) if an integration by parts is performed in α. It follows that any terms in (3.53) which are linear in $(\partial h/\partial\alpha)_B$ will vanish. For example, $g_{\rm i}$ is a flux function and so it does not contribute to (3.53). We group the nonvanishing terms into two pieces as follows:

$$\langle \boldsymbol{\Gamma}_{\rm i}\cdot\nabla\psi_{\rm t}\rangle = \Gamma_1 + \Gamma_2 \tag{3.54}$$

where

$$\Gamma_1 = \left\langle\int d^3\upsilon\frac{\partial f_{\rm i0}}{\partial\psi_{\rm t}}S\nu\mathcal{L}\{S\}\right\rangle, \tag{3.55}$$

$$\Gamma_2 = \left\langle\int d^3\upsilon\, S\nu\mathcal{L}\left\{f_{\rm i0}\frac{m_{\rm i}u_\alpha\upsilon_\parallel}{T_{\rm i}}\right\}\right\rangle, \tag{3.56}$$

and

$$u_\alpha = -\left[\int d^3\upsilon\, f_{\rm i0}\frac{m_{\rm i}\upsilon^2}{3T_{\rm i}}\nu\right]^{-1}\int d^3\upsilon\,\frac{\partial f_{\rm i0}}{\partial\psi_{\rm t}}\nu\upsilon_\parallel S \tag{3.57}$$

is the part of (3.38) which depends on α. Notice that upon applying (3.49), the $d^3\upsilon$ velocity integral in Γ_1 gives

$$\Gamma_1 \propto \int_0^\infty d\upsilon \frac{\partial f_{i0}}{\partial \psi_t} \upsilon^4 \nu. \tag{3.58}$$

Also, examining (3.57), u_α is proportional to the same factor. Therefore Γ_2 and the total flux have the same proportionality:

$$\langle \mathbf{\Gamma}_i \cdot \nabla \psi_t \rangle \propto \int_0^\infty d\upsilon \frac{\partial f_{i0}}{\partial \psi_t} \upsilon^4 \nu. \tag{3.59}$$

Consequently, when $(\partial h/\partial \alpha)_B$ is nonzero, the υ integrals can be factored out of the ambipolarity condition $\langle \mathbf{\Gamma}_i \cdot \nabla \psi_t \rangle \approx 0$ to obtain

$$0 = \int_0^\infty dx\, x^4 e^{-x^2} \nu \left[\frac{1}{p_i} \frac{dp_i}{d\psi_t} + \frac{Ze}{T_i} \frac{d\Phi}{d\psi_t} + \left(x^2 - \frac{5}{2} \right) \frac{1}{T_i} \frac{dT_i}{d\psi_t} \right]. \tag{3.60}$$

We can rearrange to solve for the radial electric field, using

$$\frac{5}{2} - \left[\int_0^\infty dx\, x^4 e^{-x^2} \nu \right]^{-1} \int_0^\infty dx\, x^6 e^{-x^2} \nu = 1.17, \tag{3.61}$$

a number which is familiar from the banana-regime analysis in a tokamak and from (3.41). The radial electric field in a long-mean-free-path-regime quasi-isodynamic stellarator is therefore

$$\frac{Ze}{T_i} \frac{d\Phi}{d\psi_t} = -\frac{1}{p_i} \frac{dp_i}{d\psi_t} + \frac{1.17}{T_i} \frac{dT_i}{d\psi_t}. \tag{3.62}$$

Physically, this formula shows an inward electric field $\mathbf{E} \approx T_i \nabla n_i / (Zen_i)$ is required to reduce the ion flux down to the level of the electron flux, corresponding to "ion root" confinement.

Note that if a pitch-angle scattering operator without the momentum conserving term u were used in the above calculation, the same radial electric field would be obtained.

The result (3.62) can be used to simplify (3.41), leaving the parallel ion flow in a long-mean-free-path-regime quasi-isodynamic stellarator as

$$V_{i\parallel} = 1.17 \frac{c}{ZeB} \frac{dT_i}{d\psi_t} \left[\left(1 - f_c \frac{B^2}{\langle B^2 \rangle} \right) K + \Upsilon \right]. \tag{3.63}$$

Notice that $V_{i\parallel} \propto dT_i/d\psi_t$ so an ion temperature gradient is required for there to be a parallel ion flow.

3.5 Bootstrap current

In a quasi-isodynamic field, the bootstrap current can be calculated exactly as in a tokamak [17], for although the $(\partial h'/\partial\alpha)_{B'}$ term in the distribution function (3.32) does not arise in a tokamak, this term vanishes whenever a flux surface average is taken, as argued following (3.53). Therefore in the evaluation of $\langle j_\parallel B\rangle$ using the standard analytical method for a tokamak [8], the $(\partial h'/\partial\alpha)_{B'}$ terms disappear from the analysis.

For the long-mean-free-path regime and arbitrary ion charge Z the result is

$$\langle j_\parallel B\rangle = f_t K c \frac{Z^2+2.21Z+0.75}{Z\left(\sqrt{2}+Z\right)}\left(\frac{dp_i}{d\psi_t}+\frac{dp_e}{d\psi_t}-\frac{2.07Z+0.88}{Z^2+2.21Z+0.75}n_e\frac{dT_e}{d\psi_t}-1.17\frac{n_e}{Z}\frac{dT_i}{d\psi_t}\right), \tag{3.64}$$

where $f_t = 1 - f_c$ is the effective trapped fraction and f_c is given by (3.42). To obtain (3.64) we have used the Spitzer function as described on page 207 of [8], and we have used the approximate Spitzer function with two Laguerre polynomials from appendix B of [49].

The total parallel current is then obtained from (3.64) using (3.30). For example, for $Z = 1$ the result is

$$\begin{aligned} j_\parallel &= 1.64\frac{f_t K c B}{\langle B^2\rangle}\left(\frac{dp_i}{d\psi_t}+\frac{dp_e}{d\psi_t}-0.74n_e\frac{dT_e}{d\psi_t}-1.17n_e\frac{dT_i}{d\psi_t}\right) \\ &\quad +\frac{c}{B}\left(\frac{dp_i}{d\psi_t}+\frac{dp_e}{d\psi_t}\right)\left[\left(1-\frac{B^2}{\langle B^2\rangle}\right)K+\Upsilon\right]. \end{aligned} \tag{3.65}$$

Another independent relation exists between $j_\parallel$ and K, for as we have noted previously, $cK/2$ is the total toroidal current inside a flux surface, and so $K(\psi_t) = (2/c)\int d^2\mathbf{a}\cdot\mathbf{j}$. Here, the surface integral is performed over a constant-ζ cross-section of the plasma, a surface which covers the region from the magnetic axis out to the flux surface ψ_t. As shown in appendix F, it follows that

$$\frac{dK}{d\psi_t} = -4\pi\frac{K}{\langle B^2\rangle}\frac{dp_{tot}}{d\psi_t}+\frac{4\pi}{c}\frac{\langle j_\parallel B\rangle}{\langle B^2\rangle}. \tag{3.66}$$

This equation is in fact true for any stellarator, just just a quasi-isodynamic one. The system of equations (3.64) and (3.66), together with the boundary condition that $K = 0$ at the magnetic axis, can be solved to give a self-consistent current profile $K(\psi_t)$. As $\langle j_\parallel B\rangle \propto K$ in (3.64), then the self-consistent solution is $K = 0$. This is the result, anticipated in [17, 20], that the bootstrap current can vanish in a quasi-isodynamic stellarator.

However, the solution $K = 0$ is fragile, and it is important to not simply set $K = 0$ in all formulae for a quasi-isodynamic plasma, for several reasons. Any small departure from (3.64) anywhere inside the flux surface of interest will alter the solution of (3.66), giving nonzero K. Departures from (3.64) are inevitable due to the impossibility of achieving *perfect* quasi-isodynamism [9] and the fact that the collisionality is not infinitesimally small. In W7-X, for example, these factors are expected to lead to a plasma current $cK/2$ of up to

~100 kA [50].

3.6 Discussion and conclusions

We have shown that perfectly quasi-isodynamic fields provide an important point of reference for understanding transport in optimized stellarator designs: while quasi-isodynamic fields are generally not quasisymmetric, neoclassical calculations are analytically tractable in a quasi-isodynamic field to the same extent as in a tokamak, with several modest modifications.

We have derived a general form for the flow in a quasi-isodynamic stellarator, given in (3.28)-(3.29). The form resembles the flow in an axisymmetric or quasisymmetric field, but a new term Υ arises in the Pfirsch-Schlüter flow due to the deviation from symmetry. Our form of the flow agrees with the previously published distribution function for the long-mean-free-path regime, but the derivation here is valid also at higher collisionality. A similar form (3.30)-(3.31) for the parallel current immediately follows. The new quantity Υ can be evaluated readily for a given $B(\theta, \zeta)$ using (3.43) or (3.45). When the enclosed toroidal current $cK/2$ vanishes in the long-mean-free-path regime, the parallel flow and current become proportional to Υ, and their flux surface averages vanish. For the more general case of nonzero K, we can use (3.45) to estimate

$$\frac{\Upsilon}{K} \sim \frac{\left(\hat{B} - \check{B}\right)}{B} \frac{I}{K} = \frac{\left(\hat{B} - \check{B}\right)}{B} \frac{i_\mathrm{p}}{i_\mathrm{t}} \tag{3.67}$$

where i_p is the poloidal current outside the flux surface (essentially equal to the total current in the external toroidal field coils) and i_t is the plasma current (the toroidal current inside the flux surface). As $i_\mathrm{p} \gg i_\mathrm{t}$ in any stellarator, the new Υ terms in $V_\parallel$ and $j_\parallel$ will dominate over the "tokamak-like" terms proportional to K even when K is not strictly zero. For example, for W7-X parameters, even with a high estimate for the bootstrap current, we expect $\Upsilon/K > 60$. To a very good approximation then,

$$\mathbf{V}_a = \frac{c}{B^2}\left(\frac{d\Phi}{d\psi_\mathrm{t}} + \frac{1}{Z_a e n_a}\frac{dp_a}{d\psi_\mathrm{t}}\right)(\mathbf{B} \times \nabla\psi_\mathrm{t} + \Upsilon\mathbf{B}) \tag{3.68}$$

for each species a and

$$\mathbf{j} = \frac{c}{B^2}\frac{dp_\mathrm{tot}}{d\psi_\mathrm{t}}(\mathbf{B} \times \nabla\psi_\mathrm{t} + \Upsilon\mathbf{B})\,. \tag{3.69}$$

Due to the departure from symmetry, the radial particle flux is not intrinsically ambipolar. We can therefore solve for the radial electric field by imposing ambipolarity. Using a momentum-conserving pitch-angle-scattering model collision operator, the electric field in the long-mean-free-path regime is found to have the concise form (3.62). In the limit of quasi-poloidal symmetry, corresponding to $(\partial h/\partial\alpha)_B = 0$, the radial ion flux (3.54)-(3.57) becomes zero even when the velocity integral in (3.59) is not, so the electric field becomes

undetermined.

These results for the flow, current, and radial electric field may be used to validate codes, since in a code it is possible to specify a perfectly quasi-isodynamic field $B(\theta, \zeta)$. Also, in an optimized stellarator which is not perfectly quasi-isodynamic but nearly so, our results may apply approximately. In a field which is not perfectly quasi-isodynamic, a $D \propto 1/\nu$ regime will reappear for the radial particle flux, so the ambipolar radial electric field (3.62) will be the first of our results to break down. However, the parallel flows and current are less sensitive to the details of the ripple-trapped particles, so our results for the flows and current should be relatively robust.

CHAPTER 4

Electric field orderings and the monoenergetic approximation

In the kinetic theory analysis in the preceding two chapters, our expansion of the drift kinetic equation

$$(\upsilon_\parallel \mathbf{b} + \mathbf{v}_\mathbf{E} + \mathbf{v}_\mathrm{m}) \cdot \nabla f = C \tag{4.1}$$

was done assuming the ordering $|\upsilon_\parallel \mathbf{b} \cdot \nabla f| \gg |\mathbf{v}_\mathbf{E} \cdot \nabla f|$. Here, $\mathbf{v}_\mathbf{E} = cB^{-2}\mathbf{E} \times \mathbf{B}$ is the $\mathbf{E} \times \mathbf{B}$ drift, and $\mathbf{v}_\mathrm{m}$ is the magnetic drift. However, starting in this chapter we will consider a stronger ordering for the radial electric field, an ordering which will be referred to as the "finite-E_r" regime, and which will be defined more precisely in the next section.

One of the most widely used tools for calculating neoclassical transport in stellarators in the finite-E_r regime is the DKES (Drift Kinetic Equation Solver) code [51, 52]. Other codes such as PENTA [53, 54] have been developed recently which use the calculations of DKES as input, compensating for the lack of momentum conservation by the collision operator used in DKES [50]. In the drift kinetic equation solved by DKES, not only is the collision operator simplified, but ad-hoc changes are also made to several other terms in order to facilitate rapid computation. These changes, which involve assuming the particle speed is a constant rather than the total (kinetic plus potential) energy, will be explained in more detail in section 4.2, and are sometimes referred to as the "monoenergetic approximation" [55]. It is natural to ask what effect the monoenergetic approximation has on the transport coefficients. To rigorously assess the validity of this approximation in neoclassical calculations, it is necessary to solve the drift kinetic equation with collisions or use a Monte-Carlo approach.

However, to avoid the complexity of the collision operator, a simpler calculation which is instructive is the determination of collisionless effective particle orbits. The characteristic curves of the kinetic equation represent effective particle trajectories, and so the effective trajectories associated with the DKES kinetic equation can be compared with the true particle trajectories. It has already been noted elsewhere that along the DKES trajectories,

neither total energy nor magnetic moment are conserved [55]. Here, using a quasisymmetric vacuum magnetic field as a model, we will calculate the guiding-center trajectories analytically for both the equations used in DKES and for the true equations of motion. We will find that when there is a nonzero radial electric field, the trajectories used by DKES are fundamentally different than the true particle trajectories, and for both trajectories we will derive the shape of the trapped-passing boundaries in velocity space. It will be shown that DKES systematically under-predicts the trapped particle fraction.

The present analytical calculation complements and provides insight into a recent numerical study by Beidler et al [55]. In that work, the particle diffusion coefficient calculated by DKES was compared to Monte-Carlo calculations, where in the latter, either the true or the monoenergetic equations of motion could be used. It was found that the DKES diffusion coefficient can be substantially erroneous once the radial electric field E_r approaches a value which was termed the "resonance" E_r^{res}. For a axisymmetric or quasisymmetric field, E_r^{res} is defined to be the value of E_r at which $\upsilon_{\text{i}}\mathbf{b}\cdot\nabla B + \mathbf{v}_{\mathbf{E}}\cdot\nabla B = 0$, where $\upsilon_{\text{i}} = \sqrt{2T_{\text{i}}/m_{\text{i}}}$ is the ion thermal speed. We too will find that substantial problems arise in monoenergetic calculations when E_r approaches E_r^{res}. These findings are relevant to the HSX stellarator [15], since E_r in this device is expected to somewhat exceed E_r^{res} near the magnetic axis [56], and so monoenergetic transport calculations are likely to be unreliable. In another recent work, Maassberg et al [50] examined the lack of momentum conservation by the collision operator in DKES. This investigation is complementary to the analysis herein, for the error in the trapped fraction discussed in the following sections is associated with the collisionless trajectories, and it is therefore unrelated to the fact that DKES uses an approximate collision operator rather than the full Fokker-Planck operator.

4.1 Orderings for the electric field

In neoclassical theory, the magnitude of the electric field can be ordered in one of three ways. The most common [8, 57, 58] is the "small-E_r," "low-flow," or "drift" ordering, which is the ordering we have used in the preceding chapters. In this ordering, $|\mathbf{v}_{\mathbf{E}}| \sim \delta\upsilon_{\text{i}}$, where $\delta \ll 1$ and the small parameter $\delta = \upsilon_{\text{i}}/(\Omega_{\text{i}}a)$ is the ion gyroradius divided by a system scale-length a. No distinction is made between radial and parallel scale-lengths. Also, all components of $\mathbf{B}$ are ordered as the same magnitude. The magnetic moment $\mu = \upsilon_\perp^2/(2B)$ is an adiabatic invariant, and the perpendicular guiding-center drifts are given to leading order by (2.6) or (2.27), the latter repeated here for convenience:

$$\mathbf{v}_{\text{d}} = (\upsilon_\parallel/\Omega)\nabla\times(\upsilon_\parallel\mathbf{b}). \tag{4.2}$$

Another ordering which is sometimes used is the "large-E_r," "large flow," or "MHD" ordering [12, 59–64], in which $|\mathbf{v}_{\mathbf{E}}|$ is taken to have a comparable magnitude to υ_{i}. Again, no distinction is made between radial and parallel scale-lengths or between different components of $\mathbf{B}$. In the large-flow ordering, the adiabatic invariant changes to $|\mathbf{v}_\perp - \mathbf{v}_{\mathbf{E}}|^2/(2B)$, and other perpendicular drifts arise which are the same order as those in (4.2).

The third ordering, which we will use for this and future chapters, may be termed "finite-E_r". In the finite-E_r ordering, we take $|\mathbf{v_E}| \ll \upsilon_\mathrm{i}$, but we allow

$$|\upsilon_\| \mathbf{b} \cdot \nabla f| \sim |\mathbf{v_E} \cdot \nabla f|. \tag{4.3}$$

As $|\mathbf{v_E}| \ll \upsilon_\mathrm{i}$ as in the finite-E_r ordering, then $\mu = \upsilon_\perp^2/(2B)$ is still an adiabatic invariant, the perpendicular drifts are still given by (4.2) to leading order, and the low-flow drift kinetic or gyrokinetic equations are applicable.

The finite-E_r ordering places a constraint on the geometry, which forces different components of $\mathbf{B}$ to be ordered differently. This result can be seen by considering a tokamak. In this case, $\mathbf{b} \cdot \nabla f = (\mathbf{b} \cdot \nabla\Theta)\partial f/\partial\Theta$, where as before, Θ is any poloidal angle, and $\mathbf{v_E} \cdot \nabla f = cI(d\Phi/d\psi_\mathrm{p})B^{-1}(\mathbf{b} \cdot \nabla\Theta)\partial f/\partial\Theta$, so (4.3) implies $cI(d\Phi/d\psi_\mathrm{p})B^{-1} \sim \upsilon_\mathrm{i}$. However, $|\mathbf{v_E}| \ll \upsilon_\mathrm{i}$ implies $c(d\Phi/d\psi_\mathrm{p})B^{-1}|\nabla\psi_\mathrm{p}| \ll \upsilon_\mathrm{i}$, and so it must be that $|\nabla\psi_\mathrm{p}| \ll I$, or equivalently, $B_\mathrm{p} \ll B_\mathrm{t}$. This analysis can be generalized to quasisymmetry using $\mathbf{b} \cdot \nabla f = (\mathbf{b} \cdot \nabla\chi)\partial f/\partial\chi$, (since as we showed in section 2.6, $(\partial f_1/\partial\zeta)_\chi = 0$.) It follows that $|\nabla\psi_\mathrm{h}|/I_\mathrm{h}$ must be $\ll 1$, or else the finite-E_r ordering is not consistent. The finite-E_r ordering for a quasisymmetric field can be written

$$1 \sim U \ll k^{-1} \tag{4.4}$$

where

$$U = \frac{\mathbf{v_E} \cdot \nabla\chi}{\upsilon_\mathrm{i}\mathbf{b} \cdot \nabla\chi}, \tag{4.5}$$

and the geometric quantity

$$k = \frac{|\nabla\psi_\mathrm{h}|}{I_\mathrm{h}} = \frac{(\iota M - N)\,|\nabla\psi_\mathrm{t}|}{MI} \tag{4.6}$$

must be $\ll 1$.

Let us determine whether the geometric constraint $k \ll 1$ is satisfied in the one existing quasisymmetric stellarator, the HSX device at the University of Wisconsin-Madison [15]. HSX has $N = 4$, $M = 1$, and $\iota \approx 1$ [15]. Figures 4 and 5 in reference [65] give values of $\left\langle |2\pi\nabla\psi_\mathrm{t}|^2 \right\rangle$ and I for HSX. Taking $|\nabla\psi_\mathrm{t}| \sim \left\langle |\nabla\psi_\mathrm{t}|^2 \right\rangle^{1/2}$, we find $k \sim 0.3$ at the last closed flux surface, with k decreasing monotonically to zero at the magnetic axis. Thus, k is indeed $\ll 1$, so the finite-E_r regime is allowed to exist in HSX if E_r has an appropriate value.

The normalized electric field U is often small compared to unity in laboratory plasmas (both stellarators and tokamaks.) However, there are several situations in which U can grow to order unity. One such situation is a transport barrier, such as the edge pedestals and internal transport barriers (ITBs) observed in both tokamaks and stellarators [66, 67]. These transport barriers are associated with a large inward E_r. While pedestals and ITBs have been observed on many stellarators [66, 67], neither feature has been observed to date on HSX, probably because HSX is a small device with relatively little heating power.

Another regime in which U can grow to order unity is the Core Electron-Root Confinement (CERC) regime, an enhanced confinement regime that has been observed in HSX

[56] and many other stellarators [68], and which has no analogue in tokamaks. The CERC regime arises when there is strong electron heating. As $T_\mathrm{e}/T_\mathrm{i}$ grows large, the electrons diffuse outward faster than the ions (opposite to the situation in a $T_\mathrm{e} \approx T_\mathrm{i}$ plasma), and the resulting charge imbalance leads to an outward E_r. An equilibrium is achieved when this E_r becomes sufficient to suppress the electron particle flux down to the level of the ion flux. However, as the electron thermal speed is so large in comparison to the $\mathbf{E}\times\mathbf{B}$ drift, the electron particle flux is relatively insensitive to E_r, and so the equilibrium E_r needs to be quite large. The CERC regime cannot arise in tokamaks because transport in axisymmetric fields is intrinsically ambipolar, meaning the ion and electron particle fluxes are equal regardless of the value of E_r. A perfectly quasisymmetric field would be intrinsically ambipolar as well [37], but the departure from perfect quasisymmetry in HSX is sufficient that the CERC regime can be observed.

The normalized radial electric field U for HSX can be estimated using

$$U = 1.2\frac{(E_r/400\,\mathrm{V/cm})\,\sqrt{m_\mathrm{i}/m_\mathrm{H}}}{(k/0.3)\,(B/1\,\mathrm{T})\,\sqrt{T_\mathrm{i}/60\,\mathrm{eV}}}. \tag{4.7}$$

The normalization for each parameter above reflects a typical HSX magnitude [56]. The radial electric field value $E_r \sim 400\,\mathrm{V/m}$ above is typical of the CERC regime [56]. The value $E_r \sim 400\,\mathrm{V/m}$ is not measured directly, but fields of this magnitude are predicted from PENTA calculations which solve for E_r using ambipolarity; the electron and ion particle fluxes are not automatically equal in these calculations because the departures of the real HSX field from perfect quasisymmetry are included. It is evident from (4.7) that U can be comparable to 1, and so the finite-E_r ordering can indeed be appropriate. One reason U can be relatively large in HSX is that there is no ion heating on the experiment, only electron cyclotron heating, so the ions are cold, and T_i enters the denominator of (4.7).

Each of the three ordering schemes (small-, finite-, and large-E_r) involves not only orderings for the electric field but also for the net plasma flow speed. For the small-E_r and large-E_r orderings, the flow speed is set by the $\mathbf{E}\times\mathbf{B}$ speed ($O(\delta v_\mathrm{i})$ for the small-E_r regime and $O(v_\mathrm{i})$ for the large-E_r regime.) For the finite-E_r ordering, we will take the net flow speed to be small compared to the thermal speed, as this ordering is appropriate for experiments. Assuming the distribution function is Maxwellian to leading order, then the center of the Maxwellian is close to the origin of velocity space ($\mathbf{v} = 0$) relative to the width of the distribution function, and so it can be further assumed that the distribution function is a *stationary* Maxwellian to leading order.

4.2 Monoenergetic guiding-center equations

In order to state the monoenergetic approximation precisely, let us first recall the "true" equations of guiding-center motion in steady electric and magnetic fields. First, $\dot{E} = 0$ where $E = v^2/2 + Ze\Phi/m$ is the total energy and the over-dot is a total time derivative d/dt,

Φ is the electrostatic potential, $\dot{\mu} = 0$ where $\mu = \upsilon_\perp^2 / (2B)$ is the magnetic moment,

$$\dot{\mathbf{r}} = \upsilon_\parallel \mathbf{b} + \mathbf{v}_\mathrm{m} + \mathbf{v}_\mathbf{E}, \tag{4.8}$$

$$\mathbf{v}_\mathbf{E} = \frac{c}{B^2}\mathbf{B} \times \nabla\Phi, \tag{4.9}$$

and

$$\mathbf{v}_\mathrm{m} = \frac{\upsilon_\perp^2}{2\Omega B^2}\mathbf{B} \times \nabla B + \frac{\upsilon_\parallel^2}{\Omega B}\mathbf{B} \times (\mathbf{b} \cdot \nabla \mathbf{b}) + \frac{\upsilon_\parallel^2}{\Omega}\mathbf{b}\mathbf{b} \cdot \nabla \times \mathbf{b}, \tag{4.10}$$

so $\mathbf{v}_\mathbf{E} + \mathbf{v}_\mathrm{m} = \mathbf{v}_\mathrm{d}$ with $\mathbf{v}_\mathrm{d}$ given by (4.2).

Now let us assume that the plasma consists of nested toroidal flux surfaces labeled by a radial coordinate ψ_t satisfying $\mathbf{B} \cdot \nabla\psi_\mathrm{t} = 0$, and let us assume Φ is a flux function. We assume MHD equilibrium so $(\nabla \times \mathbf{B}) \cdot \nabla\psi_\mathrm{t} = 0$. The radial equation of motion becomes

$$\dot{\psi}_\mathrm{t} = \frac{2\upsilon_\parallel^2 + \upsilon_\perp^2}{2\Omega B^2}\mathbf{B} \times \nabla B \cdot \nabla\psi_\mathrm{t}. \tag{4.11}$$

The guiding-center equations of motion can be cast in terms of the speed υ and the pitch angle $p = \upsilon_\parallel/\upsilon$. With a few lines of algebra, it can be shown that

$$\dot{\upsilon} = \frac{c\upsilon}{2B^3}\frac{d\Phi}{d\psi_\mathrm{t}}\left(1 + p^2\right)\mathbf{B} \times \nabla\psi_\mathrm{t} \cdot \nabla B \tag{4.12}$$

and

$$\dot{p} = -\frac{\upsilon}{2B^2}\left(1 - p^2\right)\mathbf{B} \cdot \nabla B + \frac{c}{2B^3}\frac{d\Phi}{d\psi_\mathrm{t}}p\left(1 - p^2\right)\mathbf{B} \times \nabla\psi_\mathrm{t} \cdot \nabla B - \frac{\left(1 - p^2\right)}{2pB}\mathbf{v}_\mathrm{m} \cdot \nabla B. \tag{4.13}$$

It is at this point that the monoenergetic approximation is made in DKES [51, 52, 55]. The magnetic drifts $\mathbf{v}_\mathrm{m}$ are neglected in the $\dot{\mathbf{r}}$ equation (4.8) and the $\dot{p}$ equation (4.13). Next, the $d\Phi/d\psi_\mathrm{t}$ term is dropped in (4.13), and (4.12) is replaced with $\dot{\upsilon} = 0$. Lastly, the $\mathbf{E} \times \mathbf{B}$ drift in the $\dot{\mathbf{r}}$ equation is replaced with

$$\tilde{\mathbf{v}}_\mathbf{E} = \frac{c}{\langle B^2 \rangle}\frac{d\Phi}{d\psi_\mathrm{t}}\mathbf{B} \times \nabla\psi_\mathrm{t}, \tag{4.14}$$

which differs from the true $\mathbf{v}_\mathbf{E}$ in that $\nabla \cdot \tilde{\mathbf{v}}_\mathbf{E} = 0$. The rationale for these approximations is to reduce the number of independent variables in the system by treating υ as a parameter, while maintaining a conservative structure of the equations.

To summarize, the effective equations of motion used in DKES are

$$\dot{\mathbf{r}} = \upsilon_\parallel \mathbf{b} + \tilde{\mathbf{v}}_\mathbf{E}, \tag{4.15}$$

$$\tilde{\mathbf{v}}_\mathbf{E} = \frac{c}{\langle B^2 \rangle}\frac{d\Phi}{d\psi_\mathrm{t}}\mathbf{B} \times \nabla\psi_\mathrm{t}, \tag{4.16}$$

$$\dot{p} = -\frac{\upsilon}{2B^2}\left(1-p^2\right)\mathbf{B}\cdot\nabla B, \tag{4.17}$$

and

$$\dot{\upsilon} = 0. \tag{4.18}$$

4.3 Monoenergetic trajectories for a model magnetic field

To examine how the particle trajectories are altered when these approximations are made, we consider a model magnetic field in which an analytic solution of the equations is possible, specified as follows. We consider Boozer coordinates θ and ζ satisfying

$$\mathbf{B} = \nabla\psi_t \times \nabla\theta + \iota\nabla\zeta \times \nabla\psi_t \tag{4.19}$$

with $2\pi\psi_t$ equaling the toroidal flux and $\iota(\psi_t)$ the rotational transform. We take the field to be a vacuum field so

$$\mathbf{B} = I\nabla\zeta \tag{4.20}$$

where I is position-independent. We further assume that the field is quasisymmetric, and we ignore the radial variation in B in the region of interest, so

$$B(\psi_t, \theta, \zeta) = B(\chi) \tag{4.21}$$

where

$$\chi = M\theta - N\zeta \tag{4.22}$$

is a helical angle. Finally, we take $d\Phi/d\psi_t$ to be constant.

The equations of motion (4.15)-(4.17) can then be written

$$\dot{p} = \frac{(N-\iota M)}{M}\frac{\upsilon}{2B}\left(1-p^2\right)\left(\frac{\partial B}{\partial\theta}\right)\mathbf{b}\cdot\nabla\zeta, \tag{4.23}$$

$$\dot{\zeta} = \upsilon_\parallel \mathbf{b}\cdot\nabla\zeta, \tag{4.24}$$

and

$$\dot{\theta} = \left[\iota\upsilon_\parallel + \frac{(N-\iota M)}{M}\eta\breve{u}\frac{B}{\breve{B}}\right]\mathbf{b}\cdot\nabla\zeta, \tag{4.25}$$

where $\breve{B}$ is the minimum of $B(\chi)$, $\eta = \breve{B}^2/\left\langle B^2\right\rangle$ is a geometric coefficient which is close to 1, and we have introduced the normalized radial electric field

$$\breve{u} = \frac{M}{(N-\iota M)}\frac{cI}{\breve{B}}\frac{d\Phi}{d\psi_t} \tag{4.26}$$

(a constant of the motion).

From (4.25) and (4.24) we can also form

$$\dot{B} = \frac{(N - \iota M)}{M}\left(\eta\check{u}\frac{B}{\check{B}} - \upsilon_{\|}\right)\left(\frac{\partial B}{\partial\theta}\right)\mathbf{b}\cdot\nabla\zeta. \tag{4.27}$$

Combining this result with (4.23), we obtain the following ordinary differential equation for $p\,(B)$:

$$\left(\eta\check{u}\frac{B}{\check{B}} - \upsilon p\right)\frac{dp}{dB} = \frac{\upsilon}{2B}\left(1 - p^2\right). \tag{4.28}$$

It can be verified that this equation has the solution

$$(\upsilon p - \eta\check{u}b)^2 - \upsilon^2 - \eta^2\check{u}^2b^2 = bX \tag{4.29}$$

where $b = B/\check{B}$ and X is some constant. Let us eliminate X in favor of $\check{\upsilon}_{\|}$, which is the value of $\upsilon_{\|}$ when the orbit crosses through the field minimum $\check{B}$. The result is

$$(\upsilon_{\|} - \eta\check{u}b)^2 = \left(\check{\upsilon}_{\|} - \eta\check{u}\right)^2 b - \upsilon^2 b - \eta^2\check{u}^2 b + \upsilon^2 + \eta^2\check{u}^2b^2. \tag{4.30}$$

A particle is trapped if the right-hand side of this equation is negative for $b = \hat{b}$. It follows that the trapped-passing boundary is described by

$$\check{\upsilon}_{\|} = \left(\hat{B}/\check{B}\right)\eta\check{u} \pm \check{\upsilon}_{\perp}\sqrt{\left(\hat{B}/\check{B}\right) - 1} \tag{4.31}$$

where $\check{\upsilon}_{\perp}^2 = \upsilon^2 - \check{\upsilon}_{\|}^2$.

If the variation in B is weak, i.e. $\varepsilon \ll 1$ where $\varepsilon = (\hat{B} - \check{B})/\left(2\check{B}\right)$, we can write (4.31) as

$$\check{\upsilon}_{\|} = \check{u} \pm \check{\upsilon}_{\perp}\sqrt{2\varepsilon}. \tag{4.32}$$

This is precisely the usual $d\Phi/d\psi_{\mathrm{t}} = 0$ relation for particle mirroring, but with the apex of the passing "cones" shifted by $\check{u}$ in the parallel direction.

4.4 True trajectories for the model magnetic field

For the true trajectories, it is not υ but rather the total energy $E = \upsilon_{\|}^2/2 + \mu B + Ze\Phi/m$ which is constant. We eliminate E in this relation in favor of quantities when the trajectory passes through $B = \check{B}$, denoted with the same accent:

$$\frac{\upsilon_{\|}^2}{2} + \mu B + \frac{Ze\Phi\left(\psi_{\mathrm{t}}\right)}{m} = \frac{\check{\upsilon}_{\|}^2}{2} + \mu\check{B} + \frac{Ze\Phi\left(\check{\psi}_{\mathrm{t}}\right)}{m}. \tag{4.33}$$

To analyze this equation further, we need another relation between ψ_{t} and $\check{\psi}_{\mathrm{t}}$. This relation can be obtained in a quasisymmetric field from the conservation of helical momentum. As discussed in Chapt. 2 and appendix B, the original equations of motion (4.8)-(4.10) and the

quasisymmetric condition (4.21) imply $\dot{\psi}_* = 0$ where

$$\psi_* = M\psi_\mathrm{p} - N\psi_\mathrm{t} - MI\frac{\upsilon_\parallel}{\Omega} \tag{4.34}$$

and $2\pi\psi_\mathrm{p}$ is the poloidal flux. (The fact that $K = 0$ in a vacuum has been used.) We eliminate ψ_* in (4.34) in favor of quantities when the trajectory passes through $B = \check{B}$:

$$M\psi_\mathrm{p} - N\psi_\mathrm{t} - MI\frac{\upsilon_\parallel}{\Omega} = M\check{\psi}_\mathrm{p} - N\check{\psi}_\mathrm{t} - MI\frac{\check{\upsilon}_\parallel}{\check{\Omega}} \tag{4.35}$$

and so, using $d\psi_\mathrm{p}/d\psi_\mathrm{t} = \iota$,

$$\psi_\mathrm{t} - \check{\psi}_\mathrm{t} = \frac{M}{(N - \iota M)}\frac{Icm}{Ze}\left(\frac{\check{\upsilon}_\parallel}{\check{B}} - \frac{\upsilon_\parallel}{B}\right). \tag{4.36}$$

As $\Phi(\psi_\mathrm{t}) - \Phi\left(\check{\psi}_\mathrm{t}\right) = \left(\psi_\mathrm{t} - \check{\psi}_\mathrm{t}\right) d\Phi/d\psi_\mathrm{t}$, we can use (4.36) to eliminate $\Phi(\psi_\mathrm{t})$ and $\Phi\left(\check{\psi}_\mathrm{t}\right)$ in (4.33), giving

$$\frac{\upsilon_\parallel^2}{2} + \left(\check{\upsilon}_\parallel - \upsilon_\parallel\frac{\check{B}}{B}\right)\check{u} = \frac{\check{\upsilon}_\parallel^2}{2} - \left(B - \check{B}\right)\mu. \tag{4.37}$$

Solving (4.37) for $\upsilon_\parallel$ gives

$$\upsilon_\parallel = \frac{\check{u}}{b} \pm \sqrt{\frac{\check{u}^2}{b^2} - 2\check{u}\check{\upsilon}_\parallel + \check{\upsilon}_\parallel^2 - 2\left(B - \check{B}\right)\mu}. \tag{4.38}$$

A particle is trapped if the radicand in (4.38) is negative for $B = \hat{B}$, and so the trapped-passing boundary is obtained by setting the radicand to zero:

$$\check{\upsilon}_\parallel^2 - 2\check{u}\check{\upsilon}_\parallel + \frac{\check{B}^2}{\hat{B}^2}\check{u}^2 + \left(1 - \frac{\hat{B}}{\check{B}}\right)\check{\upsilon}_\perp^2 = 0. \tag{4.39}$$

Rearranging,

$$\check{\upsilon}_\parallel = \check{u} \pm \sqrt{\left(\frac{\hat{B}}{\check{B}} - 1\right)\check{\upsilon}_\perp^2 + \left(1 - \frac{\check{B}^2}{\hat{B}^2}\right)\check{u}^2}. \tag{4.40}$$

In the $\varepsilon \ll 1$ weak-B-variation limit, this expression becomes

$$\check{\upsilon}_\parallel = \check{u} \pm \sqrt{2\varepsilon}\sqrt{\check{\upsilon}_\perp^2 + 2\check{u}^2}. \tag{4.41}$$

4.5 Trapped particle fraction

Notice that these last two equations for the true trapped-passing boundaries differ from (4.31)-(4.32) for the corresponding boundary in DKES. Figure 4-1 shows the trapped-passing boundaries for the two models. Both the DKES curve and the true curve show

trapping near $\check{v}_\parallel \approx \check{u}$, but the true trapped region is larger than the DKES prediction. If the radial electric field vanishes ($\check{u} = 0$), then the DKES equations reduce to the correct equations of motion (to leading order in the ratio of gyroradius-to-scale-length), and so DKES gives the correct prediction for the trapped-passing boundary.

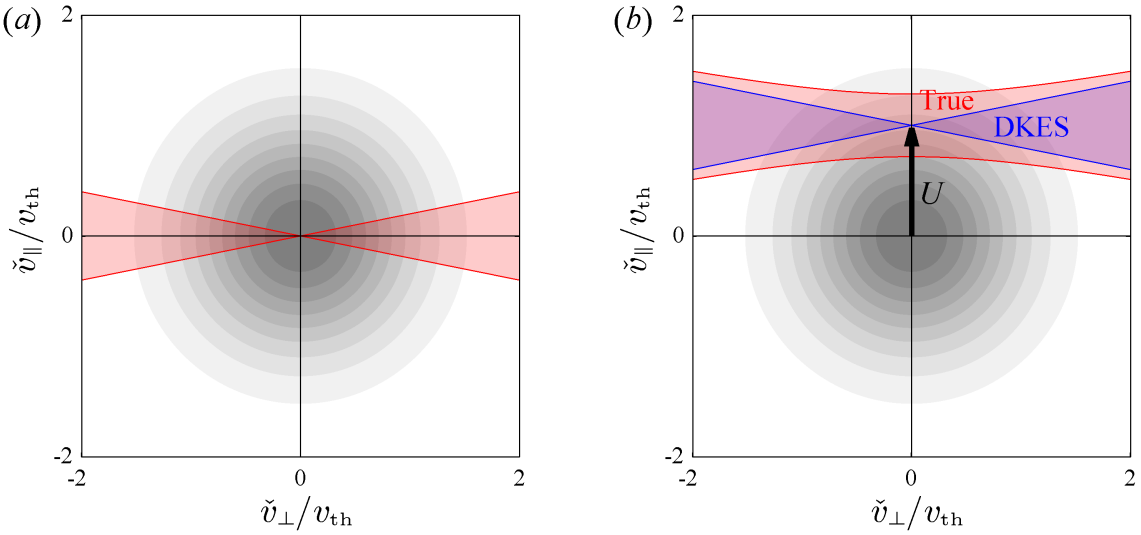

Figure 4-1: The trapped region of velocity space at a location where $B = \check{B}$. (a) DKES and the true trajectories give the same result when there is no electric field ($\check{u} = 0$) . (b) When $\check{u} \neq 0$, the actual trapped region is larger than the one obtained from the DKES equations.

To describe the difference in particle trapping between DKES and the true equations of motion, it is useful to define $\check{f}_{\rm t}$, the fraction of a stationary Maxwellian distribution which would be trapped at $B = \check{B}$:

$$\check{f}_{\rm t} = \frac{1}{v_{\rm th}^3\sqrt{\pi}} \int_0^\infty d\check{v}_\parallel^2 \int d\check{v}_\parallel \exp\left(-\frac{\check{v}_\perp^2 + \check{v}_\parallel^2}{v_{\rm th}^2}\right) \tag{4.42}$$

where $v_{\rm th} = \sqrt{2T/m}$ is the thermal speed, and the range of the $\check{v}_\parallel$ integration is taken from (4.31), (4.32), (4.40), or (4.41). For $\varepsilon \ll 1$, we can approximate the last $\check{v}_\parallel^2$ in (4.42) by $\check{u}^2$, allowing the integrals to be performed analytically, giving

$$\check{f}_{\rm t} = \begin{cases} \sqrt{2\varepsilon}e^{-\check{U}^2} & \text{(DKES)} \\ \sqrt{2\varepsilon}e^{-\check{U}^2}\left(2\sqrt{\frac{2}{\pi}}\left|\check{U}\right| + \left[1 - \operatorname{erf}\left(\sqrt{2}\left|\check{U}\right|\right)\right]e^{2\check{U}^2}\right) & \text{(actual)} \end{cases} \tag{4.43}$$

where $\check{U} = \check{u}/v_{\rm th}$. This parameter $\check{U}$ is equivalent to the value of U in (4.5) when the latter is evaluated at the field minimum $B = \check{B}$. The difference between U and $\check{U}$ is $O(\varepsilon)$ so the distinction will be neglected for the rest of this chapter. The functions in (4.43) are plotted in Figure 4-2.a.

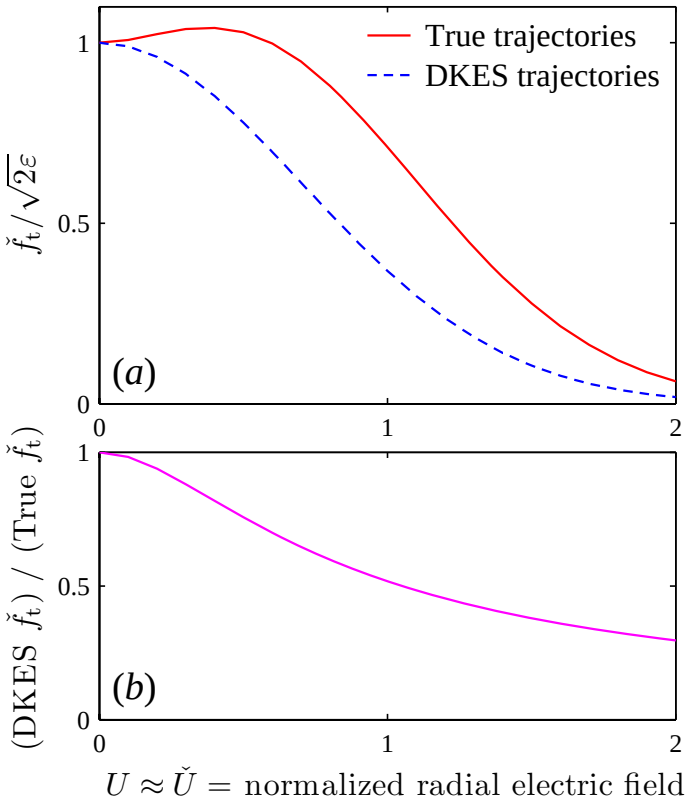

Figure 4-2: (a) Trapped particle fraction in the two models. (b) Ratio of the DKES trapped fraction divided by the actual trapped fraction.

4.6 Discussion

Both the monoenergetic and true equations show that there is an exponential ($\exp(-U^2)$) decrease in the trapped fraction as $|E_r|$ increases. Figure 4-2 show that when $E_r \neq 0$, DKES systematically underestimates the trapped particle fraction. Figure 4-2.b shows the ratio of the two functions in (4.43), showing that the discrepancy is as large as a factor of 2 for $U > 1$. Based on the estimate in section 4.1, this error will be substantial in a CERC-regime HSX plasma.

In the small-E_r ordering, U is formally $\ll 1$, while $U \sim 1$ in both the large-E_r and finite-E_r orderings. However, the analysis in this chapter is not valid in the large-E_r ordering because the drifts and magnetic moment would need to be modified.

The bootstrap current and radial fluxes in a quasisymmetric, high-aspect-ratio, low-collisionality plasma are proportional to an "effective trapped fraction"

$$f_{\mathrm{t}} = 1 - \frac{3}{4}\frac{\langle B^2\rangle}{\check{B}^2}\int_0^{\check{B}/\hat{B}} \frac{\lambda\, d\lambda}{\langle\sqrt{1-\lambda B/\check{B}}\rangle} \tag{4.44}$$

which differs the $\check{f}_{\mathrm{t}}$ defined in (4.42). It is reasonable to expect that the bootstrap current and radial fluxes calculated by the monoenergetic approach are distorted by the effect shown in figure 4-2. However, it is not correct to simply replace f_{t} in the expressions for these neoclassical quantities by the second line of (4.43). To properly evaluate the bootstrap current and radial fluxes, it is necessary to solve the drift kinetic equation with collisions. This problem will be analyzed in the next chapter.

A magnetic field cannot be perfectly quasisymmetric [33, 34], so accurate evaluation of neoclassical transport in an experimentally relevant magnetic field requires numerical computation. However, as the calculation herein shows, when E_r approaches E_r^{res}, the radial magnetic drift causes significant changes to a particle's energy through variation in the electrostatic potential, even when this potential is a flux function. Thus, proper evaluation of neoclassical transport in the regime likely requires a code which is radially nonlocal, so this radial magnetic drift can be retained.

CHAPTER 5

Finite-E_r effects in a quasisymmetric stellarator

In the previous chapter, we showed that the conventional approach to calculating the effect of E_r on neoclassical quantities in the finite-E_r regime, the monoenergetic approximation, is fundamentally flawed. In the present chapter, we propose an improved approach for neoclassical calculations in the finite-E_r regime for the case of a perfectly quasisymmetric field. The calculations in this chapter build upon techniques developed recently for tokamaks [49, 69–73]. In the next section we will begin to solve the kinetic equation. A key element of the calculations will be the use of the conserved canonical helical momentum ψ_* as a coordinate in place of the radial variable ψ_p. This change of variables requires some care to ensure that each point in phase space is counted precisely once, as we will discuss in section 5.2. Whereas in the previous chapter we were able to avoid analyzing the collision operator, in this chapter we will need to take the collision operator into account, which we do in section 5.3.1. The ion heat flux, flow, and bootstrap current in the banana regime are then calculated in the remainder of section 5.3. Although the banana regime is the collisionality ordering that is most interesting for fusion-relevant experiments, the plateau regime is also discussed briefly at the end of the chapter.

5.1 Change of variables and orderings

To evaluate neoclassical transport we must solve the drift kinetic equation

$$Df = C. \tag{5.1}$$

where $D = (v_\parallel \mathbf{b} + \mathbf{v}_\mathrm{d}) \cdot \nabla$. As before, the gradient holds the magnetic moment $\mu = v_\perp^2/(2B)$ and the total energy $E = v^2/2 + Ze\Phi/m$ fixed. When we analyzed the drift kinetic equation for a quasisymmetric stellarator in section 2.6, in accordance with the small-E_r ordering

used there, we took $\mathbf{v}_\mathrm{d}$ (which includes the $\mathbf{E}\times\mathbf{B}$ drift) to be insignificant compared to $v_\parallel\mathbf{b}$. However, when the normalized electric field U defined in (4.5) has a non-negligible magnitude, $\mathbf{v}_\mathbf{E}$ cannot be dropped in (5.1). This complication invalidates the steps used to analyze neoclassical transport in the small-E_r regime in section 2.6, so we must use a different approach to find f.

Before beginning the presentation of this new approach, it should be noted that although the ions may be in the finite-E_r regime, the electrons will essentially always be in the small-E_r regime because of their much larger thermal speed. Hence, the discussion in this and the next chapter is specific to the ions. For the rest of the calculations, then, all symbols will be assumed to refer to ions unless specified otherwise.

The first step in solving the drift kinetic equation for the finite-E_r regime is to make a change of variables. We use ψ_* instead of ψ_h as an independent variable in the kinetic equation (along with χ, ζ, μ, and E), using the chain rule for changing to a new set of variables $\left\{Q_j\right\}$:

$$Df = \sum_j \left(DQ_j\right)\left(\partial f/\partial Q_j\right) \tag{5.2}$$

where $\partial f/\partial Q_j$ holds fixed all the Q_i for $i \neq j$. We make an ansatz $(\partial f/\partial\zeta)_{\psi_*} = 0$, and the $f = f(\psi_*, \chi, \mu, E)$ we find will be consistent with this assumption. We have already shown $D\psi_* = 0$, so the kinetic equation becomes

$$(v_\parallel\mathbf{b} + \mathbf{v}_\mathrm{d})\cdot\nabla\chi\left(\frac{\partial f}{\partial\chi}\right)_{\psi_*} = C \tag{5.3}$$

Note that unlike (2.34) there is now no "radial" derivative term.

As in section 2.6, we neglect the contribution of the magnetic drifts to $\mathbf{v}_\mathrm{d}\cdot\nabla\chi$ in (5.3) compared to the adjacent $v_\parallel\mathbf{b}\cdot\nabla\chi$. However, we now keep the contribution of the $\mathbf{E}\times\mathbf{B}$ drift to $\mathbf{v}_\mathrm{d}\cdot\nabla\chi$, giving

$$(v_\parallel\mathbf{b} + \mathbf{v}_\mathrm{d})\cdot\nabla\chi \approx (v_\parallel + u)(\mathbf{b}\cdot\nabla\chi) \tag{5.4}$$

where

$$u = cI_\mathrm{h}\Phi'/B \tag{5.5}$$

and the prime denotes $\partial/\partial\psi_\mathrm{h}$. With this definition, u evaluated at the field minimum $B = \check{B}$ and in the limit $K \to 0$ gives precisely the quantity $\check{u}$ in (4.26). In the finite-E_r ordering, $u \sim v_\mathrm{i}$.

Next, we take the distribution function to be a stationary Maxwellian to leading order: $f \approx f_\mathrm{M}$ where

$$f_\mathrm{M} = \eta\left(\frac{m}{2\pi T}\right)^{3/2}\exp\left(-\frac{mE}{T}\right) \tag{5.6}$$

and where η and T are flux functions. Further motivation for this leading-order distribution is given in appendix G using an entropy production argument. We define

$$g = f - F \tag{5.7}$$

where $F(\psi_*, E)$ is obtained by replacing ψ_h with ψ_* in the arguments of η and T in f_M:

$$F = \eta(\psi_*)\left[\frac{m}{2\pi T(\psi_*)}\right]^{3/2}\exp\left[-\frac{mE}{T(\psi_*)}\right]. \tag{5.8}$$

Note that a Taylor-expansion of η and T about $\psi_* \approx \psi_\mathrm{h}$ in this definition gives $F \approx f_\mathrm{M} + F_1$ with

$$F_1 = -f_\mathrm{M}\frac{\upsilon_\parallel I_\mathrm{h}}{\Omega}\left[\frac{\eta'}{\eta} + \left(\frac{m\upsilon^2}{2T} - \frac{3}{2}\right)\frac{T'}{T}\right] = -f_\mathrm{M}\frac{\upsilon_\parallel I_\mathrm{h}}{\Omega}\left[\frac{p'}{p} + \frac{Ze\Phi'}{T} + \left(\frac{m\upsilon^2}{2T} - \frac{5}{2}\right)\frac{T'}{T}\right], \tag{5.9}$$

where primes again denote $\partial/\partial\psi_\mathrm{h}$, and η, T, p, and Φ are evaluated at ψ_h rather than ψ_*. As discussed in appendix G, the radial scale-lengths $a_\eta = \eta/(|\nabla\psi_\mathrm{h}|d\eta/d\psi_\mathrm{h})$ and $a_T = T/(|\nabla\psi_\mathrm{h}|dT/d\psi_\mathrm{h})$ are ordered as long compared to ρ/k (where $k = |\nabla\psi_\mathrm{h}|/I_\mathrm{h}$ as in section 4.1) so $|F_1| \ll f_\mathrm{M}$. It follows that the preceding Taylor expansion is a good approximation, and also, from the definition (5.7), then $|g| \ll f_\mathrm{M}$. Thus, the departure of f from the Maxwellian (5.6) has two parts: $f - f_\mathrm{M} \approx F_1 + g$, where both F_1 and g are small compared to f_M.

We next write the kinetic equation as

$$(\upsilon_\parallel + u)(\mathbf{b}\cdot\nabla\chi)(\partial g/\partial\chi)_{\psi_*} = C\{F + g\}. \tag{5.10}$$

We approximate the collision operator by the linearized ion-ion collision operator $C \approx C_{\mathrm{ii},\ell}$. Using $C_{\mathrm{ii},\ell}\{Xf_\mathrm{M}\} = 0$ for $X = 1$, $\upsilon_\parallel$, or υ^2, we can write $C\{F + g\} \approx C_{\mathrm{ii},\ell}\{g - G\}$ where

$$G = f_\mathrm{M}\frac{(\upsilon_\parallel + u)I_\mathrm{h}}{\Omega}\left[\frac{m\left(\upsilon^2 + u^2\right)}{2T} - z\right]\frac{T'}{T} \tag{5.11}$$

and z is independent of velocity. We will choose the value of z later to preserve momentum conservation by our model collision operator.

We next expand the kinetic equation and $g = g^{(0)} + g^{(1)} + ...$ for small collisionality. The leading order form of (5.10) is $\left(\partial g^{(0)}/\partial\chi\right)_{\psi_*} = 0$. The next order form is

$$(\upsilon_\parallel + u)(\mathbf{b}\cdot\nabla\chi)\left(\partial g^{(1)}/\partial\chi\right)_{\psi_*} = C_{\mathrm{ii},\ell}\left\{F + g^{(0)}\right\}. \tag{5.12}$$

5.2 Phase space structure when ψ_* is a coordinate

In conventional banana-regime analysis, the next step in the asymptotic analysis would be to annihilate the left-hand side of (5.12) using a transit average. However, we are now using ψ_* rather than ψ_p as a coordinate, so phase space has a different structure, and care is therefore required. At given (ψ_*, ζ, μ, E), the requirement $\upsilon_\parallel^2 \geq 0$ will mean that not all values of χ will be allowed, and we must determine this constraint on χ. We will also find that a new discrete degree of freedom must be specified in addition to the aforementioned

coordinates in order to uniquely identify a phase space location. Once we understand this discrete degree of freedom, we will be able to precisely state the periodicity requirements on $g^{(1)}$, and thereby define an annihilation operation.

To allow for finite radial electric fields (i.e. nonzero u), we will take into account the changes in potential Φ due to variation in a particle's radial coordinate ψ_h over its trajectory. However, we will neglect the radial variation of all magnetic quantities, treating I_h as constant. We also ignore the effect of the radial drift on B, taking.

$$B(\psi_\mathrm{h}, \chi) \approx B(\chi) = \check{B}/h(\chi) \tag{5.13}$$

where the constant $\check{B}$ represents the minimum value of $|\mathbf{B}|$ over the particle's trajectory, so $h(\chi) \leqslant 1$. This neglect of the radial variation in I_h and B amounts to ordering the scale-lengths of I_h and B as being long compared to ρ/k.

As before, we assume the potential is a flux function. Then none of the quantities in the conservation of ψ_* or E equations depend on ζ, so the range of allowed χ is independent of ζ. Stated another way, all values of ζ are always allowed regardless of (ψ_*, χ, μ, E). We will further assume the potential is a *linear* function of flux; therefore

$$\Phi(\psi_\mathrm{h}) = \Phi(\psi_*) + [\psi_\mathrm{h} - \psi_*]\,\Phi' \tag{5.14}$$

where Φ' is uniform. Combining this equation with the definitions of ψ_* and E then gives

$$\frac{\upsilon_\parallel^2}{2} + u\upsilon_\parallel + \mu B + \frac{Ze}{m}\Phi(\psi_*) - E = 0. \tag{5.15}$$

Applying the quadratic formula then yields

$$\upsilon_\parallel = -u \pm \sqrt{2E - 2\frac{Ze}{m}\Phi(\psi_*) + u^2 - 2\mu B}. \tag{5.16}$$

Notice that u and B above are functions of χ, and due to assumptions stated earlier, we are neglecting the radial variation of u and B. It is evident from the sign ambiguity in (5.16) that specifying $(\psi_*, \chi, \zeta, \mu, E)$ does not yet uniquely specify the phase-space location $(\psi, \chi, \zeta, \upsilon_\parallel, \upsilon_\perp)$: there is also the discrete degree of freedom $\sigma = \mathrm{sgn}(\upsilon_\parallel + u) = \pm 1$. In contrast to the usual situation where ψ_p (or ψ_t or ψ_h) is used as a variable, $\mathrm{sgn}(\upsilon_\parallel)$ is no longer a useful coordinate, since for example, the two phase-space locations sharing a given $(\psi_*, \chi, \zeta, \mu, E)$ may both have the same $\mathrm{sgn}(\upsilon_\parallel)$.

Since $\upsilon_\parallel$ must be real, (ψ_*, μ, E)-space is split into passing and trapped regions, defined by the sign of the radicand in (5.16) at $B = \hat{B}$. In the trapped region, single-valued functions of phase space (like the distribution f) must be independent of σ at the bounce points, the values of χ where the radicand vanishes (and so $\upsilon_\parallel + u = 0$.) This constraint is the periodicity condition we need to annihilate the $g^{(1)}$ term in (5.12) for trapped ions. We thus introduce

a new transit average operation, defined for any quantity Y by

$$\overline{Y} = \frac{\oint d\chi\, Y \left(\upsilon_\parallel + u\right)^{-1} \left(\mathbf{b}\cdot\nabla\chi\right)^{-1}}{\oint d\chi \left(\upsilon_\parallel + u\right)^{-1} \left(\mathbf{b}\cdot\nabla\chi\right)^{-1}}. \tag{5.17}$$

For regions of (E, μ, ψ_*)-space corresponding to passing particles, the integral $\oint (\cdot)\, d\chi$ indicates $\int_0^{2\pi M} (\cdot)\, d\chi$. For regions corresponding to trapped particles, the operation $\oint (\cdot)\, d\chi$ means $\sum_\sigma \sigma \int_{\chi\text{min}}^{\chi\text{max}} (\cdot)\, d\chi$. It is important to notice that since ψ_* rather than ψ_h was taken as an independent variable in the kinetic equation (5.10), the integrations in the transit average hold ψ_* rather than ψ_h fixed. Applying the new transit average to (5.12) gives

$$\overline{C_{\text{ii},\ell}\left\{g^{(0)} - G\right\}} = 0. \tag{5.18}$$

As in the standard banana-regime analysis, the $g^{(0)}$ obtained from this equation can be used to find the radial heat flux and parallel flow. We henceforth drop the superscript on $g^{(0)}$ to simplify notation.

We consider a model for the magnetic field well by taking $h(\chi) = 1 - 2\varepsilon \sin^2(\chi/2)$ with $\varepsilon \ll 1$. (We are free to shift the coordinate χ such that $\chi = 0$ aligns with $\check{B}$.) As stated earlier, in a stellarator, ε does not necessarily equal the geometric inverse aspect ratio, unlike the tokamak case. Recall from the discussion following (17) that $\mathbf{b}\cdot\nabla\chi = (M - Nq)\, B/\left(qI + K\right)$. Keeping the variation of B with χ in this definition would only give a $O(\varepsilon)$ correction to the new transit average (5.17), so we treat $\mathbf{b}\cdot\nabla\chi$ as constant in (5.17) for analytical calculations.

5.3 Banana regime neoclassical transport

5.3.1 Model collision operator

In the conventional banana-regime analysis, the collision operator is replaced with the pitch angle scattering operator

$$C_\text{pas} = \frac{\nu_\perp h \upsilon_\parallel}{2w} \frac{\partial}{\partial\lambda} \upsilon_\parallel \lambda \frac{\partial}{\partial\lambda} \tag{5.19}$$

where $w = \upsilon^2/2$, $\lambda = 2\mu\check{B}/\upsilon^2$, $\nu_\perp = \nu_\text{B} 3\sqrt{2\pi}\left[\text{erf}(x) - \Psi(x)\right]\left(2x^3\right)^{-1}$, $x = \upsilon\sqrt{m/2T}$, $\nu_\text{B} = 4\sqrt{\pi} Z^4 e^4 n_\text{i} \ln\Lambda_\text{C} / \left(3\sqrt{m} T^{3/2}\right)$ is the Braginskii ion-ion collision frequency, $\ln\Lambda_\text{C}$ is the Coulomb logarithm, $\text{erf}(x) = \pi^{-1/2} 2 \int_0^x e^{-y^2} dy$ is the error function, and $\Psi(x) = \left(2x^2\right)^{-1}\left[\text{erf}(x) - x\,\text{erf}'(x)\right]$. Use of the model operator C_pas is justified by noting that for $\varepsilon \ll 1$, the distribution function obtained using C_pas has a large $\left(O\left(\varepsilon^{-1}\right)\right)$ $\partial/\partial\lambda$ derivative [57]. Since C_pas can be obtained by keeping only $\partial/\partial\lambda$ derivatives in the operator for collisions with a Maxwellian field (as we will show shortly), it is plausible that C_pas yields accurate results. The operator C_pas does not generally satisfy the momentum conservation

property

$$\int d^3v\, v_{\|} C = 0 \tag{5.20}$$

that is satisfied by both the full Fokker-Planck ion-ion collision operator and the linearization thereof. However, (5.20) becomes true for a particular choice of the constant z in G, and so in conventional neoclassical calculations, z is selected to be this value [8].

For the present finite-E_r calculation, we will need to use a modified and generalized model collision operator. The fundamental reason that the pitch-angle scattering operator is inappropriate in the finite-E_r regime is that the trapped region is shifted away from the origin of velocity space ($\mathbf{v} = 0$). Therefore, particles are scattered into and out of the trapped region not only by pitch-angle scattering, but also by energy scattering.

Consider the properties which a good model collision operator would possess. First, the operator should give the same ion heat flux, flow, and bootstrap current as C_{pas} in the $E_r \to 0$ limit. Second, we will want to exchange the order of derivatives in the collision operator with the transit average integral in (5.18). To do so, the collision operator derivatives must be of the form $\partial/\partial X$ for some $X(\psi_*, E, \mu)$ (independent of χ), holding other combinations of (χ, ψ_*, E, μ) fixed. Lastly, the operator should keep only velocity derivatives in a direction approximately normal to the modified trapped-passing boundary described by (5.16) and the discussion following it.

Here we consider only the case of no electric field shear, $\Phi'' = 0$. By restricting our attention to the $\Phi'' = 0$ case, several expressions in the following discussion become much less complicated. Also, in a tokamak [70, 72] it was found that the most significant effect of E_r arises through the magnitude of Φ' itself rather than through its derivative: Φ' had exponential effects on neoclassical quantities (as we too shall find) while Φ'' only affects the ion heat flux through an overall algebraic multiplier, and Φ'' does not affect the ion flow or bootstrap current at all.

The model collision operator is then derived from the linearized Fokker-Planck operator. The implicit field term dramatically complicates the analysis, so it is neglected as in [57]. The explicit test-particle term then gives the standard Rosenbluth potential for collisions with a Maxwellian field. The resulting operator can then be written as

$$C_{\text{M}}\{f_1\} = \nabla_{\mathbf{v}} \cdot \left[f_{\text{M}} \overleftrightarrow{Q} \cdot \nabla_{\mathbf{v}} \left(f_1 / f_{\text{M}} \right) \right] \tag{5.21}$$

where

$$\overleftrightarrow{Q} = \left(\overleftrightarrow{I} v^2 - \mathbf{vv} \right) \frac{\nu_{\perp}}{4} + \mathbf{vv} \frac{\nu_{\|}}{2} \tag{5.22}$$

and $\nu_{\|} = \nu_{\text{B}} 3\sqrt{2\pi} \Psi(x) \left(2x^3 \right)^{-1}$.

We next cast (5.21) into a new set of velocity-space variables. The choice of variables is unusual, so we motivate it with the following argument. Suppose we could find new variables W and Λ such that

$$v_{\|} + u = \pm \sqrt{2W} \sqrt{1 - \Lambda/h} \tag{5.23}$$

so as to closely resemble the expression

$$v_\parallel = \pm \sqrt{2w}\sqrt{1-\lambda/h} \tag{5.24}$$

which is used often in the conventional calculations, but with the same $v_\parallel \to v_\parallel + u$ replacement we have needed to make in the transit average. The parallelism between (5.23)-(5.24) will allow the finite-E_r calculations to then be done in much the same way as the conventional calculations, and allow the finite-E_r results to continuously reduce to the standard $u = 0$ ones. Also, the shifted trapped-passing boundary will then be the curve $\Lambda = \min(h)$, just as the trapped-passing boundary in the $E_r \to 0$ case is the curve $\lambda = \min(h)$. Thus, keeping only $\partial/\partial\Lambda$ derivatives in the collision operator will capture the dominant velocity-space behavior for the finite-E_r regime, just as $\partial/\partial\lambda$ derivatives do in the $E_r \to 0$ case. As stated in the paragraph following (5.20), we require that W and Λ be "constants of the motion", i.e. functions of ψ_*, E, μ, $\check{B}$, etc.

However, looking at (5.16) and observing that $u \propto h^2$, the χ dependence (i.e. the h dependence) in (5.16) is fundamentally different from that in (5.23), so there is no way to define a W and Λ to make (5.23) true exactly. However, if the magnetic field does not vary much on a flux surface (i.e. if $h = 1 + O(\varepsilon)$ for $\varepsilon \ll 1$) we can make the replacement $h^2 = 3 - (2/h) + O\left(\varepsilon^2\right)$. Then (5.16) can be written

$$v_\parallel + u = \sigma\sqrt{2}\sqrt{E - \frac{Ze\Phi(\psi_*)}{m} + \frac{3}{2}\check{u}^2 - \frac{1}{h}\left(\check{u}^2 + \mu\check{B}\right) + O(\varepsilon^2 v_{\mathrm{i}}^2)} \tag{5.25}$$

where $\check{u} = u/h$ is the value of u at $B = \check{B}$ and is a constant. (The quantity in 4.26 is identical in the vacuum limit $K = 0$.) From (5.25) it can be seen that the desired form (5.23) can be achieved *approximately*, and to do so there is only one possible way to define W and Λ:

$$W = E - \frac{Ze\Phi(\psi_*)}{m} + \frac{3}{2}\check{u}^2, \tag{5.26}$$

$$\Lambda = \frac{\mu\check{B} + \check{u}^2}{W}. \tag{5.27}$$

Notice that as $E_r \to 0$, Λ reduces to λ, and $W \to w$. We will use W and Λ along with gyrophase φ as the velocity space variables in most of the remaining calculation.

We will need to relate W and Λ to $v_\parallel$ and $v_\perp$. To do so we first combine (5.16) and (5.26) to obtain

$$2W = (v_\parallel + u)^2 + \left(3 - h^2\right)\check{u}^2 + v_\perp^2. \tag{5.28}$$

Using (5.27) we then find

$$(1 - \Lambda/h)\,2W = (v_\parallel + u)^2 + \left(3 - h^2 - 2/h\right)\check{u}^2. \tag{5.29}$$

Thus, instead of (5.23), the exact relationship is

$$\upsilon_{\|} + u = \pm\sqrt{(1-\Lambda/h)\,2W - (3-h^2-2/h)\,\breve{u}^2}. \tag{5.30}$$

For $\varepsilon \ll 1$, the $O(\varepsilon)$ terms in $3-h^2-2/h$ cancel, and so (5.23) is obtained within on overall $1+O(\varepsilon)$ multiplicative factor. A particle is trapped if and only if $\upsilon_{\|}+u$ can vanish, meaning the right hand side of (5.23) vanishes as h varies while Λ and W are fixed (since Λ and W are constants of the motion.) Therefore, to a very good approximation, a particle is trapped if and only if $\Lambda > \min(h)$.

Another useful property of the variables Λ and W is found by applying a Λ derivative to (5.29):

$$\left(\frac{\partial(\upsilon_{\|}+u)}{\partial\Lambda}\right)_{W,\chi} = \left(\frac{\partial\upsilon_{\|}}{\partial\Lambda}\right)_{W,\chi} = -\frac{W}{(\upsilon_{\|}+u)\,h}. \tag{5.31}$$

This property is reminiscent of the result $(\partial\upsilon_{\|}/\partial\lambda)_w = -w/(\upsilon_{\|}h)$ which is used extensively in the conventional neoclassical calculations. The equalities (5.31) are true regardless of whether ψ_{h} or ψ_* is held fixed in the partial derivatives, since χ is fixed so u is constant.

Now consider the result of applying a velocity gradient to (5.28),

$$\nabla_{\mathbf{v}} W = (\upsilon_{\|}+u)\,\mathbf{b} + \mathbf{v}_{\perp}. \tag{5.32}$$

Applying a velocity gradient to (5.27) and using (5.32) we find

$$\nabla_{\mathbf{v}}\Lambda = -\frac{(\upsilon_{\|}+u)\,\Lambda}{W}\mathbf{b} + \frac{(1-\Lambda/h)\,h}{W}\mathbf{v}_{\perp}. \tag{5.33}$$

Then using $\nabla_{\mathbf{v}}\varphi = \upsilon_{\perp}^{-2}\mathbf{b}\times\mathbf{v}$, we obtain the Jacobian

$$J = \frac{1}{\nabla_{\mathbf{v}}W\times\nabla_{\mathbf{v}}\Lambda\cdot\nabla_{\mathbf{v}}\varphi} = \frac{W}{(\upsilon_{\|}+u)\,h}. \tag{5.34}$$

This expression closely resembles the Jacobian for the conventional variables

$$\frac{1}{\nabla_{\mathbf{v}}w\times\nabla_{\mathbf{v}}\lambda\cdot\nabla_{\mathbf{v}}\varphi} = \frac{w}{\upsilon_{\|}h} \tag{5.35}$$

with the same $\upsilon_{\|}\to\upsilon_{\|}+u$ replacement seen in (5.31).

Note that in contrast to [70], the small-ε approximation has not been used at all here to derive (5.31)-(5.34) (aside from motivating the definitions (5.26)-(5.27)).

For trapped and barely passing particles, the right hand side of (5.29) is $O\left(\varepsilon\upsilon_{\mathrm{i}}^2\right)$. Therefore $1-\Lambda/h$ must be $O(\varepsilon)$ for these particles. In light of (5.32) and (5.33), then $|\nabla_{\mathbf{v}}W|\sim\upsilon_{\mathrm{i}}$, $|\nabla_{\mathbf{v}}\Lambda|\sim\sqrt{\varepsilon}/\upsilon_{\mathrm{i}}$, and

$$\frac{|\nabla_{\mathbf{v}}\Lambda\cdot\nabla_{\mathbf{v}}W|}{|\nabla_{\mathbf{v}}\Lambda|\,|\nabla_{\mathbf{v}}W|} \sim \sqrt{\varepsilon}. \tag{5.36}$$

Therefore, in the trapped and barely passing region of velocity space, the Λ and W co-

ordinates are nearly orthogonal. Thus, $(\partial/\partial\Lambda)_W$ will act roughly normal to the shifted trapped-passing boundary, as desired. For comparison, the conventional variables satisfy $\nabla_{\mathbf{v}}\lambda \cdot \nabla_{\mathbf{v}} w = 0$ exactly.

To perform integrals later on, we will need to know the upper and lower bounds of W and Λ at given $\breve{u}$ and χ. From (5.28), W can be arbitrarily large, and the lower bound is $\left(3 - h^2\right)\breve{u}^2/2 \approx \breve{u}^2\left[1 + O\left(\varepsilon\right)\right]$. To find the bounds on Λ, we can combine (5.28) and (5.29) to write

$$\Lambda = \frac{h\upsilon_\perp^2 + 2\breve{u}^2}{\left(\upsilon_\parallel + u\right)^2 + \left(3 - h^2\right)\breve{u}^2 + \upsilon_\perp^2}. \tag{5.37}$$

It follows that at given and , the minimum of Λ is exactly 0 (which occurs when $\upsilon_\parallel \to \pm\infty$) and the maximum allowed Λ is precisely $2/\left(3 - h^2\right)$ (which occurs when $\upsilon_\parallel = -u$ and $\upsilon_\perp = 0$.) For $\varepsilon \ll 1$, this upper bound equals $h + O\left(\varepsilon^2\right)$.

Next, we use the general formula for the divergence in an arbitrary coordinate system to write (5.21) as

$$C_{\mathrm{M}}\left\{f_1\right\} = \frac{1}{J}\sum_{X,Y}\frac{\partial}{\partial X}\left[f_{\mathrm{M}} J\left(\nabla_{\mathbf{v}} X\right)\cdot\overleftrightarrow{Q}\cdot\left(\nabla_{\mathbf{v}} Y\right)\frac{\partial}{\partial Y}\left(\frac{f_1}{f_{\mathrm{M}}}\right)\right] \tag{5.38}$$

where X and Y each range over the set $\{\Lambda,\ W,\ \varphi\}$. The partial derivatives in (5.38) hold fixed the remaining elements of this set, along with ψ and χ. Recall that the collision operator appearing in the drift kinetic equation (and therefore in (5.18)) has been gyroaveraged. If we gyroaverage (5.38), the $X = \varphi$ terms vanish since the quantity in square brackets is periodic in φ. Then $\nabla_{\mathbf{v}} W \cdot \overleftrightarrow{Q} \cdot \nabla_{\mathbf{v}}\varphi = 0$ from (5.32) and $\nabla_{\mathbf{v}}\Lambda \cdot \overleftrightarrow{Q} \cdot \nabla_{\mathbf{v}}\varphi = 0$ from (5.33), so the gyroaveraged $C_{\mathrm{M}}\left\{f_1\right\}$ is given by the right hand side of (5.38) with X and Y each limited to the set $\{\Lambda,\ W\}$.

In analogy to the small-E_r case, we now drop the $\partial/\partial W$ derivatives in (5.38) in order to enable further analysis. For $u = 0$, the result of this simplification is precisely C_{pas} as defined in (5.19). For the general $u \neq 0$ case, the distribution function we obtain using our final model operator has a large Λ derivative, making it plausible that discarding the derivatives will not dramatically affect the calculations for $\varepsilon \ll 1$.

To evaluate (5.38) we must compute $\left(\nabla_{\mathbf{v}}\Lambda\right)\cdot\overleftrightarrow{Q}\cdot\left(\nabla_{\mathbf{v}}\Lambda\right)$. The algebra becomes intractable unless we use $1 - \Lambda/h \sim O\left(\varepsilon\right)$ and $\left(\upsilon_\parallel + u\right) \sim O\left(\sqrt{\varepsilon}\upsilon_{\mathrm{i}}\right)$ to discard terms which are small for trapped and barely passing particles. We thereby neglect the $\mathbf{v}_\perp$ term in (5.33) to obtain

$$\left(\nabla_{\mathbf{v}}\Lambda\right)\cdot\overleftrightarrow{Q}\cdot\left(\nabla_{\mathbf{v}}\Lambda\right) = \left(\upsilon_\parallel + u\right)^2\frac{\Lambda^2}{W^2}\left\{\frac{\nu_\perp}{4}\upsilon_\perp^2 + \frac{\nu_\parallel}{2}\upsilon_\parallel^2 + O\left(\sqrt{\varepsilon}\nu\upsilon_{\mathrm{i}}^2\right)\right\}. \tag{5.39}$$

We approximate $\upsilon_\parallel^2 \approx \breve{u}^2$, and using (5.26), we approximate $\upsilon_\perp^2 \approx 2\left(W - \breve{u}^2\right)$. Our model operator becomes

$$C\left\{f_1\right\} = \frac{\left(\upsilon_\parallel + u\right)}{2W^2}\left(\frac{\partial}{\partial\Lambda}\right)_{W,\psi}\left[\left(\upsilon_\parallel + u\right)\Lambda f_{\mathrm{M}}\left[W\nu_\perp + \breve{u}^2\left(\nu_\parallel - \nu_\perp\right)\right]\left(\frac{\partial}{\partial\Lambda}\right)_{W,\psi}\left(\frac{f_1}{f_{\mathrm{M}}}\right)\right]. \tag{5.40}$$

Notice that (5.40) has a similar form to $C_{\rm pas}$ (in (5.19)). (To obtain (5.40) we have made the replacement $\Lambda^2 \to \Lambda$, which is permissible since $\Lambda \approx 1$. In the related earlier derivation of a model collision operator for tokamaks [70], the replacement $\Lambda^2 \to 1$ was made instead. All results will be independent of the exponent on Λ because the later result (5.58) is independent of this exponent.)

Where υ appears inside $\nu_\perp$, $\nu_\parallel$, and $f_{\rm M}$ in the operator, we make the approximation

$$\upsilon \approx \sqrt{2W - u^2}. \tag{5.41}$$

The quantities $\nu_\perp$, $\nu_\parallel$, and $f_{\rm M}$ are then all constant with respect to the Λ derivative. We now apply the chain rule, so as to hold ψ_* rather than $\psi_{\rm h}$ fixed in the partial derivatives. For any quantity ξ,

$$\left(\frac{\partial \xi}{\partial \Lambda}\right)_{\psi,\chi,W} = \left(\frac{\partial \xi}{\partial \Lambda}\right)_{\psi_*,\chi,W} + \left(\frac{\partial \psi_*}{\partial \Lambda}\right)_{\psi,\chi,W} \left(\frac{\partial \xi}{\partial \psi_*}\right)_{\Lambda,\chi,W}. \tag{5.42}$$

To allow further analysis, the last term in (5.42) must be dropped for both of the partial derivatives in (5.40). Then defining

$$\nu_{\rm K} = \nu_\perp + (\nu_\parallel - \nu_\perp)\, \check{u}^2/W \tag{5.43}$$

we have

$$C = \frac{(\upsilon_\parallel + u)}{2W} f_{\rm M} \nu_{\rm K} \left(\frac{\partial}{\partial \Lambda}\right)_{W,\psi_*} \left[(\upsilon_\parallel + u)\, \Lambda \left(\frac{\partial}{\partial \Lambda}\right)_{W,\psi_*} \left(\frac{f_1}{f_{\rm M}}\right)\right]. \tag{5.44}$$

We may now plug in $f_1 \to g - G$ from (5.18). In G we use (5.41) and $\Omega \approx \check{\Omega}$. Thus

$$C_{\rm K} = \frac{(\upsilon_\parallel + u)}{2W} f_{\rm M} \nu_{\rm K} \left(\frac{\partial}{\partial \Lambda}\right)_{W,\psi_*} \left[(\upsilon_\parallel + u)\, \Lambda \left(\frac{\partial}{\partial \Lambda}\right)_{W,\psi_*} \left(\frac{g}{f_{\rm M}} - \frac{(\upsilon_\parallel + u)\, I_{\rm h} T'}{\check{\Omega} T}\left[\frac{mW}{T} - z\right]\right)\right]. \tag{5.45}$$

This operator is isomorphic to the one employed for tokamaks in [70] with $I \to I_{\rm h}$ and $\psi_{\rm p} \to \psi_{\rm h}$. Since T, T', $I_{\rm h}$, and $\check{\Omega}$ do not vary significantly over an orbit width, these quantities are all treated as constant with respect to derivatives and integrals at constant ψ_*.

We have demonstrated that many expressions for the new W, Λ variables are identical to the conventional results in the $w\,\lambda$ variables, but with the replacement $\upsilon_\parallel \to \upsilon_\parallel + u$. This pattern can be seen in the form of the model operator, the derivative (5.31), and the Jacobian (5.34). Due to the correspondence between the new expressions and the conventional ones, the steps used to calculate neoclassical quantities with the new collision operator will mirror steps in the conventional calculations. However, the replacement $\nu_\perp(w) \to \nu_{\rm K}(W)$ in the new collision operator is a significant change, for now energy diffusion as well as pitch-angle scattering is retained. This change to the effective collision frequency will cause finite-E_r modifications to the ion heat flux, ion flow, and bootstrap current.

5.3.2 Collisional constraint

We must now find the g piece of the distribution function by solving (5.18). First consider the trapped particles, for which this equation becomes

$$0 = \sum_\sigma \sigma \int_{\chi_{\min}}^{\chi_{\max}} d\chi \frac{1}{\mathbf{b}\cdot\nabla\chi}\frac{\partial}{\partial\Lambda}\left\{(v_\parallel+u)\,\Lambda\frac{\partial}{\partial\Lambda}\left[\frac{g}{f_{\rm M}}-(v_\parallel+u)\left(\frac{mW}{T}-z\right)\frac{I_{\rm h}T'}{\check{\Omega}T}\right]\right\}. \tag{5.46}$$

The T' drive term vanishes due to the σ sum. Therefore $g = 0$ is a solution for trapped particles, as in the standard banana-regime calculation.

Next we consider passing particles, for which (5.18) becomes

$$0 = \int_0^{2\pi M} d\chi \frac{\partial}{\partial\Lambda}\left\{(v_\parallel+u)\,\Lambda\frac{\partial}{\partial\Lambda}\left[\frac{g}{f_{\rm M}}-(v_\parallel+u)\left(\frac{mW}{T}-z\right)\frac{I_{\rm h}T'}{\check{\Omega}T}\right]\right\}. \tag{5.47}$$

It is permissible to switch the order of the integral and the first $\partial/\partial\Lambda$ derivative because we have constructed Λ and W to be functions of $(\psi_*,\,\mu,\,E)$. We integrate in Λ from $\Lambda = 0$ and apply (5.31) to find

$$\frac{\partial}{\partial\Lambda}\left(\frac{g}{f_{\rm M}}\right) = -\frac{HW}{\langle v_\parallel+u\rangle_*}\left(\frac{mW}{T}-z\right)\frac{I_{\rm h}T'}{\check{\Omega}T} \tag{5.48}$$

where

$$\langle\xi\rangle_* = \frac{1}{2\pi M}\int_0^{2\pi M} \xi\; d\chi|_{\psi_*,\mu,E} \tag{5.49}$$

and $H = H(h_{\min}-\Lambda)$ is a Heavyside step function which is 1 for passing particles and 0 for trapped particles.

5.3.3 Momentum conservation

We choose the parameter z by requiring

$$\int d^3v\,(v_\parallel+u)\,C_{\rm K} = 0, \tag{5.50}$$

a combination of the particle and momentum conservation properties of the ion-ion collision operator. Using a parity argument as in appendix D, it can be shown that number conservation ($\int d^3v\,C_{\rm K} = 0$) and energy conservation ($\int d^3v\,v^2 C_{\rm K} = 0$) are both satisfied to leading order regardless of z.

To evaluate velocity integrals such as (5.50) we need to write d^3v in (W,Λ) variables. Notice from (5.30) that for given W, Λ, and χ, there are two allowed values for $v_\parallel + u$, associated with $\sigma = \pm 1$. Therefore at given χ, (5.30) and (5.28) give a 1-to-1 map between $(W,\,\Lambda,\,\varphi,\,\sigma)$ and $\mathbf{v}$. The proper way to integrate a quantity ξ over velocity space in our new

variables is therefore

$$\begin{aligned}\int d^3v\, X &= \sum_\sigma \int dW \int d\Lambda \int d\varphi\, |J|\, \xi \\ &= \frac{1}{h}\sum_\sigma \sigma \int dW \int d\Lambda \int d\varphi \frac{W\xi}{(v_\parallel + u)}\end{aligned} \tag{5.51}$$

with the Jacobian J given by (5.34).

Combining (5.50)-(5.51) with our model operator (5.45) and the distribution function (5.48), we therefore require

$$0 = \int dW\, f_{\rm M} W^{3/2} \nu_{\rm K} \left(\frac{mW}{T} - z\right) \int d\Lambda \sqrt{1-\Lambda/h}\, \frac{\partial}{\partial \Lambda}\left[\Lambda - \frac{H\Lambda\sqrt{1-\Lambda/h}}{\left\langle \sqrt{1-\Lambda/h}\right\rangle_*}\right] \tag{5.52}$$

The Λ integral is independent of W so we divide it out of the equation. We then change variables from W to $y = \left(W - \check{u}^2\right) m/T$. From the earlier discussion of the lower bound on W, the lower bound on y is $O(\varepsilon)$ so effectively zero. Therefore

$$z = \frac{\int_0^\infty dy\, e^{-y}\left(y + 2U^2\right)^{3/2}\left(y\nu_\perp + 2U^2\nu_\parallel\right)}{\int_0^\infty dy\, e^{-y}\sqrt{y+2U^2}\left(y\nu_\perp + 2U^2\nu_\parallel\right)} \tag{5.53}$$

where U here is really the flux function $\check{U} = \check{u}/v_{\rm i}$ (equivalent to the definition in Chapt. 4), but here and for the rest of this chapter, we will drop the decoration to simplify notation. Using $x = \sqrt{y+U^2}$ in the definitions of $\nu_\perp$ and $\nu_\parallel$, we can now evaluate z for any given U. For $U = 0$, (5.53) gives $z = 1.33$, in agreement with conventional neoclassical theory.

5.3.4 Neoclassical ion heat flux

In appendix D we derive the following equation to relate the radial ion heat flux to an integral of the collision operator:

$$\langle \mathbf{q}\cdot\nabla\psi_{\rm h}\rangle = -\frac{I_{\rm h}}{\check{\Omega}}\left\langle h\int d^3v\, v_\parallel \frac{mv^2}{2} C\right\rangle. \tag{5.54}$$

Although this equation was derived directly from the full Fokker-Planck equation using only the quasisymmetry condition $B = B(\psi_{\rm h}, \chi)$, the same equation would result if the isomorphism substitutions (2.33) were naively applied to the analogous equation for tokamaks. Using the number, momentum, and energy conservation properties of the collision operator, as well as (5.41), then (5.54) is equivalent to

$$\langle \mathbf{q}\cdot\nabla\psi_{\rm h}\rangle = -\frac{mI_{\rm h}}{\check{\Omega}}\left\langle h\int d^3v\,(v_\parallel + u)\, WC\right\rangle. \tag{5.55}$$

Substituting in the collision operator and distribution function, we then have

$$\begin{aligned}\langle \mathbf{q}\cdot\nabla\psi_{\mathrm{h}}\rangle &= -\frac{2\pi m I_{\mathrm{h}}^2 T'}{\check{\Omega}^2 T}\int dW\, W^2 f_{\mathrm{M}}\nu_{\mathrm{K}}\left(\frac{mW}{T}-z\right) \\ &\quad\times\left\langle\int_0^h d\Lambda\,(\upsilon_{\|}+u)\,\frac{\partial}{\partial\Lambda}\left[\Lambda-\frac{(\upsilon_{\|}+u)\,H\Lambda}{\langle\upsilon_{\|}+u\rangle_*}\right]\right\rangle.\end{aligned} \tag{5.56}$$

We next integrate by parts in Λ, noting there is no contribution from the boundary. Applying (5.23) then results in

$$\begin{aligned}\langle \mathbf{q}\cdot\nabla\psi_{\mathrm{h}}\rangle &= -\frac{\sqrt{2}\pi m I_{\mathrm{h}}^2 T'}{\check{\Omega}^2 T}\int dW\, W^{5/2} f_{\mathrm{M}}\nu_{\mathrm{K}}\left(\frac{mW}{T}-z\right) \\ &\quad\times\left\langle\int_0^h d\Lambda\,\Lambda\left(\frac{1}{\sqrt{1-\Lambda/h}}-\frac{H}{\left\langle\sqrt{1-\Lambda/h}\right\rangle_*}\right)\right\rangle.\end{aligned} \tag{5.57}$$

The Λ integral can then be performed using the method in appendix B of [57]. In general,

$$\int_0^h d\Lambda\,\Lambda^\gamma\left(\frac{1}{\sqrt{1-\Lambda/h}}-\frac{H}{\left\langle\sqrt{1-\Lambda/h}\right\rangle_*}\right)=1.95\sqrt{\varepsilon}+O(\varepsilon) \tag{5.58}$$

for any $\gamma>-1$ where

$$1.95=2\sqrt{2}\left\{1+\int_0^1\frac{d\kappa}{\kappa^2}\left[1-\frac{\pi}{2E(\kappa^2)}\right]\right\} \tag{5.59}$$

and $E\left(\kappa^2\right)$ is the complete elliptic integral of the second kind. Again changing to the variable $y=\left(W-\check{u}^2\right)m/T$, then

$$\langle \mathbf{q}\cdot\nabla\psi_{\mathrm{h}}\rangle=-1.95\sqrt{\varepsilon}\frac{nI_{\mathrm{h}}^2TT'}{2\sqrt{\pi}m\check{\Omega}^2}e^{-U^2}\times\int_0^\infty dy\,e^{-y}\left(y+2U^2\right)^{3/2}\left(y+2U^2-z\right)\left(y\nu_\perp+2U^2\nu_{\|}\right). \tag{5.60}$$

Plugging in the collision frequencies,

$$\langle \mathbf{q}\cdot\nabla\psi_{\mathrm{h}}\rangle=-1.35\sqrt{\varepsilon}\frac{\nu_{\mathrm{B}}nI_{\mathrm{h}}^2TT'}{m\check{\Omega}^2}Q_{\mathrm{ban}}(U) \tag{5.61}$$

where

$$\begin{aligned}Q_{\mathrm{ban}}(U) &= 1.53e^{-U^2}\int_0^\infty dy\,e^{-y}\left(y+2U^2\right)^{3/2}\left(y+U^2\right)^{-3/2}\left(y+2U^2-z\right) \\ &\quad\times\left[y\,\mathrm{erf}\left(\sqrt{y+U^2}\right)+\left(2U^2-y\right)\Psi\left(\sqrt{y+U^2}\right)\right].\end{aligned} \tag{5.62}$$

This function is plotted in figure 5-1.a. At $U = 0$, $Q_{\rm ban} = 1$ and (5.61) recovers the conventional heat flux. Multiplying the right-hand side of (5.61) by $\sqrt{S}$ accounts for orbit squeezing effects [70], where

$$S\left(\psi_{\rm h}\right) = 1 + \frac{cI_{\rm h}^2\Phi''}{\check{B}\check{\Omega}}. \tag{5.63}$$

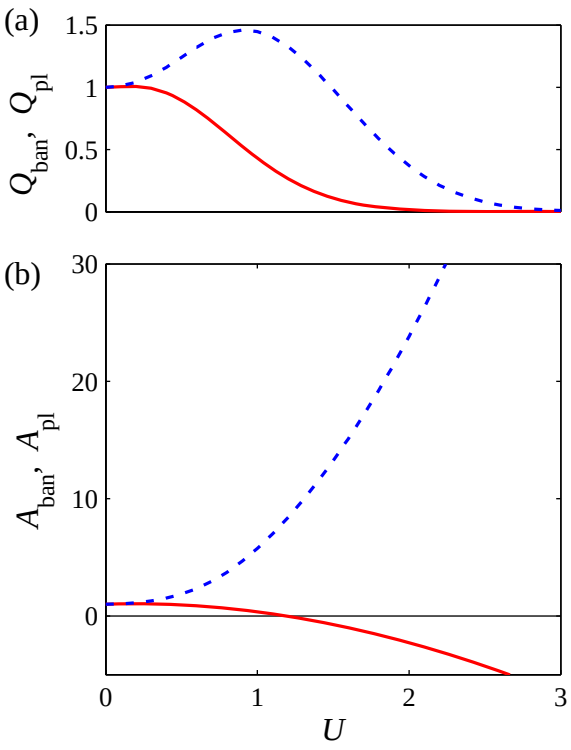

Figure 5-1: Numerical functions which appear in (a) the heat flux and (b) the parallel flow and bootstrap current. Solid (red) curves are the banana regime functions $Q_{\rm ban}$ and $A_{\rm ban}$, while dashed (blue) curves are the plateau regime functions $Q_{\rm pl}$ and $A_{\rm pl}$.

5.3.5 Ion Flow

The parallel flow is obtained by forming the integral

$$\begin{aligned} V_{\|} &= \int d^3v\, v_{\|} f \approx \int d^3v\, v_{\|} \left(F_1 + g\right) \\ &= -\frac{pI_{\rm h}}{m\Omega}\left(\frac{p'}{p} + \frac{Ze\Phi'}{T}\right) + \int d^3v\, v_{\|} g. \end{aligned} \tag{5.64}$$

We then write the remaining integral as

$$\int d^3v\, v_\parallel g = \int d^3v\, v_\parallel G + \int d^3v\, (v_\parallel + u)\,(g - G) - u \int d^3v\, (g - G)\,. \tag{5.65}$$

Using (5.11), the first integral on the right-hand side gives

$$\int d^3v\, v_\parallel G = \left(\frac{5}{2} + U^2 - z\right)\frac{pI_\mathrm{h}T'}{m\Omega T}. \tag{5.66}$$

The second integral on the right-hand side of (5.65) can be evaluated in the same manner as the integral (5.57) for the heat flux, and the result is $\sqrt{\varepsilon}$ smaller than (5.66). The last integral in (5.65) is also estimated to be $\sqrt{\varepsilon}$ smaller than (5.66), as discussed in appendix D. Thus, the final integral in (5.64) is approximately given by the right-hand side of (5.66). Defining

$$A_\mathrm{ban}\,(U) = \frac{1}{1.17}\left(\frac{5}{2} + U^2 - z\right) \tag{5.67}$$

then the parallel flow can be written

$$V_\parallel \approx -\frac{pI_\mathrm{h}}{nm\Omega}\left[\frac{p'}{p} + \frac{Ze\Phi'}{T} - 1.17\,A_\mathrm{ban}\,(U)\,\frac{T'}{T}\right] \tag{5.68}$$

The function $A_\mathrm{ban}\,(U)$ is plotted in figure 5-1.b and agrees with the corrected result from [49, 73]. Note that $A_\mathrm{ban}\,(0) = 1$, and so (5.68) recovers the conventional result for $U = 0$.

5.3.6 Bootstrap current

The bootstrap current calculation for the finite-E_r regime in a quasisymmetric stellarator proceeds exactly as for the low-flow regime in a tokamak (e.g. as shown in [8]), but with two modifications. First, the electron kinetic equation is written in (ψ_h, χ, ζ) variables and analyzed as in section 2.6 (which is appropriate as the electrons are in the small-E_r regime.) Second, the parallel ion velocity (5.68) is used. This latter change affects the electron-ion collision operator, but otherwise the conventional model electron collision operator is used. The electron distribution function in the banana regime is found in the usual way, and a velocity moment is taken to obtain the parallel current, using the Spitzer function f_s as in [8]. We approximate f_s with two Sonine polynomials, as in appendix B of [49]. The resulting bootstrap current for arbitrary Z can be written

$$\left\langle j_\parallel^\mathrm{bs} B\right\rangle \approx -\,1.46\,\sqrt{\varepsilon}cI_\mathrm{h}\frac{Z^2 + 2.21Z + 0.75}{Z\left(Z + \sqrt{2}\right)} \times\left[p'_\mathrm{e} + p'_\mathrm{i} - \frac{(2.07Z + 0.88)\,n_\mathrm{e}T'_\mathrm{e}}{(Z^2 + 2.21Z + 0.75)} - 1.17\,A_\mathrm{ban}\,(U)\,\frac{n_\mathrm{e}T'_\mathrm{i}}{Z}\right] \tag{5.69}$$

where, as usual, primes denote $\partial/\partial\psi_\mathrm{h} = q\,(M - qN)^{-1}\,\partial/\partial\psi_\mathrm{t}$. For $Z = 1$, then

$$\left\langle j_\parallel^\mathrm{bs} B \right\rangle \approx -2.42\,\sqrt{\varepsilon} c I_\mathrm{h}\,(p_\mathrm{e}' + p_\mathrm{i}' - 0.75 n T_\mathrm{e}' - 1.17\,A_\mathrm{ban} n T_\mathrm{i}')\,, \tag{5.70}$$

Setting $A_\mathrm{ban}\,(U) = 1$ in (5.70) we recover equation (5.20) from [28], Boozer's low-flow-regime result for a quasisymmetric stellarator.

5.4 Plateau regime neoclassical transport

Analysis of the plateau regime is identical to that of the banana regime through equation (5.10). Using the momentum conservation property $C_{\mathrm{ii},\ell}\,\{\upsilon_\parallel f_M\} = 0$ we can write

$$(\upsilon_\parallel + u)\left(\frac{\partial}{\partial\chi}\right)_{\psi_*}\left[\tilde{g} + f_\mathrm{M}\frac{\upsilon_\parallel I_\mathrm{h} T'}{\Omega T}\left(\frac{m\upsilon^2}{2T} - \frac{5}{2} + \frac{A_\mathrm{pl}}{2}\right)\right] = \frac{C_{\mathrm{ii},\ell}\,\{\tilde{g}\}}{(\mathbf{b}\cdot\nabla\chi)} \tag{5.71}$$

where

$$\tilde{g} = g - f_\mathrm{M}\frac{\upsilon_\parallel I_\mathrm{h} T'}{\Omega T}\left(\frac{m\upsilon^2}{2T} - \frac{5}{2} + \frac{A_\mathrm{pl}}{2}\right) \tag{5.72}$$

and A_pl is independent of velocity. Equation (5.71) has an intrinsically ambipolar form, as it should in a quasisymmetric stellarator. The equation resembles the equation for axisymmetric geometry analyzed in [49, 73], so the remaining steps are similar to those in these references. The Krook approximation $C_{\mathrm{ii},\ell} \to -\nu_\mathrm{ii}$ is made for the collision operator in (5.71), and the distribution function is found by assuming a solution of the form $\tilde{g} = \tilde{g}_s \sin\chi + \tilde{g}_c \cos\chi$. We next determine A_pl by requiring that the radial ion flux $\left\langle \int d^3\upsilon\, f \mathbf{v}_\mathrm{d}\cdot\nabla\psi_\mathrm{h}\right\rangle$ vanish, with the result

$$A_\mathrm{pl}\,(U) = \frac{1 + 4U^2 + 6U^4 + 12U^6}{1 + 2U^2 + 2U^4}. \tag{5.73}$$

The parallel ion flow is then given by

$$V_\parallel \approx -\frac{p I_\mathrm{h}}{nm\Omega}\left[\frac{p'}{p} + \frac{Ze\Phi'}{T} + \frac{A_\mathrm{pl}\,(U)}{2}\frac{T'}{T}\right]. \tag{5.74}$$

The function A_pl is plotted in figure 5-1.b. The ion heat flux is found to be

$$\langle \mathbf{q}\cdot\nabla\psi_\mathrm{h}\rangle = \left\langle \int d^3\upsilon \frac{m\upsilon^2}{2T} f \mathbf{v}_\mathrm{d}\cdot\nabla\psi_\mathrm{h}\right\rangle = -3\sqrt{\frac{\pi}{2}}\frac{\varepsilon^2\,(M - Nq)\,\check{B} I_\mathrm{h}^2 n\sqrt{T}T'}{(qI + K)\,\check{\Omega}^2 m^{3/2}} Q_\mathrm{pl}\,(U) \tag{5.75}$$

where

$$Q_\mathrm{pl} = \frac{1 + 4U^2 + 8U^4 + (16/3)\,U^6 + (4/3)\,U^8}{1 + 2U^2 + 2U^4} e^{-U^2}. \tag{5.76}$$

This numerical function is plotted in figure 5-1.a. The bootstrap current is calculated as in [49] and is found to be

$$\left\langle j_{\parallel}^{\mathrm{bs}} B \right\rangle = -\frac{\sqrt{\pi}\varepsilon^2 c I_{\mathrm{h}} T_{\mathrm{e}}^{1/2} \check{B}\,(M - Nq)}{m_e^{1/2} \nu_e\,(qI + K)} \frac{\left(\sqrt{2} + 4Z\right)}{Z\left(2 + \sqrt{2}Z\right)} \left(p_{\mathrm{e}}' + p_{\mathrm{i}}' + \frac{\sqrt{2} + 13Z}{2\sqrt{2} + 8Z} n_{\mathrm{e}} T_{\mathrm{e}}' + \frac{A_{\mathrm{pl}}}{2Z} n_{\mathrm{e}} T_{\mathrm{i}}' \right). \tag{5.77}$$

The function A_{pl} is monotonically increasing with $|U|$, so a nonzero E_r of either sign will increase the boostrap current.

5.5 Discussion and conclusions

In the preceding sections we have shown how to calculate neoclassical quantities in a quasisymmetric stellarator when the ions are in the finite-E_r regime. The technique of changing from the radial variable ψ_{p} to the canonical angular momentum ψ_* in the kinetic equation was crucial to the analysis. No analogous quantity is conserved in a non-quasisymmetric stellarator. The conservation of ψ_* enabled an analytical treatment of the particle orbits, which cannot be done to the same extent in a more general stellarator field. To define the finite-E_r regime in a quasisymmetric field, we note that the ratio $k = |\nabla\psi_{\mathrm{h}}|\,/I_{\mathrm{h}}$ plays the role that B_{p}/B plays in a tokamak, so we order $k \ll 1$. Our analysis considers relatively strong electric fields given by the ordering $E_r \sim B\upsilon_{\mathrm{i}}/\,(kc)$. As discussed in section 4.1, present estimates of E_r in the HSX stellarator suggest it may indeed be as large as in this ordering.

Through the calculations in this chapter, we have calculated the finite-E_r modifications to the banana-regime and plateau-regime ion heat flux, ion flow, and bootstrap current. These expressions turn out to match those which would be obtained by applying Boozer's isomorphism substitutions to the tokamak results in [49, 70–73]. Thus, we have shown the isomorphism can be generalized to include these neoclassical quantities in the finite-E_r regime. Table 5.1 summarizes the generalized isomorphism, including the quantities U and k which are important in the finite-E_r regime. Physically, the isomorphism holds for neoclassical quantities even in the finite-E_r regime because these quantities arise from guiding-center drift dynamics and not from additional physics such as the gyromotion. The isomorphism relates the guiding-center drifts but not the gyromotion. Roughly speaking, neoclassical processes are associated with guiding-center drifts whereas classical transport is associated with gyromotion, which helps to understand why neoclassical transport obeys the isomorphism but classical transport does not.

The modifications to banana-regime transport are obtained by generalizing the modified model collision operator proposed in [70]. Our derivation emphasizes that the (W, Λ) variables are unique, in that they are the only possible way to generalize the conventional relation $\left|\upsilon_{\parallel}\right| = \sqrt{2w}\sqrt{1 - \lambda/h}$ to the form $\left|\upsilon_{\parallel} + u\right| = \sqrt{2W}\sqrt{1 - \Lambda/h}$. The finite-$E_r$ modifications to banana-regime transport are in part due to the replacement of the deflection frequency $\nu_{\perp}$ in the usual pitch-angle scattering operator by a new frequency ν_{K} in the new collision operator. The frequency ν_{K} accounts for energy scatter across the modified trapped-passing boundary when this boundary is shifted due to E_r.

Table 5.1: Extended quasisymmetry- axisymmetry isomorphism

	Axisymmetry	**Quasisymmetry**
Symmetry of B	$B = B\left(\psi_\mathrm{p}, \Theta\right)$	$B = B\left(\psi_\mathrm{h}, \chi\right)$
Angle on which B depends	Poloidal angle Θ	Helical angle $\chi = M\theta - N\zeta$
Radial coordinate	Poloidal flux ψ_p	Helical flux $\psi_\mathrm{h} = M\psi_\mathrm{p} - N\psi_\mathrm{t}$
B component flux function	$I = RB_\mathrm{t}$	$I_\mathrm{h} = NK + MI$
Conserved quantity	$\Psi_* = \psi_\mathrm{p} - I\upsilon_\parallel/\Omega$	$\psi_* = \psi_\mathrm{h} - I_\mathrm{h}\upsilon_\parallel/\Omega$
Inverse connection length	$\mathbf{b}\cdot\nabla\Theta \approx 1/\left(qR\right)$	$\mathbf{b}\cdot\nabla\chi = (M - Nq)B/(qI + K)$
Relative B variation	$\varepsilon = a/R$	$\varepsilon = \left(\hat{B} - \check{B}\right)/\left(2\check{B}\right)$
Small ratio of **B** components	$\lvert\nabla\psi_\mathrm{p}\rvert/I = B_\mathrm{p}/B_\mathrm{t}$	$k = \lvert\nabla\psi_\mathrm{h}\rvert/I_\mathrm{h}$
Normalized electric field	$U = cI(\upsilon_\mathrm{i}\check{B})^{-1}d\Phi/d\psi_\mathrm{p}$	$U = cI_\mathrm{h}(\upsilon_\mathrm{i}\check{B})^{-1}d\Phi/d\psi_\mathrm{h}$

To understand the physical origin of the finite-E_r effects calculated here, it is useful to recall figure 4-1 and figure 4-2.a. As the radial electric field is increased from zero, the trapped-passing boundary shifts from $v_\parallel \approx 0$ to $v_\parallel \approx -u$. In the finite-E_r ordering it is consistent for the ion flow to remain subsonic, so the leading-order distribution can remain centered at $v_\parallel = 0$. The trapped fraction therefore diminishes as $\exp\left(-U^2\right)$, an effect which was discussed in Chapt. 4. Consequently, the heat flux becomes exponentially small. The parallel ion flow is mostly carried by passing particles, so for a strong radial electric field ($U \sim 1$) the flow does not become exponentially small, though it is substantially modified. The bootstrap current $j_\parallel^{\text{bs}}$ depends on the ion flow, so $j_\parallel^{\text{bs}}$ is modified as well. In the banana regime, the coefficient of the ion temperature gradient in the parallel ion flow and bootstrap current reverses sign when U exceeds ~ 1.2. Importantly, in both the banana and plateau regimes, the bootstrap current grows stronger as $|E_r|$ is increased.

CHAPTER 6

Finite-E_r effects in a quasi-isodynamic stellarator

In the previous chapter we developed techniques for analyzing the finite-E_r regime in a quasisymmetric stellarator. In the present chapter we will combine these techniques with methods of Chapt. 3 to analyze finite-E_r effects in a quasi-isodynamic device. Even in a perfectly quasi-isodynamic plasma, the kinetic equation is extremely difficult to solve outside of the small-E_r ordering. Here we present a limit in which an analytic solution is still possible. Our procedure will be to expand around the solution of the previous chapter for a quasisymmetric plasma. Terms in the kinetic equation associated with the departure from quasisymmetry are treated as a perturbation. An ordering is developed systematically so that the results of both Chapt. 3 and 5 can be recovered in the appropriate limits. In the end, modifications to the distribution function will be obtained that are driven by E_r, thereby modifying the flow and current for the small-E_r regime which were calculated in Chapt. 3. It will be possible to reuse several components of the calculations in Chapt. 3 and 5, including the model collision operator from the latter, and the numerical function $A_{\rm ban}$ will reappear. An important application of the results in this chapter is verification of numerical codes. In a code that attempts to calculate finite-E_r effects in a general stellarator, it is possible to specify a geometry, E_r, and collisionality to match the ordering developed here, and the code then must reproduce the results we now derive.

6.1 Partitioning of the drift kinetic operator

As in Chapt. 3, we write the magnetic field as $\mathbf{B} = \nabla\psi_{\rm t} \times \nabla\alpha$ where $2\pi\psi_{\rm t}$ is the toroidal flux, $\alpha = \theta - \zeta/q$ again is a field line label, and θ and ζ are the poloidal and toroidal Boozer

angles. The drift kinetic equation is $Df = C$, where

$$Df = (v_\parallel \mathbf{b}\cdot\nabla B + \mathbf{v}_\mathrm{d}\cdot\nabla B)\frac{\partial f}{\partial B} + (\mathbf{v}_\mathrm{d}\cdot\nabla\alpha)\frac{\partial f}{\partial\alpha} + (\mathbf{v}_\mathrm{d}\cdot\nabla\psi_\mathrm{t})\frac{\partial f}{\partial\psi_\mathrm{t}} \tag{6.1}$$

and $\mathbf{v}_\mathrm{d} = v_\parallel\Omega^{-1}\nabla\times(v_\parallel\mathbf{b})$, with gradients taken at fixed total energy $E = v^2/2 + Ze\Phi/m$ unless otherwise noted. The electrostatic potential $\Phi(\psi_\mathrm{t})$ is again assumed to be a flux function.

It was shown in Chapt. 3 that a quasi-isodynamic $\mathbf{B}$ can be written as

$$\mathbf{B} = B_\psi\nabla\psi_\mathrm{t} + \frac{B^2}{\mathbf{B}\cdot\nabla B}\nabla B + \left(K + \frac{\partial h}{\partial\alpha}\right)\nabla\alpha, \tag{6.2}$$

where $cK/2$ is the toroidal current inside the flux surface ψ_t, and

$$\frac{\partial^2 h}{\partial\alpha\partial B} = \frac{\partial}{\partial\alpha}\frac{B^2}{\mathbf{B}\cdot\nabla B}. \tag{6.3}$$

The components of the drifts are

$$\mathbf{v}_\mathrm{d}\cdot\nabla B = v_\parallel(\mathbf{b}\cdot\nabla B)\frac{\partial}{\partial\psi_\mathrm{t}}\left[\frac{v_\parallel}{\Omega}\left(K + \frac{\partial h}{\partial\alpha}\right)\right] - v_\parallel(\mathbf{b}\cdot\nabla B)\frac{v_\parallel}{\Omega}\frac{\partial B_\psi}{\partial\alpha}, \tag{6.4}$$

$$\mathbf{v}_\mathrm{d}\cdot\nabla\alpha = v_\parallel(\mathbf{b}\cdot\nabla B)\left[\frac{\partial}{\partial B}\left(\frac{v_\parallel}{\Omega}B_\psi\right) - \frac{\partial}{\partial\psi_\mathrm{t}}\left(\frac{v_\parallel}{\Omega}\frac{B^2}{\mathbf{B}\cdot\nabla B}\right)\right], \tag{6.5}$$

and

$$\mathbf{v}_\mathrm{d}\cdot\nabla\psi_\mathrm{t} = -v_\parallel(\mathbf{b}\cdot\nabla B)\left(K + \frac{\partial h}{\partial\alpha}\right)\left(\frac{\partial}{\partial B}\frac{v_\parallel}{\Omega}\right). \tag{6.6}$$

At this point we collect the terms of the drift kinetic operator into groups $D = D_0 + D_1 + D_2$, where we will formally take $D_0 \gg D_1$ and $D_1 \gg D_2$. As a general principle of asymptotic analysis, the terms in a given D_i need not all have the same magnitude. It is only necessary that each term in D_1 be smaller than *one* of the terms in D_0 and each term in D_2 be smaller than *one* of the terms in D_1. Thus, we are free to include small terms in D_0 and D_1 in order to facilitate the analysis.

To form the leading order group D_0, we collect all the terms that arise in a quasisymmetric field:

$$D_0 f = v_\parallel(\mathbf{b}\cdot\nabla B)\left\{\left[1 + \frac{\partial}{\partial\psi_\mathrm{t}}\left(K\frac{v_\parallel}{\Omega}\right)\right]\frac{\partial f}{\partial B} - K\left[\frac{\partial}{\partial B}\frac{v_\parallel}{\Omega}\right]\frac{\partial f}{\partial\psi_\mathrm{t}}\right\}. \tag{6.7}$$

By retaining some of the small magnetic drifts in D_0 (those that arise in a quasisymmetric field), the leading order problem will be equivalent to that of Chapt. 5, a problem which we already solved.

For the next order operator D_1 we want to include the rest of the $\mathbf{E}\times\mathbf{B}$ drift in order to capture all finite-E_r effects. We also want to include the rest of the radial magnetic drift (the

$\partial h/\partial\alpha$ term in (6.6)) since by doing so we will recover the results of Chapt. 3 associated the departure from quasisymmetry in a quasi-isodynamic field. Based on the reasoning thus far we should define D_1 as follows:

$$D_1 f = c\Phi' \frac{\partial f}{\partial \alpha} - (\mathbf{b}\cdot\nabla B)\frac{c\Phi'}{B}\left(\frac{\partial h}{\partial \alpha}\right)\frac{\partial f}{\partial B} - \upsilon_\parallel(\mathbf{b}\cdot\nabla B)\left(\frac{\partial h}{\partial \alpha}\right)\left(\frac{\partial}{\partial B}\frac{\upsilon_\parallel}{\Omega}\right)\frac{\partial f}{\partial \psi_t} \tag{6.8}$$

where $\Phi' = d\Phi/d\psi_t$. However, (6.8) is not the final expression we will use for D_1. The last two terms in (6.8) equal terms in D_0 multiplied by $K^{-1}\partial h/\partial\alpha$. To facilitate the analysis, it will turn out to be convenient to include in D_1 *all* the other D_0 magnetic drifts, multiplied by this same factor $K^{-1}\partial h/\partial\alpha$. Therefore we take

$$\begin{aligned} D_1 f =& c\Phi' \frac{\partial f}{\partial \alpha} + \frac{1}{K}\left(\frac{\partial h}{\partial \alpha}\right)\left[D_0 f - \upsilon_\parallel(\mathbf{b}\cdot\nabla B)\frac{\partial f}{\partial B}\right] \\ =& \upsilon_\parallel(\mathbf{b}\cdot\nabla B)\left[\frac{c\Phi'}{\upsilon_\parallel \mathbf{b}\cdot\nabla B}\frac{\partial f}{\partial \alpha} + \frac{1}{K}\left(\frac{\partial h}{\partial \alpha}\right)\left(\frac{\partial}{\partial \psi_t}\frac{K\upsilon_\parallel}{\Omega}\right)\frac{\partial f}{\partial B} - \left(\frac{\partial h}{\partial \alpha}\right)\left(\frac{\partial}{\partial B}\frac{\upsilon_\parallel}{\Omega}\right)\frac{\partial f}{\partial \psi_t}\right]. \end{aligned} \tag{6.9}$$

By including these particular magnetic drift terms in D_1, it becomes possible to write D_1 in terms of D_0 as in the first line of (6.9), which will simplify the calculation later in this chapter. The operator D_2 then consists of all the remaining terms in D, which correspond to $\nabla\alpha$ and ∇B components of the magnetic drifts. However, the coefficient of $\partial f/\partial B$ in (6.9) does not quite match $\mathbf{v}_d\cdot\nabla B$; in effect a small quantity

$$\upsilon_\parallel\,(\mathbf{b}\cdot\nabla B)\,\frac{\upsilon_\parallel}{\Omega}\left[\frac{1}{K}\left(\frac{\partial h}{\partial \alpha}\right)\left(\frac{\partial K}{\partial \psi_t}\right) - \frac{\partial^2 h}{\partial\alpha\partial\psi_t}\right]\frac{\partial f}{\partial B} \tag{6.10}$$

that does not correspond to any actual drift has been included in D_1. This quantity must be subtracted from D_2 to compensate. Thus, we obtain

$$\begin{aligned} D_2 f =& \upsilon_\parallel(\mathbf{b}\cdot\nabla B)\left\{\frac{\upsilon_\parallel}{\Omega}\left[-\frac{1}{K}\left(\frac{\partial h}{\partial \alpha}\right)\left(\frac{\partial K}{\partial \psi_t}\right) + \left(\frac{\partial^2 h}{\partial\alpha\partial\psi_t}\right) - \frac{\partial B_\psi}{\partial \alpha}\right]\frac{\partial f}{\partial B}\right. \\ &\left. + \left[\frac{\partial}{\partial B}\left(\frac{\upsilon_\parallel}{\Omega}B_\psi\right) - \left(\frac{\partial}{\partial \psi_t}\right)_\upsilon\left(\frac{\upsilon_\parallel}{\Omega}\frac{B^2}{\mathbf{B}\cdot\nabla B}\right)\right]\frac{\partial f}{\partial \alpha}\right\}. \end{aligned} \tag{6.11}$$

The υ subscript on the last line of (6.11) indicates that υ rather than total energy is held fixed when taking the derivative.

The equation $D = D_0 + D_1 + D_2$ is exact. In the quasisymmetric limit $\partial/\partial\alpha = 0$, then $D_1 \to 0$ and $D_2 \to 0$ so $D = D_0$.

For the remainder of this section we will manipulate D_0 and D_1 to obtain expressions that will simplify future computations. We begin by defining

$$\psi_* = \psi_t + K\frac{\upsilon_\parallel}{\Omega} \tag{6.12}$$

which is precisely what the conserved helical momentum would be in the quasisymmetric

limit $h \to 0$. Indeed, ψ_* is conserved by the D_0 operator ($D_0\psi_* = 0$). However, ψ_* will not be conserved by the full drift kinetic operator now except in the quasisymmetric limit $h = 0$. Using the definition (6.12), then (6.7) becomes

$$D_0 f = \upsilon_\parallel (\mathbf{b}\cdot\nabla B)\left[\left(\frac{\partial\psi_*}{\partial\psi_\mathrm{t}}\right)\frac{\partial f}{\partial B} - \left(\frac{\partial\psi_*}{\partial B}\right)\frac{\partial f}{\partial\psi_\mathrm{t}}\right]. \tag{6.13}$$

We can also write

$$\left(\frac{\partial X}{\partial B}\right)_\psi = \left(\frac{\partial X}{\partial B}\right)_{\psi_*} + \left(\frac{\partial\psi_*}{\partial B}\right)\left(\frac{\partial X}{\partial\psi_*}\right) = \left(\frac{\partial X}{\partial B}\right)_{\psi_*} + \left(\frac{\partial\psi_*}{\partial B}\right)\left(\frac{\partial\psi_*}{\partial\psi_\mathrm{t}}\right)^{-1}\left(\frac{\partial X}{\partial\psi_\mathrm{t}}\right) \tag{6.14}$$

to obtain

$$D_0 f = \upsilon_\parallel (\mathbf{b}\cdot\nabla B)\left(\frac{\partial\psi_*}{\partial\psi_\mathrm{t}}\right)\left(\frac{\partial f}{\partial B}\right)_{\psi_*}. \tag{6.15}$$

The first equation in (6.14) also gives

$$\left(\frac{\partial X}{\partial B}\right)_\psi = \left(\frac{\partial X}{\partial B}\right)_{\psi_*} + K\left(\frac{\partial}{\partial B}\frac{\upsilon_\parallel}{\Omega}\right)_\psi\left(\frac{\partial X}{\partial\psi_*}\right). \tag{6.16}$$

Noting

$$\left(\frac{\partial}{\partial B}\frac{\upsilon_\parallel}{\Omega}\right)_\psi = -\frac{mc}{Ze}\frac{\left(\upsilon_\parallel^2 + \mu B\right)}{\upsilon_\parallel B^2} \tag{6.17}$$

then (6.9) becomes

$$D_1 f = \frac{1}{K}\left(\frac{\partial h}{\partial\alpha}\right)\left(1 - \frac{\partial\psi_\mathrm{t}}{\partial\psi_*}\right)D_0 f + \upsilon_\parallel(\mathbf{b}\cdot\nabla B)\frac{mc}{Ze}\left(\frac{\partial h}{\partial\alpha}\right)\frac{\upsilon_\parallel^2 + \mu B}{\upsilon_\parallel B^2}\left(\frac{\partial f}{\partial\psi_*}\right) + c\Phi'\frac{\partial f}{\partial\alpha}. \tag{6.18}$$

Note also that since

$$\left(\frac{\partial X}{\partial\alpha}\right)_\psi = \left(\frac{\partial X}{\partial\alpha}\right)_{\psi_*} + \underbrace{\left(\frac{\partial\psi_*}{\partial\alpha}\right)_\psi}_{0}\left(\frac{\partial X}{\partial\psi_*}\right) = \left(\frac{\partial X}{\partial\alpha}\right)_{\psi_*} \tag{6.19}$$

then we are free to switch between holding ψ_t fixed and holding ψ_* fixed in $\partial/\partial\alpha$ derivatives.

6.2 Notation and properties of phase-space

We will reuse several expressions and conventions from Chapt. 3. First, we again define $\check{B}(\psi_\mathrm{t})$ to be the minimum of B on a flux surface, and $\hat{B}(\psi_\mathrm{t})$ to be the maximum of B on a flux surface. We will also make frequent use of the Cary-Shasharina theorem, repeated

here for convenience:

$$\frac{\partial}{\partial \alpha} \sum_{\gamma} \frac{\gamma}{\mathbf{b} \cdot \nabla B} = 0. \tag{6.20}$$

We will again assume that the potential is a linear function of flux, so Φ' is a constant.

Recall from Chapt. 3 that specifying (α, B, ψ_t) does not uniquely specify a location: there is still a choice between two *branches*, corresponding to moving forward versus backward along $\mathbf{B}$ from $\check{B}$. We again let $\gamma = \pm 1$ denote the branch. Since $\gamma = +1$ and $\gamma = -1$ refer to the same point when $B = \check{B}$, then f must be independent of γ at $B = \check{B}$.

In the following sections we will want to use ψ_* as a coordinate in place of ψ_t for much of the calculation. Consequently, as in Chapt. 5, it becomes necessary to examine the topology and geometry of phase space. The analysis of phase space structure from section 5.2, done there for a quasisymmetric field, can be repeated for a quasi-isodynamic field, substituting (B, α) for (χ, ζ) as the coordinates on a flux surface. The conclusions turn out to be very similar. Using (6.12), the definition $E = v_\parallel^2/2 + \mu B + Ze\Phi/m$, and the linearity of $\Phi(\psi_t)$, we obtain

$$v_\parallel = -u \pm \sqrt{2E - 2\frac{Ze}{m}\Phi(\psi_*) + u^2 - 2\mu B} \tag{6.21}$$

where now

$$u = -cK\Phi'/B. \tag{6.22}$$

Therefore, when $(\psi_*, B, \alpha, \gamma, \mu, E)$ are used as the phase-space coordinates instead of $(\psi_t, B, \alpha, \gamma, \mu, E)$, a point in phase space is not fully specified until the discrete coordinate $\sigma = \mathrm{sgn}(v_\parallel + u)$ is specified as well. For certain values of (ψ_*, μ, E), B is not permitted to reach $\hat{B}$ because the radicand of (6.21) becomes negative. These values of (ψ_*, μ, E) correspond to particles that would be trapped in the associated quasisymmetric field, but not necessarily to the actual trapped particles in the quasi-isodynamic field. Similarly, the rest of (ψ_*, μ, E) space corresponds to particles that would be passing in the associated quasisymmetric field, but not necessarily to the actual passing particles in the quasi-isodynamic field. Nevertheless, as a notational shortcut, we will refer to these two regions of phase space simply as the passing and trapped regions. (It is assumed that $\hat{B}$ and $\check{B}$ do not vary significantly over the radial width of an orbit, so $\hat{B}(\psi) \approx \hat{B}(\psi_*)$ and $\check{B}(\psi) \approx \check{B}(\psi_*)$.) For trapped particles, we let $B_c = B_c(\psi_*, \mu, E)$ denote the "critical" field magnitude at which the radicand of (6.21) vanishes. This value of B corresponds to the bounce points. As $\sigma = +1$ and $\sigma = -1$ refer to the same phase-space point when $B = B_c$, then f must be independent of σ at $B = B_c$.

Next, we prove another result that will be used frequently in the following sections: *for any quantity X,* $\partial X/\partial B = 0$ *implies* $\partial X/\partial \alpha = 0$ *in the passing part of phase space but not in the trapped part of phase space.*

In the passing region, $\partial X/\partial B = 0$ means that X is constant along a field line even if we follow that field line many times around the torus. On an irrational surface, we can get as close as we want to any point by starting at any other point and following a field line sufficiently far. Therefore, if we assume X is continuous, then $\partial X/\partial \alpha = 0$ on the

irrational surface. Assuming q is not a constant rational number, then continuity of X implies $\partial X/\partial\alpha = 0$ on rational surfaces as well.

In the trapped part of phase space, however, the preceding argument does not hold: we cannot follow a field line even once around toroidally because phase space "ends" when we reach the bounce point. Thus, there is no reason $\partial X/\partial\alpha$ needs to vanish for trapped particles.

6.3 Orderings and annihilation operation

We now order the terms of the drift kinetic equation. We want the ordering to meet several criteria. First, it should lead to a distribution function f that reduces, in the appropriate limits, to the distributions of Chapt. 3 and 5. Second, the ordering should allow new terms in f to be obtained that are driven by E_r, thereby capturing finite-E_r effects. Third, the ordering should result in equations that can be solved analytically. As we shall see in the rest of this chapter, an ordering that turns out to satisfy all these requirements is

$$D_0 \gg D_1 \gg C \gg D_2, \tag{6.23}$$

with

$$C/D_1 \gg D_1/D_0. \tag{6.24}$$

Not only do the inequalities (6.23)-(6.24) meet the technical requirements just mentioned, but this ordering is also physically reasonable. As D_0 contains parallel streaming motion while D_2 contains only magnetic drift terms, then $D_2/D_0 \sim \mathbf{v}_\mathrm{d}/\upsilon_\mathrm{th} \sim \rho/R$, where R is the major radius. As ρ/R is extremely small compared to one, there is room between D_0 and D_2 for intermediate scales. Laboratory plasmas are typically described in conventional neoclassical theory by the banana-plateau regime ordering $1 \gg \nu qR/\upsilon_\mathrm{th} \gg \rho/R$, which can be translated as $D_0 \gg C \gg D_2$, in agreement with (6.23). In a code that attempts to calculate finite-E_r effects in a general stellarator, the input parameters to the code can be set so the ordering (6.23)-(6.24) is satisfied. Through this procedure, the results derived here can be used to verify such codes.

To apply the ordering (6.23)-(6.24) to the kinetic equation, the distribution function is expanded $f = f_0 + f_1 + f_2 + ...$ Subscripts will not denote precisely how a quantity scales with respect to any particular small parameter, only that $f_i \gg f_{i+1}$. The first two orders of the drift kinetic equation are

$$D_0 f_0 = 0 \tag{6.25}$$

and

$$D_0 f_1 + D_1 f_0 = 0. \tag{6.26}$$

This last equation implies $f_1/f_0 \sim D_1/D_0$, and so due to (6.24),

$$C\{f_0\} \gg D_1 f_1. \tag{6.27}$$

This result and $C \gg D_2$ imply the next equation in the expansion is

$$D_0 f_2 = C\{f_0\}. \tag{6.28}$$

The term f_0 will not be Maxwellian, so the right-hand side of (6.28) will not vanish.

As in many asymptotic calculations, we will need to annihilate the largest operator, which in this case is D_0. The annihilation operation, which will be denoted by an overbar, is defined by the property $\overline{D_0 X} = 0$ for any X. For trapped particles, this operation is

$$\overline{A} = \sum_\sigma \sigma \sum_\gamma \gamma \int_{\check{B}}^{B_c} dB \frac{A}{v_\parallel \mathbf{b}\cdot\nabla B} \frac{\partial \psi_t}{\partial \psi_*} \tag{6.29}$$

for any quantity A. This operation annihilates D_0 due to two findings from section 6.2: continuous single-valued functions must be 1) independent of γ at $\check{B}$, and 2) independent of σ at B_c. For passing particles the annihilation operation is

$$\overline{A} = \sum_\gamma \gamma \int_0^{2\pi} d\alpha \int_{\check{B}}^{\hat{B}} dB \frac{A}{v_\parallel \mathbf{b}\cdot\nabla B} \frac{\partial \psi_t}{\partial \psi_*}. \tag{6.30}$$

This operation annihilates D_0 due to two facts. First, as mentioned above, continuous single-valued functions must be independent of γ at $\check{B}$. Second, consider the two curves defined by $\gamma = +1$ or $\gamma = -1$, with α varying from 0 to 2π, and holding $B = \hat{B}$ and ψ_* constant. (Along both of these paths, ψ_t is constant as well, since the difference $\psi_* - \psi_t$ is independent of α.) Assuming the plasma has N identical toroidal segments with $N > 1$, the two curves do not coincide in space, but plasma parameters along the two loops must be identical due to periodicity. Thus, when the operation (6.30) is applied to $D_0 X$, the contributions from the upper and lower boundaries of the B integration each separately cancel, leaving zero. Note that the integrals in both (6.29) and (6.30) are performed at constant ψ_*.

Applying the annihilator to the full drift kinetic equation gives

$$\overline{D_1 f} + \overline{D_2 f} = \overline{C\{f\}}. \tag{6.31}$$

This equation provides a series of constraints that must be satisfied at each order. We again apply the ordering (6.23)-(6.24). Using $D_1 \gg D_2$ and $D_1 \gg C$, the first constraint equation is

$$\overline{D_1 f_0} = 0. \tag{6.32}$$

Then using $C \gg D_2$ and (6.27), the second equation is

$$0 = \overline{C\{f_0\}}. \tag{6.33}$$

The third equation, obtained using $D_1 \gg C$, is

$$\overline{D_1 f_1} + \overline{D_2 f_0} = 0. \tag{6.34}$$

The final equation we will need is then found by applying $C \gg D_2$ to obtain

$$\overline{D_1 f_2} = \overline{C\{f_1\}}. \tag{6.35}$$

6.4 Evaluation of the distribution function

6.4.1 Zeroth order drift kinetic equation

The leading order equation (6.25) implies

$$\left(\frac{\partial f_0}{\partial B}\right)_{\psi_*} = 0 \tag{6.36}$$

so $f_0 = f_0(\psi_*, \alpha, \mu, E, \sigma)$. The distribution function f_0 cannot have any dependence on γ for either trapped or passing particles because f_0 must be independent of γ at $\check{B}$. Also, as shown at the end of section 6.2, for passing particles f_0 cannot depend on α. For now, f_0 for trapped particles can still be allowed to depend on α. For trapped particles, f_0 cannot depend on σ since f_0 must be independent of σ at the bounce points, but (for now) f_0 can still depend on σ for passing particles.

We consider the physically sensible case that f_0 is approximately Maxwellian. Let $T(\psi_t)$ be the temperature of this Maxwellian and $n(\psi_t)$ be its density. Thus, we want

$$f_0 \approx \eta(\psi_t)\left[\frac{m}{2\pi T(\psi_t)}\right]^{3/2} \exp\left(-\frac{mE}{T(\psi_t)}\right) \tag{6.37}$$

where $\eta = n\exp(Ze\Phi/T)$ is the pseudo-density. However, this Maxwellian does not satisfy (6.36). To obtain a solution of (6.36) which is approximately Maxwellian we define

$$g_0 = F - f_0 \tag{6.38}$$

where

$$F = \eta(\psi_*)\left[\frac{m}{2\pi T(\psi_*)}\right]^{3/2} \exp\left(-\frac{mE}{T(\psi_*)}\right). \tag{6.39}$$

Our task is now to find a g_0 such that the appropriate kinetic equations are satisfied. If $g_0 \ll F$, and if η' and T' are sufficiently weak that $\eta(\psi_*) \approx \eta(\psi_t)$ and $T(\psi_*) \approx T(\psi_t)$, then f_0 will be approximately Maxwellian as desired. The statements made earlier about f_0 also apply to g_0: g_0 is independent of γ for all particles, g_0 can depend on α for trapped particles but not for passing particles, and g_0 can depend on σ for passing particles but not for trapped particles.

6.4.2 Zeroth order constraint equation

Now consider the first constraint equation, (6.32), beginning with the equation for passing particles:

$$\sum_\gamma \gamma \int_0^{2\pi} d\alpha \int_{\check{B}}^{\hat{B}} dB \left[\frac{mc}{Ze} \left(\frac{\partial \psi_t}{\partial \psi_*} \right) \left(\frac{\partial h}{\partial \alpha} \right) \frac{v_\parallel^2 + \mu B}{v_\parallel B^2} \left(\frac{\partial f_0}{\partial \psi_*} \right) - \frac{c\Phi'}{v_\parallel \mathbf{b} \cdot \nabla B} \left(\frac{\partial \psi_t}{\partial \psi_*} \right) \frac{\partial f_0}{\partial \alpha} \right] = 0. \quad (6.40)$$

As discussed earlier, $\partial f_0/\partial\alpha$ is 0 in this part of phase space. The $\partial f_0/\partial\psi_*$ term gives a vanishing contribution to either the α integral or the γ sum. Thus the constraint equation for passing particles is automatically satisfied.

Now consider the constraint for trapped particles:

$$\sum_\sigma \sigma \sum_\gamma \gamma \int_{\check{B}}^{B_c} dB \left[\frac{mc}{Ze} \left(\frac{\partial \psi_t}{\partial \psi_*} \right) \left(\frac{\partial h}{\partial \alpha} \right) \frac{v_\parallel^2 + \mu B}{v_\parallel B^2} \left(\frac{\partial f_0}{\partial \psi_*} \right) - \frac{c\Phi'}{v_\parallel \mathbf{b} \cdot \nabla B} \left(\frac{\partial \psi_t}{\partial \psi_*} \right) \frac{\partial f_0}{\partial \alpha} \right] = 0. \quad (6.41)$$

The $\partial f_0/\partial\psi_*$ term vanishes in the γ sum. The $\partial f_0/\partial\alpha$ term does not automatically vanish, so $\partial f_0/\partial\alpha$ must be 0 for the trapped particles. (We already knew this for passing particles).

6.4.3 First order drift kinetic equation

The next equation to consider is (6.26), which when written out is

$$\left(\frac{\partial f_1}{\partial B} \right)_{\psi_*} = \frac{mc}{Ze} \left(\frac{\partial \psi_t}{\partial \psi_*} \right) \left(\frac{\partial h}{\partial \alpha} \right) \frac{v_\parallel^2 + \mu B}{v_\parallel B^2} \left(\frac{\partial f_0}{\partial \psi_*} \right) - \frac{c\Phi'}{v_\parallel \mathbf{b} \cdot \nabla B} \left(\frac{\partial \psi_t}{\partial \psi_*} \right) \frac{\partial f_0}{\partial \alpha}. \quad (6.42)$$

Before integrating to obtain f_1, consider the $\partial\psi_t/\partial\psi_*$ factors which appear in (6.42). If the radial variation in magnetic quantities is weak relative to the radial variation of Φ, then

$$\frac{\partial \psi_*}{\partial \psi_t} \approx \frac{v_\parallel + u}{v_\parallel}. \quad (6.43)$$

Therefore, the integral of (6.42) can be written

$$f_1 = g_1 - \left(\frac{\partial f_0}{\partial \psi_*} \right) \frac{mc}{Ze} \int_B^{\hat{B}} dB' \left(\frac{\partial h'}{\partial \alpha} \right) \frac{\left(v_\parallel' \right)^2 + \mu B'}{\left(v_\parallel' + u' \right) B'^2} \quad (6.44)$$

for passing particles and

$$f_1 = g_1 - \left(\frac{\partial f_0}{\partial \psi_*} \right) \frac{mc}{Ze} \int_B^{B_c} dB' \left(\frac{\partial h'}{\partial \alpha} \right) \frac{\left(v_\parallel' \right)^2 + \mu B'}{\left(v_\parallel' + u' \right) B'^2} \quad (6.45)$$

for trapped particles, where g_1 is an integration constant (independent of B), and primes indicate quantities are evaluated at B' rather than B. The integrals in (6.44)-(6.45) are performed at constant ψ_*.

The endpoints for the integration are chosen as shown for a reason. In the next section we will find that to satisfy a collisional constraint, we must take $g_1 = 0$ for trapped particles. However, g_1 must be consistent with the requirement that f_1 is independent of σ at the trapped-passing boundary. The choice of B_c as the integration endpoint in (6.45) means that $f_1 \to g_1$ at this boundary, so $g_1 = 0$ will satisfy the boundary condition. Had a different integration endpoint been used, $g_1 = 0$ would not satisfy the boundary condition. The choice of $\hat{B}$ as the integration endpoint in (6.44) ensures that g_1 is continuous across the trapped-passing boundary.

Since g_1 is independent of B, then for passing particles, g_1 must also be independent of α. However, for trapped particles, g_1 is free to depend on α. For trapped particles, f_1 must be independent of σ at $B \to B_c$. Therefore g_1 must be independent of σ for trapped particles, though g_1 is still free to depend on σ for passing particles.

For both passing and trapped particles, f_1 must be independent of γ at $B = \check{B}$. Therefore g_1 must be independent of γ for both passing and trapped particles. Consequently, f_1 is independent of γ everywhere.

6.4.4 First order constraint equation

We next consider (6.33), which can be written as

$$0 = \sum_\gamma \gamma \int_{\check{B}}^{\hat{B}} dB \int_0^{2\pi} d\alpha \frac{C\{f_0\}}{(v_\parallel + u)\mathbf{b}\cdot\nabla B} \tag{6.46}$$

for passing particles and

$$0 = \sum_\gamma \gamma \sum_\sigma \sigma \int_{\check{B}}^{B_c} dB \frac{C\{f_0\}}{(v_\parallel + u)\mathbf{b}\cdot\nabla B} \tag{6.47}$$

for trapped particles. Equation (6.43) has been applied. The above two constraints determine g_0. All integrals are performed at constant ψ_*. The passing constraint (6.46) is equivalent to

$$0 = \left\langle \frac{B}{v_\parallel + u} C\{f_0\} \right\rangle. \tag{6.48}$$

The distribution f_0 departs from a Maxwellian both due to g_0 and due to the difference $\psi_* - \psi_t$ in F. Thus,

$$C\{f_0\} \approx C_\ell\{g_0 + F_1\} \tag{6.49}$$

where C_ℓ is the linearized operator for self-collisions and

$$F_1 = f_{\rm M} K \frac{\upsilon_\parallel}{\Omega}\left[\frac{p'}{p} + \frac{Ze\Phi'}{T} + \left(\frac{m\upsilon^2}{2T} - \frac{5}{2}\right)\frac{T'}{T}\right]. \tag{6.50}$$

Using the conservation properties of C_ℓ, then

$$C\{f_0\} \approx C_\ell\{g_0 - G\} \tag{6.51}$$

where

$$G = -f_{\rm M} K \frac{(\upsilon_\parallel + u)}{\Omega}\left[\frac{m\left(\upsilon^2 + u^2\right)}{2T} - z\right]\frac{T'}{T}, \tag{6.52}$$

and the unknown z has been added anticipating the need to restore momentum conservation once the collision operator is replaced with a model. The next steps of the analysis proceed exactly as in the quasisymmetry case of Chapt. 5, noting $I_{\rm h} \to NK$ and $\psi_{\rm h} \to -N\psi_{\rm t}$. We use the model collision operator

$$C_{\rm K}\{g_0 - G\} = \frac{(\upsilon_\parallel + u)}{2W} f_{\rm M}\nu_{\rm K}\left(\frac{\partial}{\partial\Lambda}\right)_{W,\psi_*}\left[(\upsilon_\parallel + u)\,\Lambda\left(\frac{\partial}{\partial\Lambda}\right)_{W,\psi_*}\left(\frac{g_0}{f_{\rm M}} + K\frac{(\upsilon_\parallel + u)\,T'}{\Omega_0 T}\left[\frac{mW}{T} - z\right]\right)\right] \tag{6.53}$$

derived in Chapt. 5, and with z chosen to maintain momentum conservation. In the trapped constraint, the drive term vanishes in the σ sum, so $g_0 = 0$ is a valid solution. The passing constraint gives the g_0 we found in Chapt. 5.

6.4.5 Second order drift kinetic equation

The next order equation (6.28) can be written

$$\left(\frac{\partial f_2}{\partial B}\right)_{\psi_*} = \left(\frac{\partial\psi_{\rm t}}{\partial\psi_*}\right)\frac{C\{f_0\}}{\upsilon_\parallel \mathbf{b}\cdot\nabla B}. \tag{6.54}$$

Integrating (6.54) gives

$$f_2 = g_2 + \int_{\check{B}}^{B} dB' \frac{C\{f_0\}}{(\upsilon_\parallel + u)\,\mathbf{b}\cdot\nabla B} \tag{6.55}$$

where g_2 is independent of B. From the argument at the end of section 6.2, g_2 must also be independent of α for passing particles, but it can depend on α for trapped particles. Unlike the B' integrals in (6.44)-(6.44), we have chosen the bound of integration in (6.55) to be $\check{B}$ instead of B_c or $\hat{B}$. This choice ensures that g_2 is independent of γ (which follows from the fact that f_2 must be independent of γ at $B = \check{B}$.) The γ-independence of g_2 will be needed for a later step of the calculation.

Notice that f_2 depends on both α and γ, and it has neither even nor odd σ-parity due to the $\upsilon_\parallel$ dependence of the collision operator. However, if the model collision operator is used, then $C\{f_0\} \approx C_\ell\{g_0 - G\}$ will be odd in σ to leading order.

At $B \to B_c$ for the trapped, f_2 must be independent of σ. Therefore g_2 *does depend* on σ for the trapped, unlike previous cases. As before, g_2 can depend on σ for the passing.

One further property which will be useful later is

$$\sum_\gamma \gamma \frac{\partial f_2}{\partial \alpha} = 0 \tag{6.56}$$

for both passing and trapped.

6.4.6 Second order constraint equation

The next equation to examine is (6.34). Noting $D_2 f_0 = 0$, this constraint becomes

$$\overline{\frac{1}{K}\left(\frac{\partial h}{\partial \alpha}\right)\left(1 - \frac{\partial \psi_t}{\partial \psi_*}\right) D_0 f_1 + \upsilon_\parallel \mathbf{b}\cdot\nabla B \frac{mc}{Ze}\left(\frac{\partial h}{\partial \alpha}\right)\frac{\upsilon_\parallel^2 + \mu B}{\upsilon_\parallel B^2}\left(\frac{\partial f_1}{\partial \psi_*}\right) + c\Phi'\frac{\partial f_1}{\partial \alpha}} = 0. \tag{6.57}$$

Substituting in (6.26) and (6.18), the constraint for passing particles becomes

$$\sum_\gamma \gamma \int_0^{2\pi} d\alpha \int_{\check{B}}^{\hat{B}} dB \left[\frac{mc}{Ze}\frac{1}{K}\left(\frac{\partial h}{\partial \alpha}\right)^2\left(1 - \frac{\partial \psi_t}{\partial \psi_*}\right)\left(\frac{\partial \psi_t}{\partial \psi_*}\right)\frac{\upsilon_\parallel^2 + \mu B}{\upsilon_\parallel B^2}\left(\frac{\partial f_0}{\partial \psi_*}\right)\right. \tag{6.58}$$
$$\left. - \frac{mc}{Ze}\left(\frac{\partial \psi_t}{\partial \psi_*}\right)\left(\frac{\partial h}{\partial \alpha}\right)\frac{\upsilon_\parallel^2 + \mu B}{\upsilon_\parallel B^2}\left(\frac{\partial f_1}{\partial \psi_*}\right) - \frac{c\Phi'}{\upsilon_\parallel \mathbf{b}\cdot\nabla B}\left(\frac{\partial \psi_t}{\partial \psi_*}\right)\frac{\partial f_1}{\partial \alpha}\right] = 0.$$

Using the fact that f_0 and f_1 are independent of γ, it can be seen that this equation is always satisfied automatically. To see the $\partial f_1/\partial\alpha$ term vanishes, integrate the term by parts in α and use the identity (6.20).

For trapped particles, the constraint derived similarly from (6.57) is

$$\sum_\gamma \gamma \sum_\sigma \sigma \int_{\check{B}}^{B_c} dB \left[\frac{mc}{Ze}\frac{1}{K}\left(\frac{\partial h}{\partial \alpha}\right)^2\left(1 - \frac{\partial \psi_t}{\partial \psi_*}\right)\left(\frac{\partial \psi_t}{\partial \psi_*}\right)\frac{\upsilon_\parallel^2 + \mu B}{\upsilon_\parallel B^2}\left(\frac{\partial f_0}{\partial \psi_*}\right)\right. \tag{6.59}$$
$$\left. - \frac{mc}{Ze}\left(\frac{\partial \psi_t}{\partial \psi_*}\right)\left(\frac{\partial h}{\partial \alpha}\right)\frac{\upsilon_\parallel^2 + \mu B}{\upsilon_\parallel B^2}\left(\frac{\partial f_1}{\partial \psi_*}\right) - \frac{c\Phi'}{\upsilon_\parallel \mathbf{b}\cdot\nabla B}\left(\frac{\partial \psi_t}{\partial \psi_*}\right)\frac{\partial f_1}{\partial \alpha}\right] = 0.$$

The $\partial f_0/\partial\psi_*$ and $\partial f_1/\partial\psi_*$ terms vanish in the γ sum. However, the $\partial f_1/\partial\alpha$ term does not automatically vanish, giving the constraint

$$0 = \sum_\gamma \gamma \sum_\sigma \sigma \int_{\check{B}}^{B_c} dB \frac{1}{(\upsilon_\parallel + u)\,\mathbf{b}\cdot\nabla B}\frac{\partial f_1}{\partial \alpha} \tag{6.60}$$
$$= \sum_\gamma \gamma \sum_\sigma \sigma \int_{\check{B}}^{B_c} dB \frac{1}{(\upsilon_\parallel + u)\,\mathbf{b}\cdot\nabla B}\frac{\partial}{\partial \alpha}\left[g_1 - \left(\frac{\partial f_0}{\partial \psi_*}\right)\frac{mc}{Ze}\int_B^{B_c} dB' \left(\frac{\partial h'}{\partial \alpha}\right)\frac{\left(\upsilon_\parallel'\right)^2 + \mu B'}{\left(\upsilon_\parallel' + u'\right)B'^2}\right].$$

In the limit of vanishing radial electric field ($u \to 0$), then the drive term vanishes due to σ parity, and so $g_1 = 0$ would be a solution. However, for $u \neq 0$, (6.60) gives us a new α-dependent part of g_1 for trapped particles. We can write

$$\left(v'_\parallel\right)^2 = \left(v'_\parallel + u'\right)^2 - 2u'\left(v'_\parallel + u'\right) + (u')^2 \tag{6.61}$$

and carry out the σ sum to obtain

$$0 = \sum_\gamma \gamma \int_{\check{B}}^{B_c} dB \frac{1}{\left|v_\parallel + u\right| \mathbf{b}\cdot\nabla B} \frac{\partial}{\partial\alpha}\left[g_1 + 2\left(\frac{\partial f_0}{\partial\psi_*}\right)\frac{mc}{Ze}\int_B^{B_c} dB'\left(\frac{\partial h'}{\partial\alpha}\right)\frac{u'}{(B')^2}\right]. \tag{6.62}$$

Recalling g_1 is independent of B, we can then solve for $\partial g_1/\partial\alpha$:

$$\frac{\partial g_1}{\partial\alpha} = \frac{2c^2 K\Phi' m}{Ze}\left(\frac{\partial f_0}{\partial\psi_*}\right)\frac{\displaystyle\int_{\check{B}}^{B_c}\frac{dB}{\left|v_\parallel+u\right|}\left(\sum_\gamma\frac{\gamma}{\mathbf{b}\cdot\nabla B}\right)\int_B^{B_c}\frac{dB'}{(B')^3}\left(\frac{\partial^2 h'}{\partial\alpha^2}\right)}{\displaystyle\int_{\check{B}}^{B_c}\frac{dB}{\left|v_\parallel+u\right|}\left(\sum_\gamma\frac{\gamma}{\mathbf{b}\cdot\nabla B}\right)}. \tag{6.63}$$

An integration in α from 0 to 2π annihilates both the left-hand and right-hand sides. (The denominator is α-independent due to $\partial/\partial\alpha\left[\sum_\gamma(\gamma/\mathbf{b}\cdot\nabla B)\right] = 0$, and the numerator is a total $\partial/\partial\alpha$ derivative.) Thus, (6.63) does not provide a constraint. However, it does tell us the α-dependent part of g_1, which we display by writing

$$g_1 = \tilde{g}_1 + \bar{g}_1 \tag{6.64}$$

where

$$\tilde{g}_1 = \frac{2c^2 K\Phi' m}{Ze}\left(\frac{\partial f_0}{\partial\psi_*}\right)\frac{\displaystyle\int_{\check{B}}^{B_c}\frac{dB}{\left|v_\parallel+u\right|}\left(\sum_\gamma\frac{\gamma}{\mathbf{b}\cdot\nabla B}\right)\int_B^{B_c}\frac{dB'}{(B')^3}\left(\frac{\partial h'}{\partial\alpha}\right)}{\displaystyle\int_{\check{B}}^{B_c}\frac{dB}{\left|v_\parallel+u\right|}\left(\sum_\gamma\frac{\gamma}{\mathbf{b}\cdot\nabla B}\right)} \tag{6.65}$$

and $\bar{g}_1$ is a yet-undetermined flux function. We will determine $\bar{g}_1$ from the next (and final) constraint equation. Notice that as $u \to 0$, then $\tilde{g}_1 \to 0$ as well. Note also that we can equivalently write $\tilde{g}_1$ as a total $\partial/\partial\alpha$ derivative:

$$\tilde{g}_1 = \frac{\partial}{\partial\alpha}\left[\frac{2c^2 K\Phi' m}{Ze}\left(\frac{\partial f_0}{\partial\psi_*}\right)\frac{\displaystyle\int_{\check{B}}^{B_c}\frac{dB}{\left|v_\parallel+u\right|}\left(\sum_\gamma\frac{\gamma}{\mathbf{b}\cdot\nabla B}\right)\int_B^{B_c}\frac{h' dB'}{(B')^3}}{\displaystyle\int_{\check{B}}^{B_c}\frac{dB}{\left|v_\parallel+u\right|}\left(\sum_\gamma\frac{\gamma}{\mathbf{b}\cdot\nabla B}\right)}\right]. \tag{6.66}$$

6.4.7 Third order constraint equation

The last equation we must consider is (6.35). Applying (6.18) and (6.28), the constraint for passing particles can be written

$$\sum_\gamma \gamma \int_0^{2\pi} d\alpha \int_{\check{B}}^{\hat{B}} dB \left[\frac{1}{K} \left(\frac{\partial h}{\partial \alpha} \right) \left(1 - \frac{\partial \psi_t}{\partial \psi_*} \right) \left(\frac{\partial \psi_t}{\partial \psi_*} \right) \frac{C\{f_0\}}{\upsilon_\parallel \mathbf{b} \cdot \nabla B} \right. \tag{6.67}$$
$$\left. + \frac{mc}{Ze} \left(\frac{\partial \psi_t}{\partial \psi_*} \right) \left(\frac{\partial h}{\partial \alpha} \right) \frac{\upsilon_\parallel^2 + \mu B}{\upsilon_\parallel B^2} \left(\frac{\partial f_2}{\partial \psi_*} \right) + \frac{c\Phi'}{\upsilon_\parallel \mathbf{b} \cdot \nabla B} \left(\frac{\partial \psi_t}{\partial \psi_*} \right) \frac{\partial f_2}{\partial \alpha} - \left(\frac{\partial \psi_t}{\partial \psi_*} \right) \frac{C\{f_1\}}{\upsilon_\parallel \mathbf{b} \cdot \nabla B} \right] = 0.$$

The $C\{f_0\}$ and $\partial f_2/\partial \psi_*$ terms then both vanish after integrating by parts in α. To see that the $C\{f_0\}$ term vanishes, observe that f_0, $C\{f_0\}$, and h are all independent of γ, and apply (6.20). The $\partial f_2/\partial \psi_*$ term vanishes due to the property (6.56). The remaining terms are

$$c\Phi' \sum_\gamma \gamma \int_0^{2\pi} d\alpha \int_{\check{B}}^{\hat{B}} dB \frac{1}{\upsilon_\parallel \mathbf{b} \cdot \nabla B} \left(\frac{\partial \psi_t}{\partial \psi_*} \right) \frac{\partial}{\partial \alpha} \left[\int_B^{\hat{B}} dB' \left(\frac{\partial \psi_t}{\partial \psi_*} \right) \frac{C\{f_0\}}{\upsilon_\parallel \mathbf{b} \cdot \nabla B} \right] \tag{6.68}$$
$$= \sum_\gamma \gamma \int_0^{2\pi} d\alpha \int_{\check{B}}^{\hat{B}} dB \left(\frac{\partial \psi_t}{\partial \psi_*} \right) \frac{1}{\upsilon_\parallel \mathbf{b} \cdot \nabla B} C \left\{ g_1 - \frac{mc}{Ze} \left(\frac{\partial f_0}{\partial \psi_*} \right) \int_B^{\hat{B}} dB' \left(\frac{\partial h'}{\partial \alpha} \right) \frac{\left(\upsilon_\parallel' \right)^2 + \mu B'}{\left(\upsilon_\parallel' + u' \right) (B')^2} \right\}.$$

It can be seen that the $\partial f_0/\partial \psi_*$ drive term vanishes if it is integrated by parts in α. It also turns out that the $C\{f_0\}$ term vanishes. To see this is so, first define

$$y(B, \alpha, \gamma) = \frac{1}{\mathbf{b} \cdot \nabla B}. \tag{6.69}$$

The identity (6.20) is equivalent to

$$\frac{\partial}{\partial \alpha} y(B, \alpha, +) = \frac{\partial}{\partial \alpha} y(B, \alpha, -). \tag{6.70}$$

Integrating,

$$y(B, \alpha, +) = y(B, \alpha, -) + A(B) \tag{6.71}$$

for some function $A(B)$. The $C\{f_0\}$ term in (6.68) is proportional to a B and B' integral of X where

$$X = \int_0^{2\pi} d\alpha \left[y(B, \alpha, +) \frac{\partial}{\partial \alpha} y(B', \alpha, +) - y(B, \alpha, -) \frac{\partial}{\partial \alpha} y(B', \alpha, -) \right]. \tag{6.72}$$

Applying (6.71) to the first term,

$$X = \int_0^{2\pi} d\alpha \left[A \frac{\partial}{\partial \alpha} y(B', \alpha, +) + y(B, \alpha, -) \frac{\partial}{\partial \alpha} y(B', \alpha, -) - y(B, \alpha, -) \frac{\partial}{\partial \alpha} y(B', \alpha, -) \right]. \tag{6.73}$$

The first term vanishes since it is a total derivative, and the second and third terms cancel each other, leaving $X = 0$.

Thus, the top line in (6.68) vanishes, so we are left with

$$0 = \sum_\gamma \gamma \int_0^{2\pi} d\alpha \int_{\check{B}}^{\hat{B}} dB \left(\frac{\partial \psi_t}{\partial \psi_*}\right) \frac{1}{\upsilon_\parallel \mathbf{b}\cdot\nabla B} C\{g_1\}. \tag{6.74}$$

There is no drive left for g_1, so the physically sensible solution is $g_1 = 0$.

For trapped particles, we again apply (6.18) and (6.28) to the constraint equation (6.35), this time obtaining

$$\begin{aligned}\sum_\gamma \gamma \sum_\sigma \sigma \int_{\check{B}}^{B_c} dB \Bigg[&\frac{1}{K}\left(\frac{\partial h}{\partial \alpha}\right)\left(1 - \frac{\partial \psi_t}{\partial \psi_*}\right)\left(\frac{\partial \psi_t}{\partial \psi_*}\right)\frac{C\{f_0\}}{\upsilon_\parallel \mathbf{b}\cdot\nabla B} \\ &+ \frac{mc}{Ze}\left(\frac{\partial \psi_t}{\partial \psi_*}\right)\left(\frac{\partial h}{\partial \alpha}\right)\frac{\upsilon_\parallel^2 + \mu B}{\upsilon_\parallel B^2}\left(\frac{\partial f_2}{\partial \psi_*}\right) + \frac{c\Phi'}{\upsilon_\parallel \mathbf{b}\cdot\nabla B}\left(\frac{\partial \psi_t}{\partial \psi_*}\right)\frac{\partial f_2}{\partial \alpha} - \left(\frac{\partial \psi_t}{\partial \psi_*}\right)\frac{C\{f_1\}}{\upsilon_\parallel \mathbf{b}\cdot\nabla B}\Bigg] = 0.\end{aligned} \tag{6.75}$$

This equation contains two yet-unknown quantities: $\bar{g}_1$ and g_2. It will turn out that if (6.75) is integrated in α, the g_2 dependence disappears, leaving a simpler equation to determine $\bar{g}_1$. The original α-dependent constraint equation (6.75) is still solvable due to the freedom remaining in g_2.

In the α-averaged equation, the $C\{f_0\}$ and $\partial f_2/\partial \psi_*$ terms vanish upon integrating by parts in α and applying (6.20) and (6.56). We are left with

$$\begin{aligned}\int_0^{2\pi} d\alpha \int_{\check{B}}^{B_c} dB \sum_\gamma \gamma \sum_\sigma \sigma \frac{c\Phi'}{\upsilon_\parallel \mathbf{b}\cdot\nabla B}\left(\frac{\partial \psi_t}{\partial \psi_*}\right)\frac{\partial}{\partial \alpha}\left[g_2 + \int_{\check{B}}^{B} dB' \left(\frac{\partial \psi_t}{\partial \psi_*}\right)\frac{C\{f_0\}}{\upsilon_\parallel \mathbf{b}\cdot\nabla B}\right] \\ = \int_0^{2\pi} d\alpha \int_{\check{B}}^{B_c} dB \sum_\gamma \gamma \sum_\sigma \sigma \left(\frac{\partial \psi_t}{\partial \psi_*}\right)\frac{1}{\upsilon_\parallel \mathbf{b}\cdot\nabla B}\times \\ C\left\{\bar{g}_1 + \tilde{g}_1 - \frac{mc}{Ze}\left(\frac{\partial f_0}{\partial \psi_*}\right)\int_B^{\hat{B}} dB' \left(\frac{\partial h'}{\partial \alpha}\right)\frac{\left(\upsilon_\parallel'\right)^2 + \mu B'}{\left(\upsilon_\parallel' + u'\right)(B')^2}\right\}.\end{aligned} \tag{6.76}$$

Since g_2 is independent of γ, the g_2 term vanishes upon integration by parts in α. The $C\{f_0\}$ term will vanish for the same reason as described in (6.72)-(6.73). The $\tilde{g}_1$ term vanishes if we recognize that $\tilde{g}_1$ is a total $\partial/\partial\alpha$ derivative (6.66) and is γ-independent, so upon integrating by parts in α, the Cary-Shasharina theorem (6.20) can be applied. The $\partial f_0/\partial \psi_*$ term similarly vanishes. We are left with

$$0 = \int_0^{2\pi} d\alpha \int_{\check{B}}^{B_c} dB \sum_\gamma \gamma \sum_\sigma \sigma \left(\frac{\partial \psi_t}{\partial \psi_*}\right)\frac{1}{\upsilon_\parallel \mathbf{b}\cdot\nabla B} C\{\bar{g}_1\}. \tag{6.77}$$

There is consequently no drive for $\bar{g}_1$, and so the only physically sensible solution is $\bar{g}_1 = 0$.

We have now completely determined the distribution function through order f_1.

6.4.8 Summary of distribution function

We make one last approximation, replacing $\partial f_0/\partial\psi_* \to \partial F/\partial\psi_*$ in f_1. Then the distribution function through order f_1 for passing particles is

$$f \approx F + g_0 - \frac{mc}{Ze}\left(\frac{\partial F}{\partial \psi_*}\right)\int_B^{\hat{B}} dB'\left(\frac{\partial h'}{\partial \alpha}\right)\frac{\left(v_\parallel'\right)^2 + \mu B'}{\left(v_\parallel' + u'\right)(B')^2} \tag{6.78}$$

where, again,

$$F = \eta(\psi_*)\left[\frac{m}{2\pi T(\psi_*)}\right]^{3/2}\exp\left(-\frac{mE}{T(\psi_*)}\right). \tag{6.79}$$

The equation for g_0, given by (6.48), is completely independent of α and it is identical to the quasisymmetric case. From the model collision operator developed in Chapt. 5, g_0 is given to leading order in $\sqrt{\varepsilon}$ by (5.48). For trapped particles,

$$f \approx F + \tilde{g} - \frac{mc}{Ze}\left(\frac{\partial F}{\partial \psi_*}\right)\int_B^{B_c} dB'\left(\frac{\partial h'}{\partial \alpha}\right)\frac{\left(v_\parallel'\right)^2 + \mu B'}{\left(v_\parallel' + u'\right)(B')^2} \tag{6.80}$$

where

$$\tilde{g} = \frac{2c^2 K\Phi' m}{Ze}\left(\frac{\partial F}{\partial \psi_*}\right)\frac{\displaystyle\int_{\check{B}}^{B_c}\frac{dB}{\left|v_\parallel + u\right|}\left(\sum_\gamma \frac{\gamma}{\mathbf{b}\cdot\nabla B}\right)\int_B^{B_c}\frac{dB'}{(B')^3}\left(\frac{\partial h'}{\partial \alpha}\right)}{\displaystyle\int_{\check{B}}^{B_c}\frac{dB}{\left|v_\parallel + u\right|}\left(\sum_\gamma \frac{\gamma}{\mathbf{b}\cdot\nabla B}\right)}. \tag{6.81}$$

The $\tilde{g}$ and $\partial F/\partial\psi_*$ terms in (6.80) are formally the same order, so either one can dominate the other.

6.4.9 Consistency of the ordering

Now that the distribution functions f_0 and f_1 are known, the regime of validity of the ordering in section 6.3 can be further investigated. The asymptotic procedure required $f_1 \ll f_0$, which will be consistent if $\tilde{g} \ll F$ and $f_{\rm QI} \ll F$, where

$$f_{\rm QI} = -\frac{mc}{Ze}\left(\frac{\partial F}{\partial \psi_*}\right)\int_B^{B_x} dB'\left(\frac{\partial h'}{\partial \alpha}\right)\frac{\left(v_\parallel'\right)^2 + \mu B'}{\left(v_\parallel' + u'\right)(B')^2}. \tag{6.82}$$

Here B_x=B_c for trapped particles and $B_x = \hat{B}$ for the passing particles. From (3.17) and $K \ll I$ we estimate $\partial h/\partial\alpha \sim I \sim RB$ where R is the major radius. As shown in figure

3-2, $\partial h/\partial\alpha$ in practice tends to be smaller than this estimate, so we refine the estimate to $\partial h/\partial\alpha \sim \delta RB$ where $\delta \leq 0.3$. We also estimate $2\pi\psi_t \sim \pi r^2 B$ where r is the minor radius, so $|\nabla\psi_t| \sim rB$. Then $\partial F/\partial\psi_* \sim \partial F/\partial\psi_t \sim |\nabla\psi_t|^{-1}\partial F/\partial r \sim F/(rBr_T)$, where r_T is the scale length for temperature or pseudo-density. We thereby estimate

$$\frac{f_{\rm QI}}{F} \sim \delta\frac{R}{r}\frac{\rho}{r_T}, \tag{6.83}$$

where $\rho = \upsilon_i/\Omega$ is the thermal ion gyrofrequency. In typical stellarators, $R/r \sim 10$. The last factor ρ/r_T above is usually very small compared to 0.3 in stellarator experiments, and so $f_{\rm QI} \ll F$ should be a good approximation.

Similarly, we estimate

$$\frac{\tilde{g}}{F} \sim \frac{2c^2K\Phi' m}{Ze|\nabla\psi_t|r_T B^2}\frac{\partial h}{\partial\alpha} \sim 2\delta\left(\frac{R}{r}\right)^2\frac{K}{I}\frac{\rho}{r_T}M_E \tag{6.84}$$

where $M_E = cE_r/(\upsilon_i B)$ is the Mach number associated with the $\mathbf{E}\times\mathbf{B}$ flow. In a non-quasisymmetric device, M_E must be small compared to unity [12], and indeed, M_E is typically small in any laboratory experiment. The fraction K/I is the ratio of plasma to coil current, so it will be very small. (Recall from the discussion in the conclusion to Chapt. 3 that K/I will be $< 1/60$ in W7-X.) The ordering $\tilde{g} \ll F$ thus seems quite appropriate.

6.5 Flows and current

The parallel flow can in principle be obtained by forming the integral $V_\parallel = n^{-1}\int d^3\upsilon\,\upsilon_\parallel f$ of the distribution function above. However, this task is daunting due to the complexity of the terms in f. The calculation can be dramatically simplified by exploiting several results from Chapt. 3. Recall that in section 3.3.1, it was found that

$$V_\parallel = \frac{B\langle V_\parallel B\rangle}{\langle B^2\rangle} + V_\parallel^{\rm PS}, \tag{6.85}$$

where

$$V_\parallel^{\rm PS} = \frac{c}{B}\left(\frac{d\Phi}{d\psi_t} + \frac{1}{Zen}\frac{dp}{d\psi_t}\right)\left[\left(1 - \frac{B^2}{\langle B^2\rangle}\right)K + \Upsilon\right] \tag{6.86}$$

is the Pfirsch-Schlüter flow, satisfying $\left\langle V_\parallel^{\rm PS}B\right\rangle = 0$, and

$$\Upsilon = 2B^2\frac{qI+K}{q}\int_{\zeta_x}^{\zeta}\frac{d\zeta'}{B'^3}\left(\frac{\partial B'}{\partial\theta'}\right)_{\zeta'}. \tag{6.87}$$

These results were derived using only incompressibility $\nabla\cdot(n\mathbf{V}) = 0$ and the form of the perpendicular flow $\mathbf{V}_\perp = cB^{-2}\left[(d\Phi/d\psi_t) + c\,(dp/d\psi_t)\,/\,(Zen)\right]\mathbf{B}\times\nabla\psi_t$, two results which remain true in the finite-E_r ordering. Hence, we need only evaluate $\langle V_\parallel B\rangle$ rather than $V_\parallel$

itself, for once $\langle V_\parallel B\rangle$ is known, the full $V_\parallel$ can be constructed using (6.85).

In evaluating $\langle V_\parallel B\rangle = \langle n^{-1} B \int d^3v\, v_\parallel f\rangle$, none of the α-dependent terms in the distribution function contribute, due to the property $\langle \partial X/\partial\alpha\rangle = 0$ for any branch-independent X. Consequently,

$$\langle V_\parallel B\rangle = \langle n^{-1} B \int d^3v\, v_\parallel (F + g_0)\rangle. \tag{6.88}$$

The only terms that remain on the right-hand side are the ones which arise in a quasi-poloidally symmetric plasma. For the main ions, then, we can use the result from section 5.3.5:

$$\langle V_{\mathrm{i}\parallel} B\rangle = \frac{KcT_\mathrm{i}}{Ze}\left[\frac{1}{p_\mathrm{i}}\frac{dp_\mathrm{i}}{d\psi_\mathrm{t}} + \frac{Ze}{T_\mathrm{i}}\frac{d\Phi}{d\psi_\mathrm{t}} - 1.17\frac{A_\mathrm{ban}(U)}{T_\mathrm{i}}\frac{dT_\mathrm{i}}{d\psi_\mathrm{t}}\right] \tag{6.89}$$

where $A_\mathrm{ban}(U)$ is the dimensionless function in figure 5-1.b. Above we have set $\psi_\mathrm{h} \to -N\psi_\mathrm{t}$ and $I_\mathrm{h} \to NK$ to specialize from general to poloidal quasisymmetry. Using (6.85), then the total parallel flow is

$$V_{\mathrm{i}\parallel} = -1.17 A_\mathrm{ban}(U)\frac{KcB}{Ze\langle B^2\rangle}\frac{dT_\mathrm{i}}{d\psi_\mathrm{t}} + \frac{c}{B}\left(\frac{d\Phi}{d\psi_\mathrm{t}} + \frac{1}{Zen_\mathrm{i}}\frac{dp_\mathrm{i}}{d\psi_\mathrm{t}}\right)(K + \Upsilon)\,. \tag{6.90}$$

Now that the ion flow is known, the parallel current can be determined as described in section 3.5. The result is

$$j_\parallel = \frac{B\langle j_\parallel B\rangle}{\langle B^2\rangle} + j_\parallel^\mathrm{PS}, \tag{6.91}$$

where

$$j_\parallel^\mathrm{PS} = \frac{c}{B}\left(\frac{dp}{d\psi_\mathrm{t}}\right)\left[\left(1 - \frac{B^2}{\langle B^2\rangle}\right)K + \Upsilon\right] \tag{6.92}$$

is the Pfirsch-Schlüter current, satisfying $\left\langle j_\parallel^\mathrm{PS} B\right\rangle = 0$, $p = p_\mathrm{e} + p_\mathrm{i}$ is the total pressure, and

$$\begin{aligned}\langle j_\parallel B\rangle =& f_\mathrm{t} Kc\frac{Z^2 + 2.21Z + 0.75}{Z\left(\sqrt{2} + Z\right)} \\ &\times\left(\frac{dp_\mathrm{i}}{d\psi_\mathrm{t}} + \frac{dp_\mathrm{e}}{d\psi_\mathrm{t}} - \frac{2.07Z + 0.88}{Z^2 + 2.21Z + 0.75}n_\mathrm{e}\frac{dT_e}{d\psi_\mathrm{t}} - 1.17A_\mathrm{ban}(U)\frac{n_\mathrm{e}}{Z}\frac{dT_\mathrm{i}}{d\psi_\mathrm{t}}\right).\end{aligned} \tag{6.93}$$

As in Chapt. 3, $f_\mathrm{t} = 1 - f_\mathrm{c}$ is the effective trapped fraction and f_c is given by (3.42).

6.6 Radial fluxes and electric field

To evaluate the radial particle flux, we can reuse equation (3.50) from the small-E_r analysis in Chapt. 3:

$$\langle \boldsymbol{\Gamma}\cdot\nabla\psi_\mathrm{t}\rangle = -\left\langle \int d^3v\, v_\parallel \Delta\mathbf{b}\cdot\nabla f\right\rangle \tag{6.94}$$

where $\Delta = -K\upsilon_\parallel\Omega^{-1} + S$ and

$$S = -\frac{mc}{Ze}\int_B^{B_x} dB' \left(\frac{\partial h'}{\partial \alpha}\right)_{B'} \frac{(\upsilon_\parallel')^2 + \mu B'}{\upsilon_\parallel'(B')^2}. \tag{6.95}$$

It can be verified that these equations are all still valid in the finite-E_r ordering. Notice the integral in (6.95) is performed at constant ψ_t rather than constant ψ_*. Substituting the drift kinetic equation into (6.94) gives

$$\langle \mathbf{\Gamma}\cdot\nabla\psi_\mathrm{t}\rangle = -\left\langle \int d^3\upsilon\, \Delta\,(C - \mathbf{v}_\mathrm{d}\cdot\nabla f)\right\rangle. \tag{6.96}$$

In the small-E_r ordering, the $\mathbf{v}_\mathrm{d}\cdot\nabla f$ term above can be approximated by $(\mathbf{v}_\mathrm{d}\cdot\nabla\psi_\mathrm{t})(\partial f_\mathrm{M}/\partial\psi_\mathrm{t})$, and the latter does not contribute to the integral in (6.96) due to $\mathrm{sgn}(\upsilon_\parallel)$ parity. However, in the ordering developed in this chapter, other $(\mathbf{v}_\mathrm{d}\cdot\nabla\psi_\mathrm{t})(\partial f/\partial\psi_\mathrm{t})$ and $\mathbf{v}_\mathbf{E}\cdot\nabla f$ terms become equally important and they give nonvanishing contributions to (6.96). Due to the complexity of the terms in f it is not possible in general to obtain the radial particle flux analytically.

Analytic progress becomes possible, however, in the limit $K \to 0$. This limit is interesting as it corresponds to a self-consistent current profile when there is absolutely no departure from omnigenity anywhere inside the flux surface of interest and also no current driven by RF, neutral beams, or a transformer, as discussed at the end of section 3.5. Examining the definition (6.12), the distinction between ψ_* and ψ_t disappears in this limit. Furthermore, $u \propto K$ so $u \to 0$. In this case the calculation of E_r reduces to the problem solved in section 3.4, and so we recover the radial electric field derived there:

$$\frac{Ze}{T_\mathrm{i}}\frac{d\Phi}{d\psi_\mathrm{t}} = -\frac{1}{p_\mathrm{i}}\frac{dp_\mathrm{i}}{d\psi_\mathrm{t}} + \frac{1.17}{T_\mathrm{i}}\frac{dT_\mathrm{i}}{d\psi_\mathrm{t}}. \tag{6.97}$$

Thus, the radial electric field reduces to the one obtained in Chapt. 3 in the limit $K \to 0$. For other values of K, presumably E_r will be different from (6.97). If so, then if plasma current is driven using neutral beams or RF waves, K can be experimentally controlled, thereby allowing some control over E_r, unlike the small-E_r case in which E_r is fixed by (6.97).

6.7 Discussion and conclusion

In this chapter we have constructed an ordering in which finite-E_r effects can be derived analytically for a quasi-isodynamic plasma. The procedure is based upon a novel grouping of the terms in the drift kinetic equation, exploiting the fact that in any asymptotic expansion, small terms can always be added or subtracted from expressions having terms of larger magnitude. We can thereby arrange for the leading-order drift kinetic equation to be one in which a quantity ψ_* is conserved, even though this quantity is not conserved by the full drift

kinetic operator. The leading order equation then resembles the problem solved in Chapt. 5, and so results from that earlier chapter can be reused. However, in the quasi-isodynamic case, the terms in the higher order kinetic equations lead to new α-dependent terms in the distribution function which did not appear in the quasisymmetric case. One such term, the last term in (6.78) and (6.80), resembles a term from the small-E_r quasi-isodynamic distribution function (3.32), but with $v_\parallel \to v_\parallel + u$. Another term (6.81) appears which has no analogue in any of the previous calculations.

The results in this chapter continuously reduce to results from previous chapters in the appropriate limits. Specifically, in the quasisymmetric limit $h \to 0$, the distribution function, flow, and bootstrap current in this chapter reduce to the corresponding expressions in Chapt. 5. Also, if h is nonzero but the normalized electric field U is much less than unity, expressions from the present chapter reduce to those of Chapt. 3.

Exploiting general results from Chapt. 3 that give the form of $V_\parallel$ and $j_\parallel$ required to satisfy $\nabla \cdot n\mathbf{V} = 0$ and $\nabla \cdot \mathbf{j} = 0$, it has been possible to find $V_\parallel$ and $j_\parallel$ for a finite-E_r quasi-isodynamic plasma without directly integrating all the terms in the distribution function. The expression for the radial drifts is more complicated in the finite-E_r quasi-isodynamic case compared to the finite-E_r quasisymmetric case or the small-E_r quasi-isodynamic case due to the $\mathbf{v}_\mathrm{d} \cdot \nabla f$ term in (6.96). Consequently, an explicit expression for the radial electric field does not exist in general. However, analytic solution for E_r does become possible in the interesting and important limit $K \to 0$, in which case the result of Chapt. 3 is recovered.

The results herein are perhaps most useful for verification of codes that attempt to calculate finite-E_r effects in general stellarators, since experiments like W7-X are not and cannot be precisely quasi-isodynamic. In such codes, the collisionality, E_r, and magnetic geometry can be specified so the ordering developed here is satisfied.

CHAPTER 7

Conclusion

In the preceding chapters, neoclassical transport in optimized stellarators has been analyzed in two regimes: the conventional small-E_r ordering and the finite-E_r ordering. In the small-E_r regime, the $\mathbf{E} \times \mathbf{B}$ drift is taken to be much smaller than any component of the parallel speed. In the finite-E_r ordering, the $\mathbf{E} \times \mathbf{B}$ drift is still smaller than the parallel speed in overall magnitude, but due to geometric effects, the ∇f components of the $\mathbf{E} \times \mathbf{B}$ drift and parallel velocity can be comparable. The finite-E_r ordering can be appropriate for HSX and other stellarators that exhibit Core Electron-Root Confinement [56, 68], as well as for pedestals and internal transport barriers observed in stellarators [66, 67].

The new results derived in this thesis fall into four categories, corresponding to Chapt. 3-6. First, in Chapt. 3, we have calculated compact expressions for the flows, current, and radial electric field in a quasi-isodynamic stellarator, using the conventional small-E_r ordering. These expressions are all new, although other authors had argued previously that a self-consistent state free of toroidal current would be possible [17, 20], in agreement with the calculation here. In a general stellarator, the Pfirsch-Schlüter flows and Pfirsch-Schlüter current can only be written as the solution of a partial differential equation, but we have shown that in a quasi-isodynamic field, these quantities can be written explicitly in terms of Υ, which is an integral of $B(\theta, \zeta)$. The Pfirsch-Schlüter flows and Pfirsch-Schlüter current we have derived are, by definition, independent of collisionality. Our expressions for the remaining terms in the flow and current, as well as the equation for the radial electric field, are derived for the long-mean-free-path regime. Our findings demonstrate that quasi-isodynamic fields are a useful ideal to consider: they can be a reasonable model for W7-X-like stellarators, they are more general than poloidally symmetric fields, and yet they permit explicit analytic results to be derived that are nearly as compact as results for quasisymmetric or axisymmetric fields.

Second, in Chapt. 4, we have shown that there is a fundamental problem with previous treatments of the finite-E_r regime in stellarators. We have done so by analytically calculating the particle orbits in a quasisymmetric field for both the true equations of motion and for

the monoenergetic DKES equations. We derived new analytic expressions for the fraction of trapped particles in each model. While both models correctly find the trapped fraction to scale as $\exp(-U^2)$ where U is a normalized radial electric field, DKES systematically under-predicts the trapped fraction, and the amount of this error can exceed a factor of two in experimentally relevant conditions. Trapped particles play a central role in neoclassical theory, and so DKES is likely making errors of this same relative size.

Third, to correct this problem, in Chapt. 5 we have presented a new analysis of the finite-E_r regime in a quasisymmetric stellarator. Our analysis does not employ the problematic monoenergetic approximation. Expressions were calculated for the ion heat flux, flow, and bootstrap current in both the banana and plateau regimes. All of these quantities turn out to be modified in a similar manner to the corresponding quantities in a tokamak pedestal. The heat flux exhibits $\exp(-U^2)$ scaling as it is proportional to the trapped particle fraction. Another important finding is that the bootstrap current is enhanced in the finite-E_r regime compared to the small-E_r regime, regardless of the sign of E_r.

Finally, in Chapt. 6 we have analyzed finite-E_r effects in a quasi-isodynamic stellarator. A regime of finite E_r and collisionality was identified in which the kinetic equation can be solved analytically and without making the problematic monoenergetic approximation. The radial electric field drives modifications to the distribution function that have no analogue in the quasisymmetric finite-E_r or the quasi-isodynamic small-E_r cases. Explicit formulae were derived for the ion flow and bootstrap current. In appropriate limits, the distribution function, flow, current, and ambipolar E_r reduce to results from the previous chapters.

One primary implication of the results herein is that a new continuum neoclassical code should be developed to replace DKES (and the derivative code PENTA). The new code would need to be radially nonlocal, to account for the change in potential energy over an orbit. Such finite-orbit-effects on *radial* transport can be examined with Monte-Carlo codes, but in calculating parallel flows and the bootstrap current, the near cancelation between $v_\parallel > 0$ and $v_\parallel < 0$ particles leads to large noise in any estimate of parallel transport [74]. Thus, the new code should be Eulerian (continuum). The analytic results derived in Chapt. 5 and 6 can be used for benchmarking. The new code would ideally use the full Fokker-Planck collision operator (either in the original nonlinear form or linearized about a Maxwellian), for as shown in Chapt. 5, a momentum-conserving pitch-angle-scattering operator will not be an accurate approximation. The proposed new code would then be the first to solve the drift kinetic equation without further approximation, making it the first to include all the physics necessary for accurate modeling of HSX and other CERC-regime stellarators.

The code would be useful not just for stellarators but also for tokamaks. Even for a perfectly axisymmetric tokamak, no continuum neoclassical code presently exists to calculate the finite-orbit-width effects in an H-mode pedestal, and so the new code would fill this gap. The code would enable calculation of the finite-orbit-width-induced modification of the bootstrap current in the pedestal, which will impact studies of ELM stability. Also, the code could be used to calculate the neoclassical toroidal viscosity (NTV) associated with tokamak error fields. The finite-orbit-width physics in the code would be important in the pedestal where ripple is relatively large compared to the core. As NTV damps toroidal ro-

tation, increasing susceptibility to locked modes and disruptions, the code would therefore enable improved calculation of the error field tolerance for ITER.

APPENDIX A

Omnigenity

In this appendix we will first prove the equivalence of the two definitions of omnigenity: 1) the bounce-averaged radial drift vanishes, and 2) the longitudinal adiabatic invariant is a flux function. Then, we will derive (3.3).

We begin by considering a general (not necessarily optimized) stellarator equilibrium. Using (2.27) we can write $\mathbf{v}_\mathrm{d}\cdot\nabla\psi_\mathrm{t} = (v_\parallel/\Omega)\nabla\cdot[(v_\parallel/\Omega)\mathbf{B}\times\nabla\psi_\mathrm{t}]$. Next, we consider Boozer coordinates θ and ζ, defining a field line label $\alpha = \theta - \iota\zeta$ so $\mathbf{B} = \nabla\psi_\mathrm{t}\times\nabla\alpha$. Treating $(\psi_\mathrm{t},\alpha,\zeta)$ as independent variables, then from the form of the divergence in general coordinates,

$$\mathbf{v}_\mathrm{d}\cdot\nabla\psi_\mathrm{t} = \frac{mc}{Ze}v_\parallel\mathbf{b}\cdot\nabla\zeta\left[\left(\frac{\partial}{\partial\alpha}\right)_\zeta\left(\frac{v_\parallel}{\mathbf{b}\cdot\nabla\zeta}\right) - \left(\frac{\partial}{\partial\zeta}\right)_\alpha\left(\frac{Kv_\parallel}{B}\right)\right]. \tag{A.1}$$

Next, we define the bounce average, which for any quantity A is

$$\bar{A} = \frac{1}{\tau}\oint\frac{A\,d\ell}{v_\parallel} \qquad \text{where} \qquad \tau = \oint\frac{d\ell}{v_\parallel}. \tag{A.2}$$

Here, ℓ is the distance along a field line, and $\oint$ indicates an integral along a full bounce. Equivalently, in terms of the ζ coordinate,

$$\bar{A} = \frac{1}{\tau}\sum_\varsigma \varsigma\int_{\zeta_-}^{\zeta_+}\frac{A\,d\zeta}{v_\parallel\mathbf{b}\cdot\nabla\zeta} \qquad \text{where} \qquad \tau = \sum_\varsigma\varsigma\int_{\zeta_-}^{\zeta_+}\frac{d\zeta}{v_\parallel\mathbf{b}\cdot\nabla\zeta}, \tag{A.3}$$

$\varsigma = \mathrm{sgn}(v_\parallel)$, and ζ_- and ζ_+ are the two bounce points (where $v_\parallel = 0$). Notice that the integrals in (A.2)-(A.3) are performed at constant α. Applying the bounce average to (A.1) gives

$$\overline{\mathbf{v}_\mathrm{d}\cdot\nabla\psi_\mathrm{t}} = \frac{mc}{Ze\tau}\sum_\varsigma\varsigma\int_{\zeta_-}^{\zeta_+}d\zeta\left(\frac{\partial}{\partial\alpha}\right)_\zeta\left(\frac{v_\parallel}{\mathbf{b}\cdot\nabla\zeta}\right). \tag{A.4}$$

Even though ζ_- and ζ_+ depend on α, it is valid to pull the $\partial/\partial\alpha$ derivative in front of the integral in (A.4) because the integrand vanishes at these endpoints. Thus,

$$\overline{\mathbf{v}_\mathrm{d}\cdot\nabla\psi_\mathrm{t}} = \frac{mc}{Ze\tau}\frac{\partial}{\partial\alpha}\sum_\varsigma \varsigma\int_{\zeta_-}^{\zeta_+} d\zeta\left(\frac{v_\parallel}{\mathbf{b}\cdot\nabla\zeta}\right). \tag{A.5}$$

Now, consider the longitudinal invariant for trapped particles:

$$J(\psi_\mathrm{t},\alpha,v,\lambda) = \oint v_\parallel\, d\ell \tag{A.6}$$

where the integration is again carried out along a full bounce. Using $d\ell = d\zeta/\mathbf{b}\cdot\nabla\zeta$ in this definition, then (A.5) can be written

$$\overline{\mathbf{v}_\mathrm{d}\cdot\nabla\psi_\mathrm{t}} = \frac{mc}{Ze\tau}\frac{\partial J}{\partial\alpha}. \tag{A.7}$$

Consequently, the bounce-averaged radial drift vanishes if and only if the longitudinal invariant J is a flux function, and so the two definitions of omnigenity are equivalent.

Now we move on to the proof that (3.3) must hold in an omnigenous field. Here we rewrite J using $d\ell = dB/\mathbf{b}\cdot\nabla B$ to obtain

$$J = 2v\int_{\check{B}}^{\check{B}/\lambda} dB\,\sqrt{1-\lambda B/\check{B}}\sum_\gamma \frac{\gamma}{\mathbf{b}\cdot\nabla B} \tag{A.8}$$

where the factor of 2 arises from a sum over ς, and the integral is performed at fixed ψ_t, α, λ, and v. Applying a $(\partial/\partial\alpha)_{\psi_\mathrm{t},v,\lambda}$ derivative, and noting that $\partial J/\partial\alpha = 0$ due to omnigenity, then

$$0 = \int_{\check{B}}^{x} dB\, g_\mathrm{CS}\,\sqrt{x-B} \tag{A.9}$$

where

$$g_\mathrm{CS}(\psi,\,\alpha,\,B) = \left(\frac{\partial}{\partial\alpha}\right)_B\sum_\gamma\frac{\gamma}{\mathbf{b}\cdot\nabla B} \tag{A.10}$$

and $x = \check{B}/\lambda$. The original definition of the longitudinal invariant (A.6) was valid for all trapped particles (i.e. for $\lambda > \check{B}/\hat{B}$ and $\lambda < 1$), and so (A.9) is true for any x between $\check{B}$ and $\hat{B}$.

It is proven in the appendix of [9] that in this situation, g_CS must vanish at all locations. We repeat the argument here for convenience. First, (A.10) is divided by $\sqrt{y-x}$, where y is any value in the range $(\check{B},\hat{B})$, and the result is integrated in x from $\check{B}$ to y. The order of

the B and x integrals is reversed, giving

$$0 = \int_{\check{B}}^{y} dB\, g_{\mathrm{CS}}(B) \int_{B}^{y} dx \sqrt{\frac{x-B}{y-x}} = \frac{\pi}{2} \int_{\check{B}}^{y} dB\, g_{\mathrm{CS}}(B)(y-B). \tag{A.11}$$

Differentiating once with respect to y and dropping the $\pi/2$ gives

$$0 = \underbrace{g_{\mathrm{CS}}(y)(y-y)}_{=0} + \int_{\check{B}}^{y} dB\, g_{\mathrm{CS}}(B) = \int_{\check{B}}^{y} dB\, g_{\mathrm{CS}}(B). \tag{A.12}$$

Differentiating again with respect to y gives $g_{\mathrm{CS}}(y) = 0$. As y was allowed to have any value in the range $(\check{B}, \hat{B})$, then g_{CS} must vanish everywhere, proving the Cary-Shasharina theorem (3.3).

APPENDIX B

Conservation of canonical momentum

Here we establish a few technical results related to the conservation of canonical momentum in axisymmetric and quasisymmetric fields.

Vanishing of $\mathbf{v}_\mathrm{d} \cdot \nabla(I\upsilon_\parallel/\Omega)$ in axisymmetry

Consider $X = \mathbf{v}_\mathrm{d} \cdot \nabla(I\upsilon_\parallel/\Omega)$, a term that was neglected in deriving the conservation of Ψ_* in section 2.1.1 since it was formally small. Here we prove that X is in fact exactly zero, so the term could have been retained in section 2.1.1. Using the form of the drifts $\mathbf{v}_\mathrm{d} = (\upsilon_\parallel/\Omega)\,\nabla \times (\upsilon_\parallel \mathbf{b})$, a form that includes the parallel velocity correction, then

$$\begin{aligned} X &\propto \nabla \times \left(\frac{\upsilon_\parallel}{B}\mathbf{B}\right) \cdot \nabla\left(\frac{I\upsilon_\parallel}{B}\right) \qquad \text{(B.1)} \\ &= \frac{\upsilon_\parallel^2}{B^2}\nabla \times \mathbf{B} \cdot \nabla I + \left[\nabla\left(\frac{\upsilon_\parallel}{B}\right) \times \mathbf{B} \cdot \nabla I\right]\frac{\upsilon_\parallel}{B} + \frac{I\upsilon_\parallel}{B}\nabla \times \mathbf{B} \cdot \nabla\left(\frac{\upsilon_\parallel}{B}\right). \end{aligned}$$

The first term in the last line vanishes because $\nabla \times \mathbf{B} \cdot \nabla\psi_\mathrm{p} = 0$ and $\nabla I = I'\nabla\psi_\mathrm{p}$ where $I' = dI/d\psi_\mathrm{p}$. Thus,

$$X \propto I'\nabla S \cdot \mathbf{B} \times \nabla\psi_\mathrm{p} + I\nabla \times \mathbf{B} \cdot \nabla S \qquad \text{(B.2)}$$

where $S = \upsilon_\parallel/B$. As $\mathbf{B} \times \nabla\psi_\mathrm{p} = I\mathbf{B} - R^2B^2\nabla\phi$ and $\partial S/\partial\phi = 0$, then the first right-hand-side term in (B.2) equals $II'\mathbf{B} \cdot \nabla S$. The last term in (B.2) is evaluated using

$$\nabla \times \mathbf{B} \cdot \nabla S = \nabla \cdot (\mathbf{B} \times \nabla S) = \nabla \cdot \Big[(\nabla\phi \times \nabla\psi_\mathrm{p}) \times \nabla S + I\nabla\phi \times \nabla S\Big] = \nabla\phi \times \nabla S \cdot \nabla I = -I'\mathbf{B} \cdot \nabla S \qquad \text{(B.3)}$$

Thus, the two terms in (B.2) cancel, so $X = 0$.

Exact conservation of ψ_* in quasisymmetry

We now give another proof of the conservation of $\psi_* = \psi_\mathrm{h} - I_\mathrm{h}\upsilon_\parallel/\Omega$ in quasisymmetric fields, where $\psi_\mathrm{h} = M\psi_\mathrm{p} - N\psi_\mathrm{t}$ and $I_\mathrm{h} = NK + MI$. The proof will be more general than the one given in Chapt. 2 in that it allows for both a time-dependent electrostatic potential Φ as well as for variation of Φ on a flux surface. Along the way we will derive the identity (2.35), repeated here for convenience:

$$\mathbf{v}_\mathrm{d}\cdot\nabla\psi_\mathrm{h} = \upsilon_\parallel\mathbf{b}\cdot\nabla\left(I_\mathrm{h}\upsilon_\parallel/\Omega\right) = \upsilon_\parallel\left(\mathbf{b}\cdot\nabla\chi\right)\frac{\partial}{\partial\chi}\left(I_\mathrm{h}\upsilon_\parallel/\Omega\right) \tag{B.4}$$

where $\chi = M\theta - N\zeta$. Proofs of ψ_* conservation have been given previously in references [14], [28], and [75].

Both the conservation of ψ_* and (B.4) require that the potential, if it varies at all on a flux surface, have the same helicity as B: $\Phi = \Phi(\psi_\mathrm{h}, \chi, t)$. In this case, since $\upsilon_\parallel^2 = 2\left(E - \mu B - Ze\Phi/m\right)$, then $M\,\partial\left(\upsilon_\parallel/B\right)/\partial\zeta = -N\,\partial\left(\upsilon_\parallel/B\right)/\partial\theta$. This result, together with the Boozer representations for $\mathbf{B}$ in (2.17) and (2.19), gives

$$\upsilon_\parallel\mathbf{b}\cdot\nabla\left(\frac{I_\mathrm{h}\upsilon_\parallel}{\Omega}\right) = \frac{I_\mathrm{h}\upsilon_\parallel}{\Omega}\left(\nabla\psi_\mathrm{p}\cdot\nabla\theta\times\nabla\zeta\right)\left(1 - \frac{Nq}{M}\right)\frac{\partial}{\partial\theta}\left(\frac{\upsilon_\parallel}{B}\right). \tag{B.5}$$

Also, using $\mathbf{v}_\mathrm{d} = \left(\upsilon_\parallel/\Omega\right)\nabla\times\left(\upsilon_\parallel\mathbf{b}\right)$, we can similarly show

$$\mathbf{v}_\mathrm{d}\cdot\nabla\psi_\mathrm{p} = \frac{I_\mathrm{h}\upsilon_\parallel}{\Omega}\left(\nabla\psi_\mathrm{p}\cdot\nabla\theta\times\nabla\zeta\right)\frac{1}{M}\frac{\partial}{\partial\theta}\left(\frac{\upsilon_\parallel}{B}\right). \tag{B.6}$$

The identity (B.4) immediately follows. To avoid dividing by zero in the $M = 0$ case, $(1 - Nq/M)\,\partial\left(\upsilon_\parallel/B\right)/\partial\theta$ in (B.5) can be replaced by $q\,\partial\left(\upsilon_\parallel/B\right)/\partial\zeta$, and $M^{-1}\partial\left(\upsilon_\parallel/B\right)/\partial\theta$ in (B.6) can be replaced by $-N^{-1}\partial\left(\upsilon_\parallel/B\right)/\partial\zeta$.

Next, we prove another intermediate result: B depends on θ and ζ only through the combination $M\theta - N\zeta$ (i.e. the field is quasisymmetric) if and only if L in (2.19) has this same property. We begin by casting the equilibrium condition $(\nabla\times\mathbf{B})\times\mathbf{B}/4\pi = \nabla p$ into Boozer coordinates. Then applying $\nabla\psi_\mathrm{p}\cdot\nabla\theta\times\nabla\zeta = B^2/\left(qI + K\right)$ (which follows from the scalar product of (2.17) with (2.19)) we obtain

$$\frac{\partial L}{\partial\theta} + q\frac{\partial L}{\partial\zeta} - \frac{dK}{d\psi_\mathrm{p}} - q\frac{dI}{d\psi_\mathrm{p}} = \frac{4\pi\left(qI + K\right)}{B^2}\frac{dp}{d\psi_\mathrm{p}}. \tag{B.7}$$

Note that the only quantities in this equation which vary in θ or ζ are B and L. By expanding (B.7) in Fourier series in θ and ζ, it follows that L depends on θ and ζ only through the combination $M\theta - N\zeta$ if and only if B does the same.

In a quasisymmetric field therefore $M\,\partial L/\partial\zeta = -N\,\partial L/\partial\theta$. Using (2.17) and (2.19) we can then show $\mathbf{v}_\mathrm{d}\cdot\nabla\left(I_\mathrm{h}\upsilon_\parallel/\Omega\right) = 0$. Combining this result with (2.35), we obtain $\left(\upsilon_\parallel\mathbf{b} + \mathbf{v}_\mathrm{d}\right)\cdot$

$\nabla\psi_* = 0$. It quickly follows that

$$\left[\frac{\partial}{\partial t} + (\upsilon_\parallel \mathbf{b} + \mathbf{v}_\mathrm{d}) \cdot \nabla + \frac{Ze}{m}\left(\frac{\partial \Phi}{\partial t}\right)\frac{\partial}{\partial E}\right]\psi_* = 0. \tag{B.8}$$

This equation represents the generalized version of ψ_* conservation.

APPENDIX C

Quasisymmetry in other coordinate systems

In this appendix, we prove that B has a single helicity in Boozer coordinates if and only if B has a single helicity in Hamada coordinates. The result which is proved is actually more general, that symmetry is equivalent for any magnetic coordinate system in which the Jacobian is proportional to some power of B. Preliminary results are derived in the next three sections which are used for the proof in the last section.

Transformations between magnetic coordinates

Consider two sets of magnetic coordinates, (θ_x, ζ_x) and (θ_y, ζ_y), satisfying

$$\begin{aligned} \mathbf{B} &= \nabla\psi_\mathrm{t} \times \nabla\theta_x + \iota\nabla\zeta_x \times \nabla\psi_\mathrm{t} \\ &= \nabla\psi_\mathrm{t} \times \nabla\theta_y + \iota\nabla\zeta_y \times \nabla\psi_\mathrm{t} \end{aligned} \tag{C.1}$$

where $2\pi\psi_\mathrm{t}$ is the toroidal flux. Suppose the transformation from one system to the other was written as

$$\theta_y = \theta_x + F\left(\psi_\mathrm{t}, \theta_x, \zeta_x\right) \tag{C.2}$$

$$\zeta_y = \zeta_x + G\left(\psi_\mathrm{t}, \theta_x, \zeta_x\right) \tag{C.3}$$

where F and G are periodic in both the poloidal and toroidal angles. Substituting (C.2)-(C.3) into (C.1),

$$\nabla\psi_\mathrm{t} \times \nabla F + \iota\nabla G \times \nabla\psi_\mathrm{t} = 0. \tag{C.4}$$

The $\nabla\theta_x$ component of this equation tells us $\partial F/\partial\zeta_x = \iota\,\partial G/\partial\zeta_x$, so upon integrating,

$$F = \iota G + y\left(\psi_\mathrm{t}, \theta_x\right). \tag{C.5}$$

Here and throughout this appendix, $\partial/\partial\zeta_x$ holds θ_x fixed, $\partial/\partial\theta_x$ holds ζ_x fixed, $\partial/\partial\zeta_y$ holds θ_y fixed, and $\partial/\partial\theta_y$ holds ζ_y fixed. The $\nabla\zeta_x$ component of (C.4) implies $\partial F/\partial\theta_x = \iota\,\partial G/\partial\theta_x$, so

$$F = \iota G + w\left(\psi_\mathrm{t}, \zeta_x\right). \tag{C.6}$$

Comparing (C.5) with (C.6), F must equal ιG plus a flux function, so

$$\theta_y = \theta_x + \iota G + a\left(\psi_\mathrm{t}\right) \tag{C.7}$$

and

$$\zeta_y = \zeta_x + G \tag{C.8}$$

for some flux function $a\left(\psi_\mathrm{t}\right)$.

Coordinates in which the Jacobian is proportional to a power of B

Suppose the Jacobian for the (θ_x, ζ_x) coordinates is proportional to B^x:

$$\nabla\psi_\mathrm{t} \cdot \nabla\theta_x \times \nabla\zeta_x = A_x\left(\psi_\mathrm{t}\right) B^x \tag{C.9}$$

for some flux function $A_x\left(\psi_\mathrm{t}\right)$. Hamada coordinates have $x = 0$ and Boozer coordinates have $x = 2$. The flux surface average of a quantity Q is

$$\langle Q \rangle = \frac{1}{V'} \int_0^{2\pi} d\theta_x \int_0^{2\pi} d\zeta_x \frac{Q}{\nabla\psi_\mathrm{t} \cdot \nabla\theta_x \times \nabla\zeta_x} \tag{C.10}$$

where $V\left(\psi_\mathrm{t}\right)$ is the volume enclosed by a flux surface, and the prime denotes $d/d\psi_\mathrm{t}$. Observe that

$$\langle B^x \rangle = \frac{4\pi^2}{V' A_x}, \tag{C.11}$$

so

$$\nabla\psi_\mathrm{t} \cdot \nabla\theta_x \times \nabla\zeta_x = \frac{4\pi^2}{V'} \frac{B^x}{\langle B^x \rangle}. \tag{C.12}$$

Therefore the Hamada Jacobian is $\nabla\psi_\mathrm{t} \cdot \nabla\theta_0 \times \nabla\zeta_0 = 4\pi^2/V'$.

Useful identities

Now we again consider the two magnetic coordinate systems (θ_x, ζ_x) and (θ_y, ζ_y), and we suppose that the latter also has a property analogous to (C.9):

$$\nabla\psi_\mathrm{t} \cdot \nabla\theta_y \times \nabla\zeta_y = A_y\left(\psi_\mathrm{t}\right) B^y. \tag{C.13}$$

Then from (C.12),

$$\nabla\psi_\mathrm{t} \cdot \nabla\theta_x \times \nabla\zeta_x = \frac{B^x}{\langle B^x \rangle} \frac{\langle B^y \rangle}{B^y} \nabla\psi_\mathrm{t} \cdot \nabla\theta_y \times \nabla\zeta_y. \tag{C.14}$$

Next, we apply the chain rule to G from (C.7)-(C.8):

$$\frac{\partial G}{\partial \theta_y} = \frac{\partial \theta_x}{\partial \theta_y}\frac{\partial G}{\partial \theta_x} + \frac{\partial \zeta_x}{\partial \theta_y}\frac{\partial G}{\partial \zeta_x}. \tag{C.15}$$

By applying $\partial/\partial\theta_y$ to (C.7) and (C.8), we find $1 = \partial\theta_x/\partial\theta_y + \iota\partial G/\partial\theta_y$ and $0 = \partial\zeta_x/\partial\theta_y + \partial G/\partial\theta_y$, so (C.15) implies

$$\frac{\partial G}{\partial \theta_y} = \left(1 - \iota\frac{\partial G}{\partial \theta_y}\right)\frac{\partial G}{\partial \theta_x} - \frac{\partial G}{\partial \theta_y}\frac{\partial G}{\partial \zeta_x}. \tag{C.16}$$

Rearranging,

$$\left(1 + \iota\frac{\partial G}{\partial \theta_x} + \frac{\partial G}{\partial \zeta_x}\right)\frac{\partial G}{\partial \theta_y} = \frac{\partial G}{\partial \theta_x}. \tag{C.17}$$

Now, apply $\mathbf{B}\cdot\nabla$ to (C.8) to obtain

$$\nabla\psi_\mathrm{t}\times\nabla\theta_y\cdot\nabla\zeta_y = \nabla\psi_\mathrm{t}\times\nabla\theta_x\cdot\nabla\zeta_x + \mathbf{B}\cdot\nabla G. \tag{C.18}$$

Noting (C.14), then (C.18) can be written

$$\frac{\langle B^x\rangle}{B^x}\frac{B^y}{\langle B^y\rangle} = 1 + \frac{\partial G}{\partial \zeta_x} + \iota\frac{\partial G}{\partial \theta_x}. \tag{C.19}$$

Substituting this expression into (C.17) then gives

$$\frac{B^x}{\langle B^x\rangle}\frac{\partial G}{\partial \theta_x} = \frac{B^y}{\langle B^y\rangle}\frac{\partial G}{\partial \theta_y}. \tag{C.20}$$

A similar calculation gives

$$\frac{B^x}{\langle B^x\rangle}\frac{\partial G}{\partial \zeta_x} = \frac{B^y}{\langle B^y\rangle}\frac{\partial G}{\partial \zeta_y}. \tag{C.21}$$

Next, applying $\partial/\partial\theta_x$ to (C.19) and commuting the derivatives on the right-hand side,

$$(y-x)\frac{\langle B^x\rangle}{\langle B^y\rangle}B^{y-x-1}\frac{\partial B}{\partial \theta_x} = \left[\frac{\partial}{\partial \zeta_x} + \iota\frac{\partial}{\partial \theta_x}\right]\frac{\partial G}{\partial \theta_x}. \tag{C.22}$$

Recalling that $\mathbf{B}\cdot\nabla = \nabla\psi_\mathrm{t}\times\nabla\theta_x\cdot\nabla\zeta_x\left[(\partial/\partial\zeta_x) + \iota\,(\partial/\partial\theta_x)\right]$, then (C.22) is equivalent to

$$\mathbf{B}\cdot\nabla\frac{\partial G}{\partial \theta_x} = \frac{4\pi^2}{V'}\frac{(y-x)}{\langle B^y\rangle}B^{y-1}\frac{\partial B}{\partial \theta_x}, \tag{C.23}$$

where we have also applied (C.12). We could have applied $\partial/\partial\zeta_x$ to (C.19) instead of $\partial/\partial\theta_x$, and so it is also true that

$$\mathbf{B}\cdot\nabla\frac{\partial G}{\partial \zeta_x} = \frac{4\pi^2}{V'}\frac{(y-x)}{\langle B^y\rangle}B^{y-1}\frac{\partial B}{\partial \zeta_x}. \tag{C.24}$$

Boozer and Hamada symmetry are equivalent

Suppose B has only a single helicity in the (θ_x, ζ_x) coordinates: $B = B(M\theta_x - N\zeta_x)$ for some integers M and N, or equivalently,

$$N\frac{\partial B}{\partial \theta_x} + M\frac{\partial B}{\partial \zeta_x} = 0. \tag{C.25}$$

Then from (C.23)-(C.24),

$$\mathbf{B}\cdot\nabla\left(N\frac{\partial G}{\partial \theta_x} + M\frac{\partial G}{\partial \zeta_x}\right) = 0. \tag{C.26}$$

It follows that

$$N\frac{\partial G}{\partial \theta_x} + M\frac{\partial G}{\partial \zeta_x} = S\,(\psi_t) \tag{C.27}$$

for some flux function $S\,(\psi_t)$. Integrating (C.27) in θ_x and ζ_x from 0 to 2π in both variables, we obtain $0 = (2\pi)^2\, S$, so $S = 0$. Then applying (C.20) and (C.21),

$$N\frac{\partial G}{\partial \theta_y} + M\frac{\partial G}{\partial \zeta_y} = 0. \tag{C.28}$$

Finally, we form

$$\begin{aligned} N\frac{\partial B}{\partial \theta_y} + M\frac{\partial B}{\partial \zeta_y} &= N\left(\frac{\partial \theta_x}{\partial \theta_y}\frac{\partial B}{\partial \theta_x} + \frac{\partial \zeta_x}{\partial \theta_y}\frac{\partial B}{\partial \zeta_x}\right) + M\left(\frac{\partial \theta_x}{\partial \zeta_y}\frac{\partial B}{\partial \theta_x} + \frac{\partial \zeta_x}{\partial \zeta_y}\frac{\partial B}{\partial \zeta_x}\right) \\ &= N\left(\left[1 - \iota\frac{\partial G}{\partial \theta_y}\right]\frac{\partial B}{\partial \theta_x} - \frac{\partial G}{\partial \theta_y}\frac{\partial B}{\partial \zeta_x}\right) + M\left(-\iota\frac{\partial G}{\partial \zeta_y}\frac{\partial B}{\partial \theta_x} + \left[1 - \frac{\partial G}{\partial \zeta_y}\right]\frac{\partial B}{\partial \zeta_x}\right). \end{aligned} \tag{C.29}$$

The first equality above is the chain rule, and to get the second line we have used the $\partial/\partial\theta_y$ and $\partial/\partial\zeta_y$ derivatives of (C.7) and (C.8). The last line vanishes due to (C.28), and so

$$N\frac{\partial B}{\partial \theta_x} + M\frac{\partial B}{\partial \zeta_x} = 0 \;\Rightarrow\; N\frac{\partial B}{\partial \theta_y} + M\frac{\partial B}{\partial \zeta_y} = 0. \tag{C.30}$$

The right equality in (C.30) also implies the left one, since x and y were arbitrary in the proof. For the specific case of $x = 0$ and $y = 2$, then B has a single helicity in Boozer coordinates if and only if B has a single helicity in Hamada coordinates.

APPENDIX D

Moment equations for the radial particle and heat fluxes

We now derive the result (5.54) which relates the radial heat flux to a moment of the collision operator in a quasisymmetric stellarator. Along the way, we will also derive an analogous relation for the particle flux. We first note the identity

$$\mathbf{B} \times \nabla \psi_{\mathrm{h}} \cdot \nabla B = I_{\mathrm{h}} \mathbf{B} \cdot \nabla B, \tag{D.1}$$

obtained by writing $\mathbf{B}$ in the Boozer representations (2.17) and (2.19) and using $M\,\partial B/\partial \zeta = -N\,\partial B/\partial \theta$.

Next, we follow [37, 76] and define the vector

$$\mathbf{y} = \frac{1}{B^2}\mathbf{B} \times \nabla \psi_{\mathrm{h}} - \frac{I_{\mathrm{h}}}{B^2}\mathbf{B}. \tag{D.2}$$

Using (D.1) and $[(\nabla \times \mathbf{B}) \times \mathbf{B}] \times \nabla \psi_h = 0$ we find the useful properties

$$\nabla \cdot \mathbf{y} = 0 \ \text{ and } \ \mathbf{b} \cdot (\nabla \mathbf{y}) \cdot \mathbf{b} = 0. \tag{D.3}$$

In the axisymmetric limit, $\mathbf{y} \to -R^2 \nabla \phi$ where ϕ is the conventional toroidal angle in cylindrical $(R,\ \phi,\ Z)$ coordinates.

Now take the full Fokker-Planck equation, multiply it by any function $X\,(\mathbf{r}, \mathbf{v})$, integrate over velocity, and apply a flux surface average. The result can be written

$$\left\langle \int d^3\upsilon\, f \dot{X} \right\rangle = \left\langle \frac{\partial}{\partial t} \int d^3\upsilon\, X f \right\rangle + \frac{1}{V'} \frac{d}{d\psi_{\mathrm{h}}} \left(V' \left\langle \int d^3\upsilon\, X f \mathbf{v} \cdot \nabla \psi_{\mathrm{h}} \right\rangle \right) - \left\langle \int d^3\upsilon\, X C \right\rangle \tag{D.4}$$

where the overdot indicates the Vlasov operator $\partial_t + \mathbf{v} \cdot \nabla + Zem^{-1}\left(\mathbf{E} + c^{-1}\mathbf{v} \times \mathbf{B}\right) \cdot \nabla_{\mathbf{v}}$ with $V' = (1 - Nq/M)^{-1} \oint d\theta \oint d\zeta\, (\mathbf{B} \cdot \nabla \theta)^{-1}$. Consider the choice $X = \upsilon^2 \mathbf{v} \cdot \mathbf{y}$. Assuming

$\mathbf{E} = -\nabla\Phi$ with Φ a flux function, then

$$\dot{X} = \upsilon^2 \mathbf{v}\cdot(\nabla \mathbf{y})\cdot\mathbf{v} - 2\frac{Ze\Phi'}{m}\mathbf{y}\cdot\mathbf{v}\mathbf{v}\cdot\nabla\psi_\mathrm{h} - \frac{Ze}{mc}\upsilon^2\mathbf{v}\cdot\nabla\psi_\mathrm{h} \tag{D.5}$$

where a prime denotes $d/d\psi_\mathrm{h}$ as usual.

We now proceed to order the various terms in (D.4) using the conventional drift orderings rather than the finite-E_ψ orderings. We use the small parameter $\delta = \rho/a$ with $\rho = \upsilon_\mathrm{i}/\Omega$ and a a macroscopic scale length. We expand the full distribution function as $f = \sum_j f_j$ with $f_j \sim \delta^j f_0$ and f_0 the Maxwellian of (5.6). We order $\partial_t \sim \delta^2\Omega$, $\nu \sim \delta\Omega$, $T/|\nabla T| \sim \eta/|\nabla\eta| \sim B^{-1}|\nabla\psi_\mathrm{h}| \sim \mathbf{y} \sim a$, and $|\mathbf{E}| \sim \delta B\upsilon_\mathrm{i}/c$.

We define $\langle\cdot\rangle_\varphi$ to be a gyroaverage holding ψ, θ, ζ, $\mu = \upsilon_\perp^2/2B$, and E fixed. We then define $\tilde{f} = f - \langle f\rangle_\varphi$. By the standard drift kinetic procedure [43],

$$\tilde{f}_1 = \frac{s}{\Omega}f_0\mathbf{b}\times\nabla\psi_\mathrm{h}\cdot\mathbf{v} \quad \text{where} \quad s(\upsilon,\psi_h) = \frac{p'}{p} + \frac{Ze\Phi'}{T} + \left(\frac{m\upsilon^2}{2T} - \frac{5}{2}\right)\frac{T'}{T}. \tag{D.6}$$

In (D.4), the time derivative term is $O\left(\delta^2\upsilon_\mathrm{i}^4 n\right)$ and therefore negligible compared to the collision term, which is $O\left(\delta\upsilon_\mathrm{i}^4 n\right)$. In the V' term, the contribution from $\langle f\rangle_\varphi$ is proportional to $\int d^3\upsilon\ \langle f\rangle_\varphi \upsilon^2 s(\upsilon)\,\mathbf{v}\mathbf{v} = \int d^3\upsilon\ \langle f\rangle_\varphi \upsilon^2 s(\upsilon)\langle\mathbf{v}\mathbf{v}\rangle_\varphi$. Due to

$$\langle\mathbf{v}\mathbf{v}\rangle_\varphi = \upsilon_\parallel^2\mathbf{b}\mathbf{b} + \left(\upsilon_\perp^2/2\right)\left(\overleftrightarrow{I} - \mathbf{b}\mathbf{b}\right) \tag{D.7}$$

then $\mathbf{y}\cdot\langle\mathbf{v}\mathbf{v}\rangle_\varphi\cdot\nabla\psi_\mathrm{h} = 0$, so $\langle f\rangle_\varphi$ does not contribute to the term. The contribution to the V' term from $\tilde{f}_1$ is proportional to $\int d^3\upsilon\, f_0\upsilon^2 s(\upsilon)\,\mathbf{v}\mathbf{v}\mathbf{v} = 0$. Thus, the largest contribution to the V' term in (D.4) comes from $\tilde{f}_2$, making the V' term $O\left(\delta^2\upsilon_\mathrm{i}^4 n\right)$ and negligible. From (D.4) we therefore have

$$\begin{aligned}\frac{Ze}{mc}\left\langle\int d^3\upsilon\, f\upsilon^2\mathbf{v}\cdot\nabla\psi_\mathrm{h}\right\rangle &= \left\langle\int d^3\upsilon\,\upsilon^2\mathbf{v}\cdot\mathbf{y}C\right\rangle + \left\langle\int d^3\upsilon\, f\upsilon^2\mathbf{v}\cdot(\nabla\mathbf{y})\cdot\mathbf{v}\right\rangle \\ &\quad -2\frac{Ze\Phi'}{m}\left\langle\mathbf{y}\cdot\int d^3\upsilon\, f\mathbf{v}\mathbf{v}\cdot\nabla\psi_\mathrm{h}\right\rangle + O\left(\delta^2\upsilon_\mathrm{i}^4 n\right).\end{aligned} \tag{D.8}$$

Due to (D.7) and (D.3), $\langle f\rangle_\varphi$ does not contribute to the $\nabla\mathbf{y}$ term in (D.8). The contribution to the term from $\tilde{f}_1$ vanishes since $\int d^3\upsilon\, f_0\upsilon^2 s(\upsilon)\,\mathbf{v}\mathbf{v}\mathbf{v} = 0$. Thus, the largest contribution to the term in (D.8) comes from $\tilde{f}_2$, making the term $O\left(\delta^2\upsilon_\mathrm{i}^4 n\right)$ and therefore negligible compared to the collision term.

Now consider the Φ' term in (D.8). Noting $\int d^3\upsilon\,\langle f\rangle_\varphi\,\mathbf{v}\mathbf{v} = \int d^3\upsilon\,\langle f\rangle_\varphi\,\langle\mathbf{v}\mathbf{v}\rangle_\varphi$ and (D.7), then $\langle f\rangle_\varphi$ does not contribute to this term. The contribution from $\tilde{f}_1$ is proportional to $\int d^3\upsilon\, f_0 s(\upsilon)\,\mathbf{v}\mathbf{v}\mathbf{v} = 0$. The largest contribution to the term in (D.8) therefore comes from $\tilde{f}_2$. This term is $O\left(\delta^2\upsilon_\mathrm{i}^4 n\right)$ and therefore negligible (though it would remain if $\mathbf{E}$ were ordered larger.)

To restrict our attention to neoclassical transport and exclude classical transport, we keep the parallel component of $\mathbf{y}$ in the collision term, but drop the perpendicular component. This leaves

$$\left\langle \int d^3\upsilon\, f\upsilon^2 \mathbf{v}\cdot\nabla\psi_{\mathrm{h}} \right\rangle \approx -\frac{I_{\mathrm{h}}}{\Omega_0}\left\langle h\int d^3\upsilon\, \upsilon^2\upsilon_{\|}C\right\rangle. \tag{D.9}$$

The particle flux can be found by repeating the preceding argument using $X = \mathbf{v}\cdot\mathbf{y}$ in (D.4). We find

$$\dot{X} = \mathbf{v}\cdot(\nabla\mathbf{y})\cdot\mathbf{v} - \frac{Ze}{mc}\mathbf{v}\cdot\nabla\psi_{\mathrm{h}}. \tag{D.10}$$

The ordering of terms in (D.4) proceeds as before, and so

$$\left\langle \int d^3\upsilon\, f\mathbf{v}\cdot\nabla\psi_{\mathrm{h}} \right\rangle = \frac{mc}{Ze}\left\langle \mathbf{y}\cdot\int d^3\upsilon\,\mathbf{v}C\right\rangle + O\left(\delta^2\upsilon_{\mathrm{i}}^2\frac{nmc}{Ze}\right). \tag{D.11}$$

For a plasma with a single species of ions, $C \approx C_{\mathrm{ii}}$ in the ion kinetic equation, and so the collision term in (D.11) vanishes to leading order in $\sqrt{m_{\mathrm{e}}/m_{\mathrm{i}}}$.

In light of this result and (D.9), the ion heat flux can be written as

$$\langle \mathbf{q}\cdot\nabla\psi_{\mathrm{h}}\rangle = \left\langle \int d^3\upsilon\, f\left(\frac{m\upsilon^2}{2}-\frac{5T}{2}\right)\mathbf{v}\cdot\nabla\psi_{\mathrm{h}}\right\rangle \approx \left\langle \int d^3\upsilon f\frac{m\upsilon^2}{2}\mathbf{v}\cdot\nabla\psi_{\mathrm{h}}\right\rangle, \tag{D.12}$$

which when combined with (D.9) gives (5.54) as desired.

APPENDIX E

Construction of quasi-isodynamic fields

Here we review the procedure described in [9] for constructing a field $B(\theta, \zeta)$ with the property (3.19) and with $\hat{B}$ straight in Boozer coordinates. While the original construction in [9] was given for a field in which the B contours may close toroidally or helically, here we specialize to the case where the contours close poloidally. We have also modified the notation slightly to account for the possibility of multiple toroidal periods. As shown following (3.19), any field generated by the construction which follows will be quasi-isodynamic.

We assume the stellarator has N identical toroidal periods, with the $B = \hat{B}$ curves falling along $\zeta = 2\pi N^{(0)}/N$ for any integer $N^{(0)}$. We also assume there is a single $B = \check{B}$ curve in each of the N periods, and there are no local maxima or minima in B aside from the global extrema $\hat{B}$ and $\check{B}$. We define $\varepsilon_r = \left(\hat{B} - \check{B}\right) / \left(2\check{B}\right)$ and define η by the relation

$$B/\check{B} = 1 + \varepsilon_r + \varepsilon_r \cos\eta, \tag{E.1}$$

so contours of $B(\theta, \zeta)$ are contours of $\eta(\theta, \zeta)$. We stipulate that $\eta = 0$ at $\zeta = 0$, varying continuously to $\eta = 2\pi$ at $\zeta = 2\pi/N$. Our goal will be to construct $\eta(\theta, \zeta)$ for the single period $0 \leqslant \zeta \leqslant 2\pi/N$. We define

$$G_{\mathrm{CS}} = N\zeta - \eta. \tag{E.2}$$

For η in the range $0 \leqslant \eta \leqslant \pi$, G_{CS} is then specified to be some continuous function of θ and η such that $G_{\mathrm{CS}} = 0$ when $\eta = 0$. For example, the model field shown in the figures was obtained using $G_{\mathrm{CS}}(\theta, \eta) = [0.6 + 0.9\sin\theta]\sin(\eta/2)$. A function $\Delta\zeta(\eta)$ is also chosen such that $\Delta\zeta(0) = 2\pi/N$ and $\Delta\zeta(\pi) = 0$, and it must satisfy the periodicity condition $\Delta\zeta(\eta) = \Delta\zeta(2\pi - \eta)$. For the figures we choose the inverted tent function $\Delta\zeta = 2|\eta - \pi|/N$. While we chose $G_{\mathrm{CS}}(\theta, \eta)$ freely in the range $0 \leqslant \eta \leqslant \pi$, in the range $\pi < \eta \leqslant 2\pi$, $G_{\mathrm{CS}}(\theta, \eta)$ is fixed by the requirement (3.19). To derive the mathematical constraint which is placed on G_{CS} by this requirement, consider points x and y in figure 3-1, two points on the same field

line and at the same value of B but on opposite sides of $\check{B}$. Suppose point $x$has coordinates $\zeta = \zeta_0, \theta = \theta_0$, and $\eta = \eta_0$. Then point y has coordinates $\zeta = \zeta_0 - \Delta\zeta(\eta_0), \theta = \theta_0 - \Delta\zeta(\eta_0)/q$, and $\eta = 2\pi - \eta_0$. Writing out (E.2) for each point, algebraically eliminating ζ_0, and dropping the subscripts, we obtain

$$G_{\mathrm{CS}}(\theta, \eta) = 2\pi - 2\eta + G_{\mathrm{CS}}(\theta - \Delta\zeta(\eta)/q, 2\pi - \eta) + N\Delta\zeta(\eta). \tag{E.3}$$

This formula, which determines G_{CS} for $\pi < \eta \leqslant 2\pi$ in terms of the G_{CS} we chose for $0 \leqslant \eta \leqslant \pi$, ensures (3.19) is satisfied. Next, the relationship $\zeta(\theta, \eta) = [\eta + G_{\mathrm{CS}}(\theta, \eta)]/N$ is inverted numerically to obtain $\eta(\theta, \zeta)$, and finally $B(\theta, \zeta)$ can be computed from (E.1).

For the model field shown in the figures, we have chosen $\varepsilon_r = 0.15$, $q = 1.079$, and $N = 5$.

APPENDIX F

Relations for the current in a general stellarator

Here we calculate several relations which are satisfied by the current in a general stellarator. The results are important for understanding the principle that the bootstrap current can vanish in a quasi-isodynamic stellarator, but in this appendix, we will consider the more general case of any MHD equilibrium with nested toroidal flux surfaces.

We begin by noting that the perpendicular current is $\mathbf{j}_\perp = c\,(dp/d\psi_\mathrm{t})\,B^{-2}\mathbf{B}\times\nabla\psi_\mathrm{t}$, where p is the sum of the pressures of each species and a flux function. The condition $\nabla\cdot\mathbf{j}=0$ then implies

$$\mathbf{B}\cdot\nabla\left(j_\parallel/B\right) = -c\,(dp/d\psi_\mathrm{t})\,\mathbf{B}\times\nabla\psi_\mathrm{t}\cdot\nabla\left(1/B^2\right). \tag{F.1}$$

This equation only determines $j_\parallel$ up to a flux function times B. We define the Pfirsch-Schlüter current $j_\parallel^\mathrm{PS}$ to be the solution of (F.1) with this free flux function chosen such that $\left\langle j_\parallel^\mathrm{PS} B\right\rangle = 0$. The true parallel current and the Pfirsch-Schlüter current then may differ by a flux function times B, and we call this flux function $A\,(\psi_\mathrm{t})$: $j_\parallel = j_\parallel^\mathrm{PS} + AB$. Multiplying this equation by B and flux surface averaging gives $\langle j_\parallel B\rangle = A\left\langle B^2\right\rangle$, so

$$j_\parallel = j_\parallel^\mathrm{PS} + \frac{\langle j_\parallel B\rangle\, B}{\langle B^2\rangle}. \tag{F.2}$$

The total current vector is therefore

$$\mathbf{j} = \frac{c}{B^2}\frac{dp}{d\psi_\mathrm{t}}\mathbf{B}\times\nabla\psi_\mathrm{t} + \frac{j_\parallel^\mathrm{PS}}{B}\mathbf{B} + \frac{\langle j_\parallel B\rangle}{\langle B^2\rangle}\mathbf{B}. \tag{F.3}$$

Next, recall that the coefficient $K\,(\psi_\mathrm{t})$ in the covariant Boozer representation 2.19 equals $2/c$ times the toroidal current inside a flux surface. Therefore $K\,(\psi_\mathrm{t}) = (2/c)\int d^2\mathbf{a}\cdot\mathbf{j}$, where the surface integral is performed over a constant-ζ cross-section of the plasma, a

surface which covers the region from magnetic axis out to the flux surface ψ_t. The area element is $d^2\mathbf{a} = d\psi_t d\theta \left(\nabla\psi_t \cdot \nabla\theta \times \nabla\zeta\right)^{-1} \nabla\zeta$, and so

$$\frac{c}{2}K\left(\psi_t\right) = -c\int_0^{\psi_t} d\psi_t' K \frac{dp}{d\psi_t}\int_0^{2\pi} d\theta \frac{1}{B^2} + \int_0^{\psi_t} d\psi_t' \int_0^{2\pi} d\theta \frac{j_\parallel^{\mathrm{PS}}}{B} + 2\pi\int_0^{\psi_t} d\psi_t' \frac{\langle j_\parallel B\rangle}{\langle B^2\rangle}, \quad \text{(F.4)}$$

where each integrand is evaluated at ψ_t' rather than ψ_t. We next integrate (F.4) over all ζ. Recalling that the flux surface average can be written

$$\langle X\rangle = \frac{\int_0^{2\pi} d\theta \int_0^{2\pi} d\zeta \left(X/B^2\right)}{\int_0^{2\pi} d\theta \int_0^{2\pi} d\zeta \left(1/B^2\right)}, \quad \text{(F.5)}$$

then the ζ integral of the $j_\parallel^{\mathrm{PS}}$ term in (F.4) becomes an integral of $\left\langle j_\parallel^{\mathrm{PS}} B\right\rangle = 0$, and so it vanishes. Also noting $\left\langle B^2\right\rangle = 4\pi^2 / \int_0^{2\pi} d\theta \int_0^{2\pi} d\zeta \left(1/B^2\right)$, then we are then left with

$$K\left(\psi_t\right) = -4\pi\int_0^{\psi_t} d\psi_t' \frac{K}{\langle B^2\rangle}\frac{dp}{d\psi_t} + \frac{4\pi}{c}\int_0^{\psi_t} d\psi_t' \frac{\langle j_\parallel B\rangle}{\langle B^2\rangle}. \quad \text{(F.6)}$$

Differentiating in ψ_t,

$$\frac{dK}{d\psi_t} = -4\pi\frac{K}{\langle B^2\rangle}\frac{dp}{d\psi_t} + \frac{4\pi}{c}\frac{\langle j_\parallel B\rangle}{\langle B^2\rangle}. \quad \text{(F.7)}$$

Importantly, the Pfirsch-Schlüter current does not contribute to K. If another equation for $\langle j_\parallel B\rangle$ in terms of K can be obtained from kinetic theory (as we have done for a quasi-isodynamic stellarator in 3.64), then this equation can be used with (F.6) to calculate a self-consistent current profile. In integrating (F.7), the initial condition $K = 0$ at $\psi_t = 0$ is used. For a quasi-isodynamic stellarator this procedure is done at the end of section 3.5.

APPENDIX G

Leading-order solution of the drift kinetic equation

We first prove a theorem regarding the time-independent drift kinetic equation

$$Df = C\{f\} \qquad \text{where} \qquad D = (\upsilon_\parallel \mathbf{b} + \mathbf{v}_\mathrm{d}) \cdot \nabla, \tag{G.1}$$

f is gyrophase-independent, $C\{f\}$ is the (nonlinear) Fokker-Planck operator for self collisions, and the magnetic field is quasisymmetric. We look for solutions f which are independent of ζ at fixed χ. Casting into $(\psi_*, \chi, \zeta, E, \mu)$ variables as in (5.3) we obtain $(D\chi)(\partial f/\partial\chi)_{\psi_*} = C\{f\}$. We multiply both sides by $(\ln f)/D\chi$ and recognize a perfect derivative:

$$\left(\frac{\partial}{\partial\chi}\right)_{\psi_*} (f \ln f - f) = \frac{C\{f\} \ln f}{D\chi}. \tag{G.2}$$

Now multiply by $\sigma = \operatorname{sgn}(D\chi)$, integrate over all allowed χ, and sum over σ and (in the case of trapped particles) all helical wells. These operations annihilate the left-hand side. Next, integrate over all allowed ψ_*, μ, and E, so we have integrated over all of position- and velocity-space (except for the unimportant ζ coordinate). This leaves

$$0 = \sum_\sigma \int d\mu\, dE\, d\psi_*\, d\chi\, |D\chi|^{-1}\, C\{f\} \ln f. \tag{G.3}$$

We now change from ψ_* to ψ_h as an integration variable. This is done using the remarkable identity

$$\frac{\partial\psi_*}{\partial\psi_\mathrm{h}} = \frac{(\upsilon_\parallel \mathbf{b} + \mathbf{v}_\mathrm{d}) \cdot \nabla\chi}{\upsilon_\parallel \mathbf{b} \cdot \nabla\chi} \tag{G.4}$$

which can be shown with a few lines of algebra using the techniques of appendix B. Then (G.3) becomes

$$0 = \sum_{\varsigma} \int d\mu\, dE\, d\psi_{\mathrm{h}}\, d\chi \left| \upsilon_{\parallel} \mathbf{b} \cdot \nabla \chi \right|^{-1} C\{f\} \ln f \tag{G.5}$$

where $\varsigma = \mathrm{sgn}(\upsilon_{\parallel})$. This can be rewritten as

$$0 = \int d\psi_{\mathrm{h}} \int (\mathbf{B} \cdot \nabla \chi)^{-1}\, d\chi \int d^3\upsilon\, C\{f\} \ln f. \tag{G.6}$$

Using the Landau form of the operator for self-collisions, the Cauchy-Schwartz inequality as usual implies $\int d^3\upsilon\, C\{f\} \ln f \leq 0$ for any f. Thus, (G.6) implies that $\int d^3\upsilon\, C\{f\} \ln f = 0$ at all positions, so f must be Maxwellian

$$f = \eta \left(\frac{m}{2\pi T} \right)^{3/2} \exp\left(-\frac{m}{T} \left(E - \mathbf{v} \cdot \mathbf{V} + \frac{V^2}{2} \right) \right), \tag{G.7}$$

where, for the moment, η, T, and $\mathbf{V}$ may depend on position. Next, (G.1) becomes $(\partial f / \partial \chi)_{\psi_*} = 0$, so f can vary only through ψ_*, μ, and E. Using this fact, a brief calculation then shows η, T, and V must be position-independent.

Thus, we have proven that the only ζ-independent exact solutions of the equilibrium drift kinetic equation (G.1) in a quasisymmetric field are Maxwellians as in (5.6) but with no gradients in temperature, mean flow, or pseudo-density η.

We now consider the related problem of finding the leading-order distribution function for the neoclassical transport analysis in a quasisymmetric field. If the leading-order kinetic equation is taken to be $(\upsilon_{\parallel} \mathbf{b} + \mathbf{v}_{\mathrm{d}}) \cdot \nabla f_0 = C\{f_0\}$, the proof following (G.1) applies and f_0 must be Maxwellian. If we restrict our attention to the case in which the mean flow is small compared to the thermal speed, then it is permissible to take $\mathbf{V} = 0$ to leading order. Although the gradients T' and η' are nonzero in a realistic plasma, we interpret the proof as indication these gradients are weak. If we instead expand the kinetic equation for small collisionality, to leading order $Df \approx 0$, so f must be a function of the constants of the motion (ψ_*, μ, E). Since we want f to also be nearly Maxwellian, we therefore must take $f \approx F(\psi_*, E)$ with F given by (5.8), and we demand that F be Maxwellian to leading order. A Taylor-expansion of η and T in F about $\psi_* \approx \psi_{\mathrm{h}}$ gives $F \approx f_{\mathrm{M}} + F_1$ where

$$F_1 = -f_{\mathrm{M}} \frac{\upsilon_{\parallel} I_{\mathrm{h}}}{\Omega} \left[\frac{\eta'}{\eta} + \left(\frac{mE}{T} - \frac{3}{2} \right) \frac{T'}{T} \right] \tag{G.8}$$

with η and T evaluated at ψ_{h} rather than ψ_*. (This F_1 is equivalent to (5.9).) Therefore $F_1 / f_{\mathrm{M}} \sim \rho / (k r_T)$ where $k = |\nabla \psi_{\mathrm{h}}| / I_{\mathrm{h}}$ is the quasisymmetry generalization of $B_{\mathrm{p}}/B_{\mathrm{t}}$ defined in section (4.1), and r_T is the scale length for η and T. For f to remain Maxwellian to leading order, T and η can vary only on a scale length which is long compared to ρ/k. It is still possible that the true density n and the potential Φ vary on the length scale ρ/k as long as their combination in $\eta = n \exp(Ze\Phi/T)$ varies more slowly.

APPENDIX H

Integral for the parallel flow

Here we argue that

$$\int d^3v\,(g-G) \sim \sqrt{\varepsilon}\frac{nI_{\rm h}T'}{v_{\rm i}m\Omega} \tag{H.1}$$

and therefore that the last integral in (5.65) can be dropped. We begin by writing the integral in terms of (W,Λ) variables:

$$\int d^3v\,(g-G) = \frac{2\pi}{h}\sum_\sigma \iint dW\,d\Lambda \frac{(g-G)\,W}{\left|v_\parallel+u\right|} = -2\pi\sum_\sigma \iint dW\,d\Lambda\,(g-G)\,\frac{\partial}{\partial\Lambda}\left|v_\parallel+u\right|. \tag{H.2}$$

We are free to add a constant behind the derivative, so

$$\int d^3v\,(g-G) = 2\pi\sum_\sigma \iint dW\,d\Lambda\,\sqrt{2W}\,(g-G)\,\frac{\partial}{\partial\Lambda}\left(1-\sqrt{1-\Lambda/h}\right). \tag{H.3}$$

We next integrate by parts in Λ. There is no contribution from the lower boundary $\Lambda = 0$ because the last quantity in parentheses vanishes there. There is also no contribution from the upper boundary since $G = 0$ there and $g = 0$ in this trapped region to leading order. Thus,

$$\int d^3v\,(g-G) = 2\pi\sum_\sigma \iint dW\,d\Lambda\,\sqrt{2W}\left(\sqrt{1-\Lambda/h}-1\right)\left[f_{\rm M}\frac{\partial}{\partial\Lambda}\frac{(g-G)}{f_{\rm M}}+\frac{(g-G)}{f_{\rm M}}\frac{\partial f_{\rm M}}{\partial\Lambda}\right]. \tag{H.4}$$

To leading order in $\sqrt{\varepsilon}$, $f_{\rm M}$ is independent of Λ, so the $\partial f_{\rm M}/\partial\Lambda$ term vanishes. Also, from (5.48), $f_{\rm M}\partial\left[(g-G)/f_{\rm M}\right]/\partial\Lambda$ is odd in σ to leading order, and so it vanishes in the σ sum. To properly calculate the leading nonvanishing contribution to the integral above, we would need to find not only the next correction to $f_{\rm M}$ in the $\sqrt{\varepsilon}$ expansion, but also the next correction to g, which is not feasible. In any event, since the right-hand side of (H.4) vanishes in leading order, the estimate (H.1) is adequate.

Bibliography

[1] Boozer, A. H. What is a stellarator? *Phys. Plasmas*, **5**, 1647 (1998).

[2] Freidberg, J. *Plasma Physics and Fusion Energy*. Cambridge University Press, Cambridge (2007).

[3] I. E. Tamm. vol. 1 of *Plasma Physics and the problem of controlled thermonuclear reactions*, p. 35. Pergamon, New York (1961).

[4] Wakatani, M. *Stellarator and Heliotron Devices*. Oxford University Press, Oxford (1998).

[5] Ho, D. D.-M. and Kulsrud, R. M. Neoclassical transport in stellarators. *Phys. Fluids*, **30**, 442 (1987).

[6] Hirsch, M., et al. Major results from the stellarator Wendelstein 7-AS. *Plasma Phys. Controlled Fusion*, **50**, 053001 (2008).

[7] Hall, L. S., and McNamara, B. Three-dimensional equilibrium of the anisotropic, finite-pressure guiding-center plasma: Theory of the magnetic plasma. *Phys. Fluids*, **18**, 552 (1975).

[8] Helander, P. and Sigmar, D. J. *Collisional Transport in Magnetized Plasmas*. Cambridge University Press, Cambridge (2002).

[9] Cary, J. R. and Shasharina, S. G. Omnigenity and quasihelicity in helical plasma confinement systems. *Phys. Plasmas*, **4**, 3323 (1997).

[10] Cary, J. R. and Shasharina, S. G. Helical plasma confinement devices with good confinement properties. *Phys. Rev. Lett.*, **78**, 647 (1997).

[11] Catto, P. J., and Hazeltine, R. D. Omnigenous equilibria. *Phys. Fluids B*, **4**, 2081 (1992).

[12] Helander, P. On rapid plasma rotation. *Phys. Plasmas*, **14**, 104501 (2007).

[13] Boozer, A. H. Quasi-helical symmetry in stellarators. *Plasma Phys. Controlled Fusion*, **37**, A103 (1995).

[14] Nührenberg, J. and Zille, R. Quasi-helically symmetric toroidal stellarators. *Phys. Lett. A*, **129**, 113 (1988).

[15] Anderson, F., Almagri, A., Anderson, D., Matthews, P., Talmadge, J., and Shohet, J. *Fusion Tech.*, **27**, 273 (1995).

[16] Zarnstorff, M., et al. Physics of the compact advanced stellarator NCSX. *Plasma Phys. Controlled Fusion*, **43**, A237 (2001).

[17] Helander, P., and Nührenberg, J. Bootstrap current and neoclassical transport in quasi-isodynamic stellarators. *Plasma Phys. Controlled Fusion*, **51**, 055004 (2009).

[18] Nührenberg, J. Development of quasi-isodynamic stellarators. *Plasma Phys. Controlled Fusion*, **52**, 124003 (2010).

[19] Gori, S., Lotz, W., and Nührenberg, J. *Theory of Fusion Plasmas (Bologna: Editrice Compositori)*, p. 335 (1996).

[20] Subbotin, A. A. et al. Integrated physics optimization of a quasi-isodynamic stellarator with poloidally closed contours of the magnetic field strength. *Nucl. Fusion*, **46**, 921 (2006).

[21] Mikhailov, M. I., Shafranov, V. D., and Nührenberg, J. *Plasma Phys. Rep.*, **35**, 529 (2009).

[22] Mynick, H. E. Transport optimization in stellarators. *Phys. Plasmas*, **13**, 058102 (2006).

[23] Beidler, C., et al. Physics and engineering design for Wendelstein VII-X. *Fusion Tech.*, **17**, 148 (1990).

[24] Lotz, W., Nührenberg, J., and Schwab, C. Proc. 13th Int. Conf. on Plasma Physics and Controlled Nuclear Fusion Research (Washington), Paper IAEA-CN-53-C-III-5, IAEA, Vienna (1991).

[25] Grieger, G., et al. Physics optimization of stellarators. *Phys. Fluids B*, **4**, 2081 (1992).

[26] Wobig, H. Theory of advanced stellarators. *Plasma Phys. Controlled Fusion*, **41**, A159 (1999).

[27] Johnson, J. L., et al. External kink modes in a large helical device (LHD) equilibrium with self-consistent bootstrap current. *Phys. Plasmas*, **6**, 2513 (1999).

[28] Boozer, A. H. Transport and isomorphic equilibria. *Phys. Fluids*, **26**, 496 (1983).

[29] Landreman, M. and Catto, P. J. Effects of the radial electric field in a quasisymmetric stellarator. *Plasma Phys. Controlled Fusion*, **53**, 015004 (2011).

[30] Landreman, M. and Catto, P. J. Neoclassical flow, current, and electric field in a quasi-isodynamic stellarator. *Plasma Phys. Controlled Fusion*, **53**, 035016 (2011).

[31] Landreman, M. The monoenergetic approximation in stellarator neoclassical calculations. *Submitted to Plasma Phys. Controlled Fusion, also available at arXiv:1102.2508v1* (2011).

[32] Simakov, A. N. and Helander, P. Plasma rotation in a quasi-symmetric stellarator. *Plasma Phys. Controlled Fusion*, **53**, 024005 (2011).

[33] Garren, D. A., and Boozer, A. H. Magnetic field strength of toroidal plasma equilibria. *Phys. Fluids B*, **3**, 2805 (1991).

[34] Garren, D. A., and Boozer, A. H. Existence of quasihelically symmetric stellarators. *Phys. Fluids B*, **3**, 2822 (1991).

[35] Garabedian, P. R. Stellarators with the magnetic symmetry of a tokamak. *Phys. Plasmas*, **3**, 2483 (1996).

[36] Garabedian, P. R. Recent progress in the design of stellarator experiments. *Phys. Plasmas*, **4**, 1617 (1997).

[37] Helander, P. and Simakov, A. N. Intrinsic ambipolarity and rotation in stellarators. *Phys. Rev. Lett.*, **101**, 145003 (2008).

[38] Fitzpatrick, R., and Aydemir, A. Y. Stabilization of the resistive shell mode in tokamaks. *Nucl. Fusion*, **36**, 11 (1996).

[39] Diamond, P. H., Itoh, S.-I., Itoh, K., and Hahm, T. S. Zonal flows in plasma - a review. *Plasma Phys. Controlled Fusion*, **47** (2005).

[40] Bateman, G. *MHD Instabilities*. MIT Press, Cambridge, Mass. (1978).

[41] Boozer, A. Physics of magnetically confined plasmas. *Rev. Mod. Phys.*, **76**, 1071 (2004).

[42] Boozer, A. H. Establishment of magnetic coordinates for a given magnetic field. *Phys. Fluids*, **25**, 520 (1982).

[43] Hazeltine, R. Recursive derivation of drift-kinetic equation. *Plasma Phys.*, **15**, 77 (1973).

[44] Spong, D. A., Hirshman, S. P., Berry, L. A., Lyon, J. F., Fowler, R. H., Strickler, D. J., Cole, M. J., Nelson, B., N., Williamson, D. E., Ware, A. S., Alban, D., Sanchez, R., Fu, G. Y., Monticello, D. A., Miner, W. H., and Valanju, P. M. Physics issues of compact drift optimized stellarators. *Nucl. Fusion*, **41**, 711 (2001).

[45] Talmadge, J. N., et al. Experimental tests of quasisymmetry in HSX. *Plasma Fusion Res.*, **3**, S1002 (2008).

[46] Gerhardt, S. P., Talmadge, J. N., Canik, J. M., and Anderson, D. T. Measurements and modeling of plasma flow damping in the Helically Symmetric eXperiment. *Phys. Plasmas*, **12**, 056116 (2005).

[47] Canik, J. M. et al. Experimental demonstration of improved neoclassical transport with quasihelical symmetry. *Phys. Rev. Lett.*, **98**, 085002 (2007).

[48] Pytte, A. and Boozer, A. H. Neoclassical transport in helically symmetric plasmas. *Phys. Fluids*, **24**, 88 (1981).

[49] Pusztai, I. and Catto, P. J. Neoclassical plateau regime transport in a tokamak pedestal. *Plasma Phys. Controlled Fusion*, **52**, 075016 (2010).

[50] Maassberg, H., Beidler, C. D., and Turkin, Y. Momentum correction techniques for neoclassical transport in stellarators. *Phys. Plasmas*, **16**, 072504 (2009).

[51] Hirshman, S. P., Shaing, K. C., van Rij, W. I., Beasley, Jr., C. O., and Crume, Jr., E. C. Plasma transport coefficients for nonsymmetric toroidal confinement systems. *Phys. Fluids*, **29**, 2951 (1986).

[52] van Rij, W. I., and Hirshman, S. P. Variational bounds for transport coefficients in three-dimensional toroidal plasmas. *Phys. Fluids B*, **3**, 563 (1989).

[53] Sugama, H. and Nishimura, S. How to calculate the neoclassical viscosity, diffusion, and current coefficients in general toroidal plasmas. *Phys. Plasmas*, **9**, 4637 (2002).

[54] Spong, D. A. Generation and damping of neoclassical plasma flows in stellarators. *Phys. Plasmas*, **12**, 056114 (2005).

[55] Beidler, C. D., et al. ICNTS - impact of incompressible $\mathbf{E} \times \mathbf{B}$ flow in estimating mono-energetic transport coefficients. *Proceedings of the 17th International Toki Conference and 16th International Stellarator/Heliotron Workshop, Toki* (2007).

[56] Lore, J. et al. Internal electron transport barrier due to neoclassical ambipolarity in the Helically Symmetric Experiment. *Phys. Plasmas*, **17**, 056101 (2010).

[57] Rosenbluth, M. N., Hazeltine, R. D., and Hinton, F. L. Plasma transport in toroidal confinement systems. *Phys. Fluids*, **15**, 116 (1972).

[58] Hinton, F. L., and Hazeltine, R. D. Theory of plasma transport in toroidal confinement systems. *Rev. Mod. Phys.*, **48**, 239 (1976).

[59] Hinton, F. L., and Wong, S. K. Neoclassical ion transport in rotating axisymmetric plasmas. *Phys. Fluids*, **28**, 3082 (1985).

[60] Catto, P. J., Bernstein, I. B., Tessarotto, M. Ion transport in toroidally rotating tokamak plasmas. *Phys. Fluids*, **30**, 2784 (1987).

[61] Hazeltine, R. D., and Hinton, F. L. Kinetic theory of flowing, magnetized plasma. *Phys. Plasmas*, **12**, 102506 (2005).

[62] Brizard, A. J. Nonlinear gyrokinetic Vlasov equation for toroidally rotating axisymmetric tokamaks. *Phys. Plasmas*, **2**, 459 (1995).

[63] Cary, J. R., and Brizard, A. J. Hamiltonian theory of guiding-center motion. *Rev. Mod. Phys.*, **81**, 693 (2009).

[64] Ramos, J. J. Finite-Larmor-radius kinetic theory of a magnetized plasma in the macroscopic flow reference frame. *Phys. Plasmas*, **15**, 082106 (2008).

[65] Talmadge, J. N., and Garhardt, S. P. Numerical calculation of the Hamada basis vectors for three-dimensional toroidal magnetic configurations. *Phys. Plasmas*, **12**, 072513 (2005).

[66] Wagner, F., Hirsch, M., Hartfuss, H.-J., Laqua, H. P., and Maassberg, H. H-mode and transport barriers in helical systems. *Plasma Phys. Controlled Fusion*, **48**, A217 (2006).

[67] Akiyama, T., Hirsch, M., Estrada, T., Hidalgo, C., and Mizuuchi, T. Status of a stellarator/heliotron H-mode database. *Contrib. Plasma Phys.*, **50**, 590 (2010).

[68] Yokoyama, M., Maassberg, H., Beidler, C. D., Tribaldos, V., Ida, K., Estrada, T., Castejon, F., Fujisawa, A., Minami, T., Shimozuma, T., Takeiri, Y., Dinklage, A., Murakami, S., and Yamada, H. Core electron-root confinement (CERC) in helical plasmas. *Nucl. Fusion*, **47**, 1213 (2007).

[69] Kagan, G. and Catto, P. J. Arbitrary poloidal gyroradius effects in tokamak pedestals and transport barriers. *Plasma Phys. Controlled Fusion*, **50**, 085010 (2008).

[70] Kagan, G. and Catto, P. J. Neoclassical ion heat flux and poloidal flow in a tokamak pedestal. *Plasma Phys. Controlled Fusion*, **52**, 055004 (2010).

[71] Kagan, G. and Catto, P. J. Corrigendum: Neoclassical ion heat flux and poloidal flow in a tokamak pedestal. *Plasma Phys. Controlled Fusion*, **52**, 079801 (2010).

[72] Kagan, G. and Catto, P. J. Enhancement of the bootstrap current in a tokamak pedestal. *Phys. Rev. Lett.*, **105**, 045002 (2010).

[73] Pusztai, I. and Catto, P. J. Corrigendum: Neoclassical plateau regime transport in a tokamak pedestal. *Plasma Phys. Controlled Fusion*, **52**, 119801 (2010).

[74] Tribaldos, V., and Guasp, J. Neoclassical global flux simulations in stellarators. *Plasma Phys. Controlled Fusion*, **47**, 545 (2005).

[75] Isaev, M. Yu., Mikhailov, M. I., and Shafranov, V. D. Quasi-symmetric toroidal magnetic systems. *Plasma Phys. Rep.*, **20**, 319 (1994).

[76] Simakov, A. N. and Helander, P. Neoclassical momentum transport in a collisional stellarator and a rippled tokamak. *Phys. Plasmas*, **16**, 042503 (2009).